Hadron Spectroscopy at COMPASS

Jan M. Friedrich

Physik-Department, TU München

COMPASS collaboration

September 26, 2016

COmmon Muon and Proton Apparatus for Structure and Spectroscopy

COmmon Muon and Proton Apparatus for Structure and Spectroscopy

CERN SPS: protons $\sim$ 450 GeV (5 – 10 sec spills)

- secondary $\pi, K, (\bar{p})$: up to $2 \cdot 10^7$/s (typ. $5 \cdot 10^6$/s)
  Nov. 2004, 2008-09, 2012, 2015:
  hadron spectroscopy, Primakoff, Drell-Yan
- tertiary muons: $4 \cdot 10^7$ / s
  2002-04, 2006-07, 2010-11, 2016: nucleon spin structure

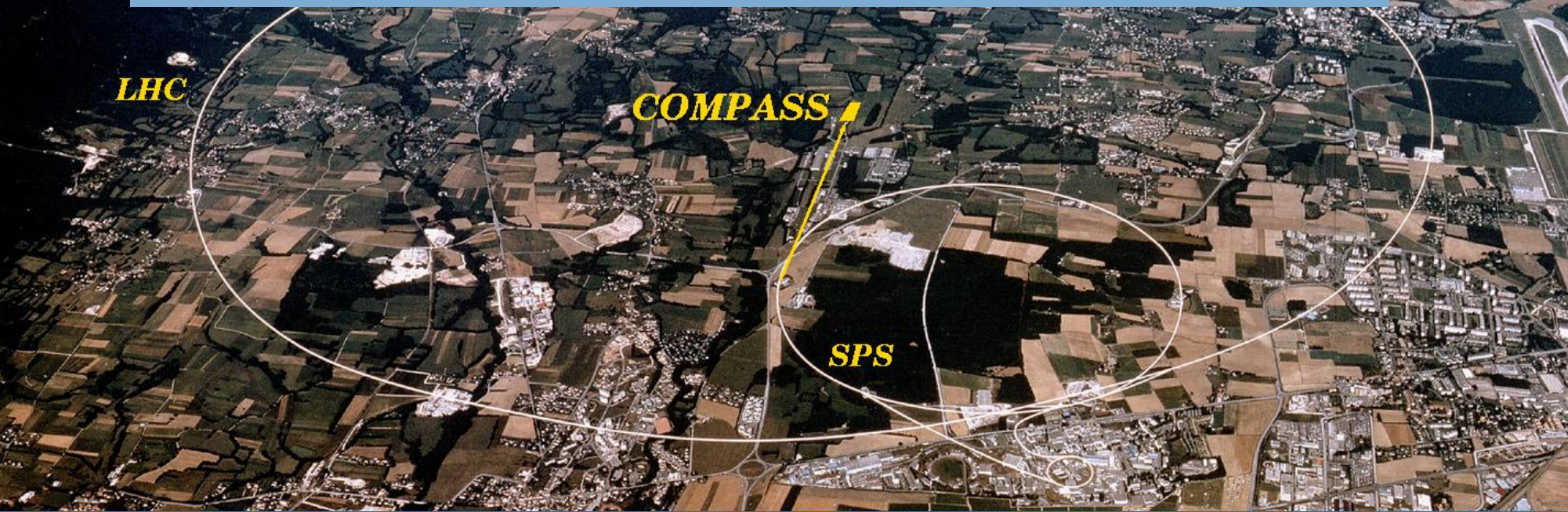

Physics fields at COMPASS

- lepton scattering
  $\rightarrow$ partonic nucleon structure at high momentum transfer

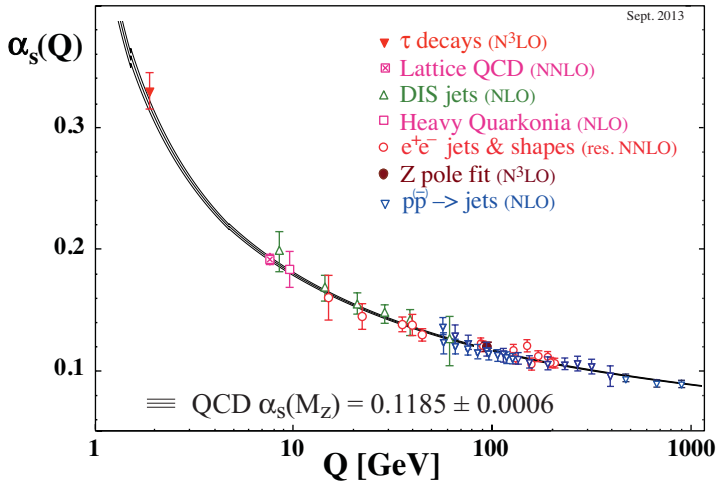

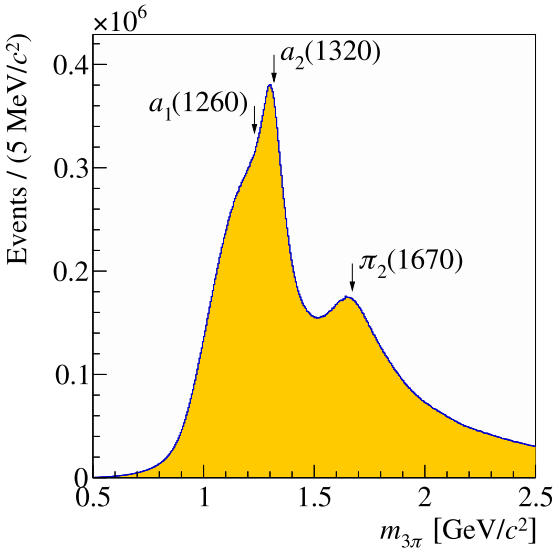

- diffractive dissociation of pions and kaons
  $\rightarrow$ meson resonances and dynamics

- scattering of pions (and kaons) in nuclear Coulomb field
  $\rightarrow$ low-energetic meson-photon reactions $\pi\gamma \rightarrow \pi\gamma$, $\pi\gamma \rightarrow 3\pi$

Physics fields at COMPASS

- lepton scattering
  → partonic nucleon structure
  talks by N. Makke, S. Sirtl, M. Gorzellik, L. Silva, B. Parsamyan, G. Nukazuka, K. Klimaszewski, M. Wilfert, A. Ferrero, J. Matousek

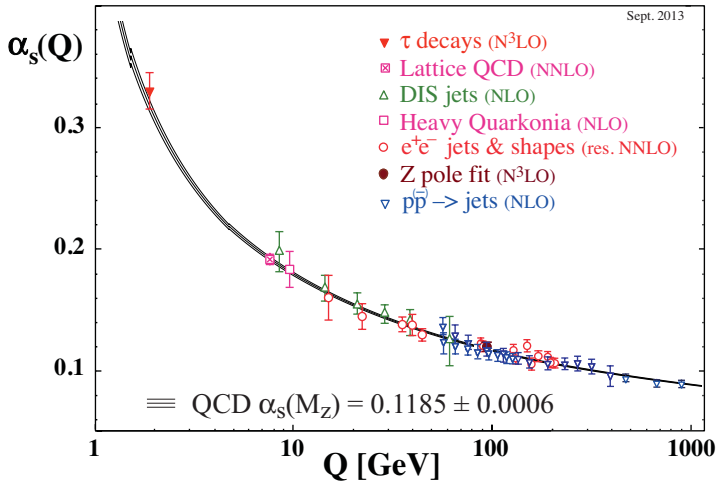

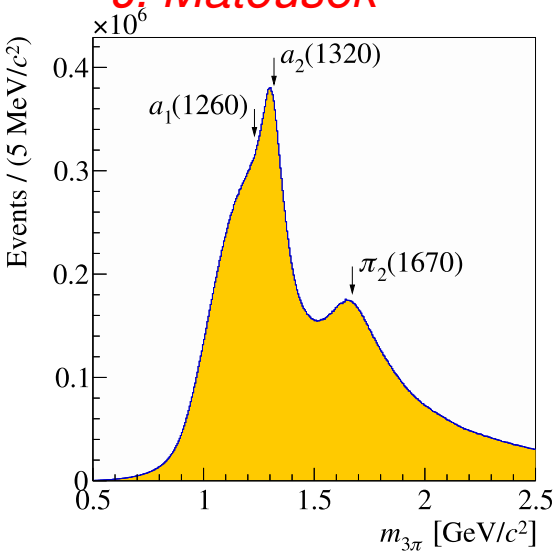

- diffractive dissociation of pions and kaons
  → meson resonances and dynamics
  this talk

- scattering of pions (and kaons) in nuclear Coulomb field
  → low-energetic meson-photon reactions $\pi\gamma \to \pi\gamma$, $\pi\gamma \to 3\pi$

Fixed-target experiment

- two-stage magnetic spectrometer
- high-precision, high-rate tracking, PID, calorimetry

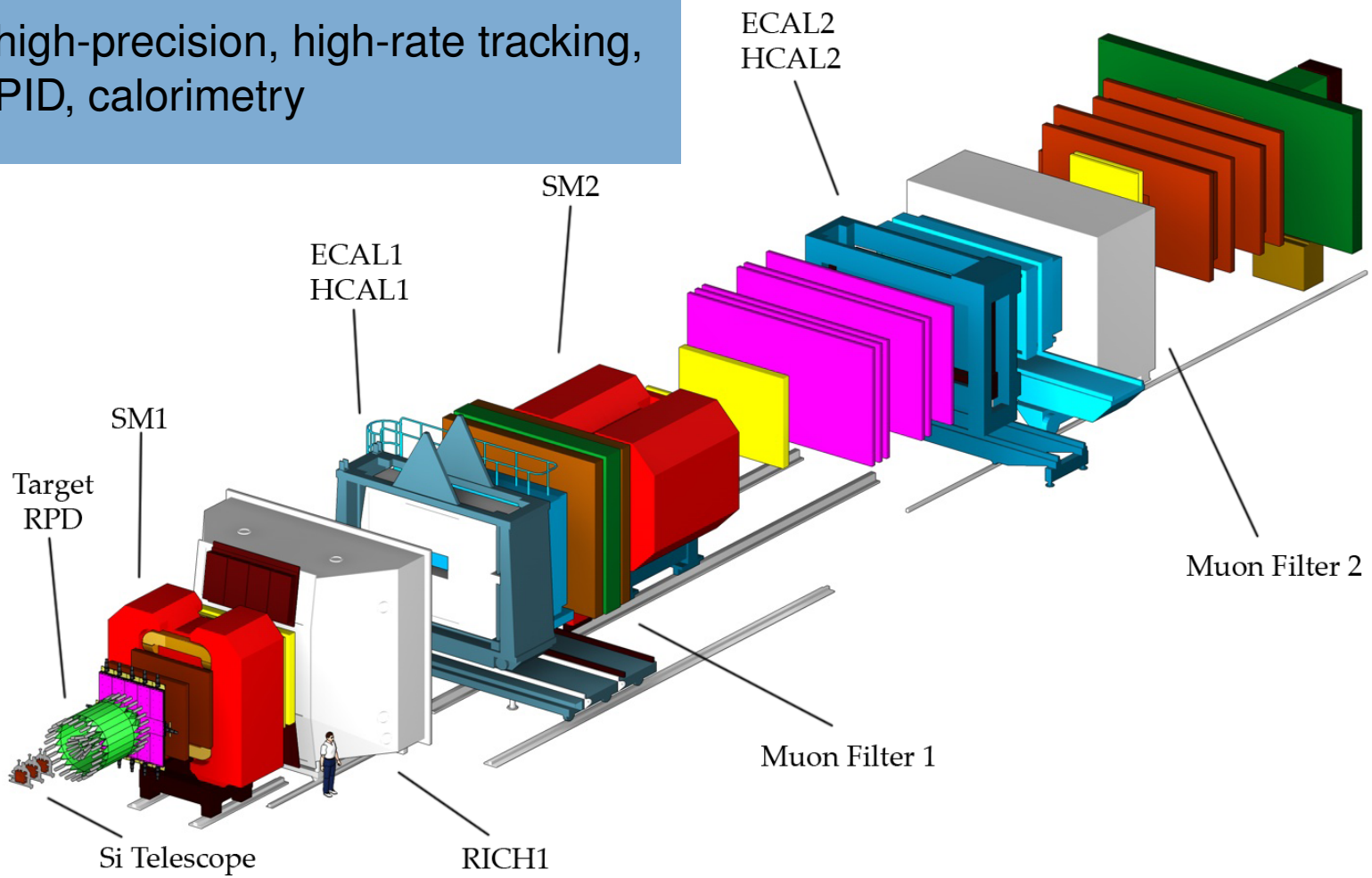

Fixed-target experiment

- two-stage magnetic spectrometer
- high-precision, high-rate tracking, PID, calorimetry

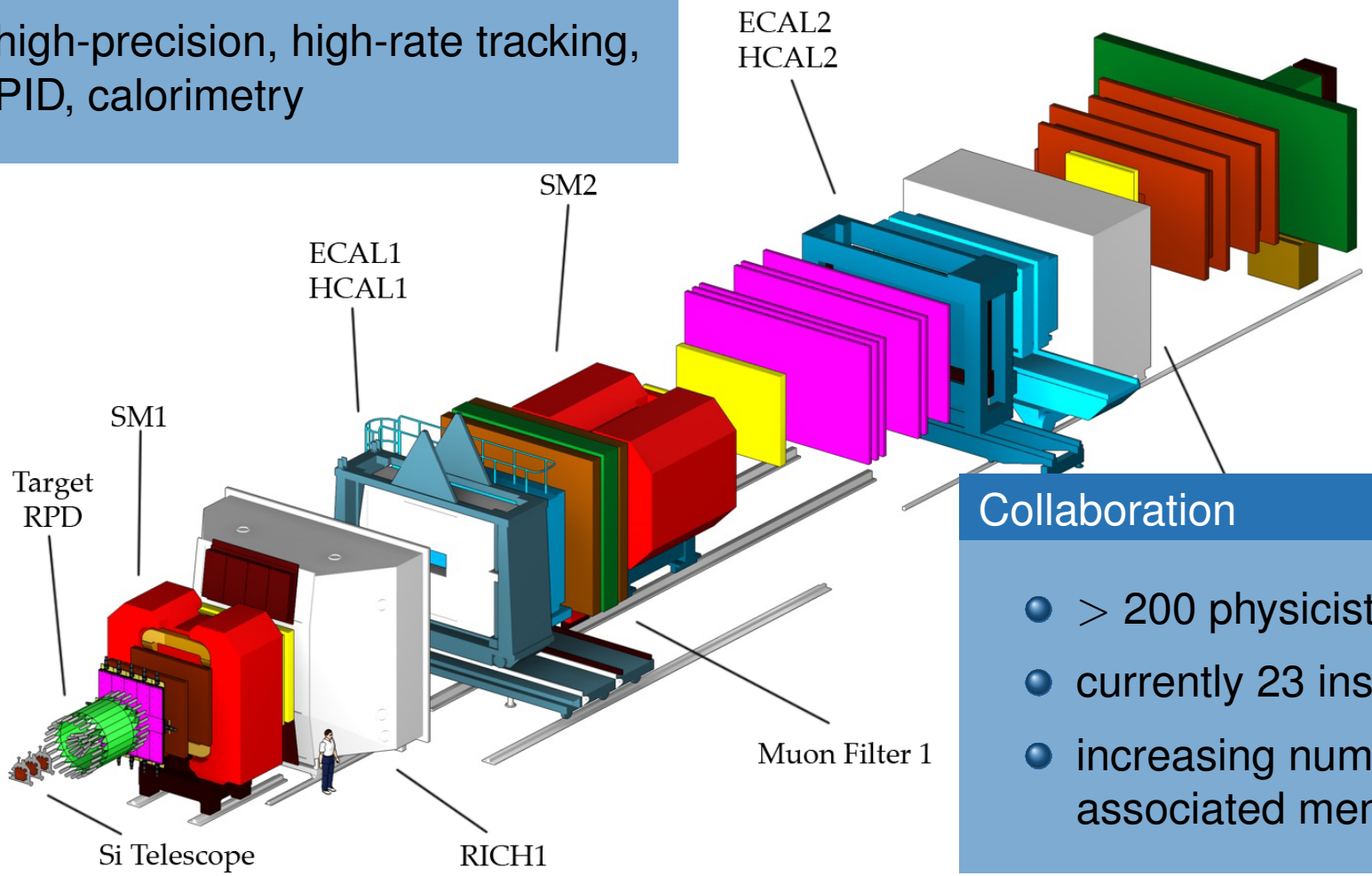

Collaboration

- $>$ 200 physicists
- currently 23 institutes
- increasing number of associated members

$h = \pi^- / K^- / \bar{p}$ or $h = p / K^+ \pi^+$

$$h + p \rightarrow \begin{cases} p + h + \eta \\ p + h + \pi^0 + \pi^0 \\ p + h + \pi^- + \pi^+ \quad \Longleftarrow \\ p + h + (\pi^0\pi^0)^a + (\pi^-\pi^+)^b \\ p + h + (K^0\bar{K}^0)^c + (K^-K^+)^d \end{cases}$$

$$h + \gamma^{(*\text{Primakoff})} \rightarrow \begin{cases} h + \gamma \\ h + \pi^0 \ / \ \eta \\ h + (\pi^0\pi^0)^a + (\pi^-\pi^+)^b \end{cases}$$

Diffractive 3π production

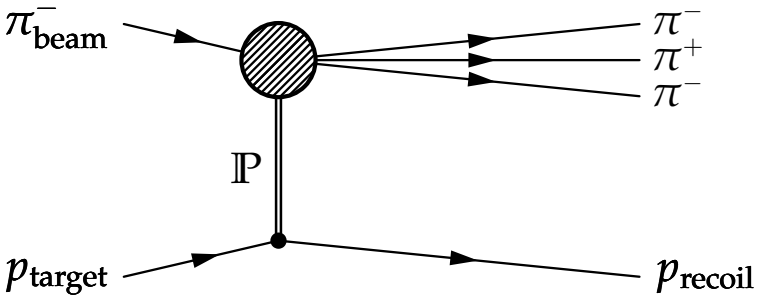

- exclusive measurement

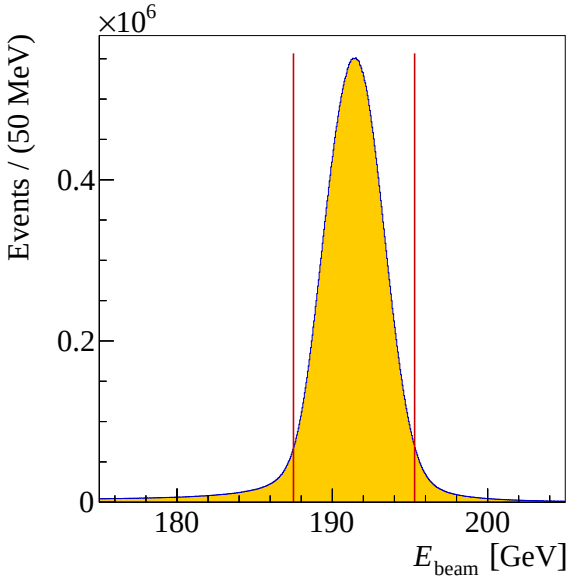

Diffractive 3π production

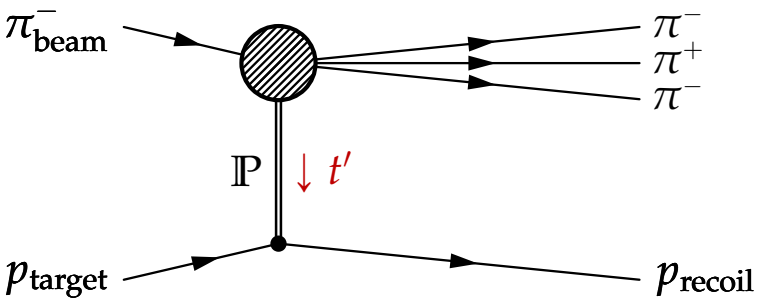

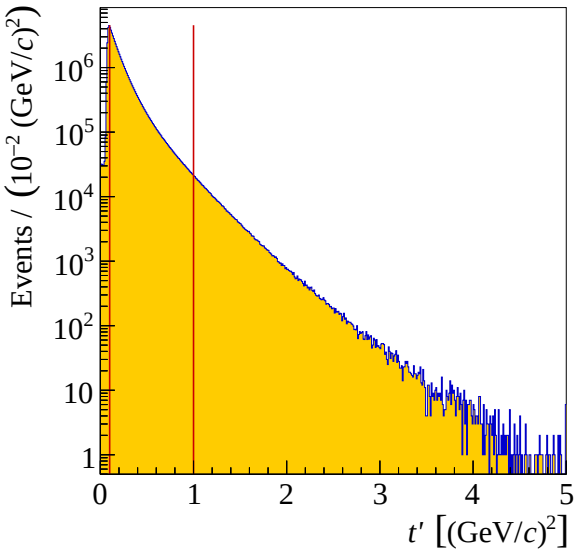

- exclusive measurement
- four-momentum transfer t'
  $< 0.5\,\text{GeV}$: Pomeron exchange $\mathbb{P}$

Diffractive 3π production

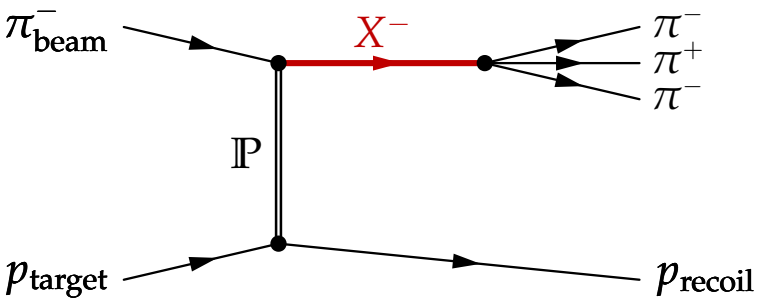

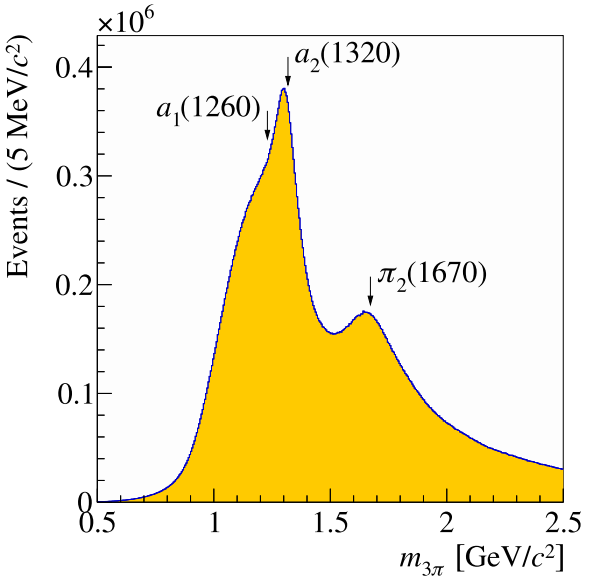

- exclusive measurement
- four-momentum transfer t'
  $< 0.5\,\text{GeV}$: Pomeron exchange $\mathbb{P}$
- rich structure in $\pi^-\pi^+\pi^-$ mass spectrum...

Diffractive 3π production

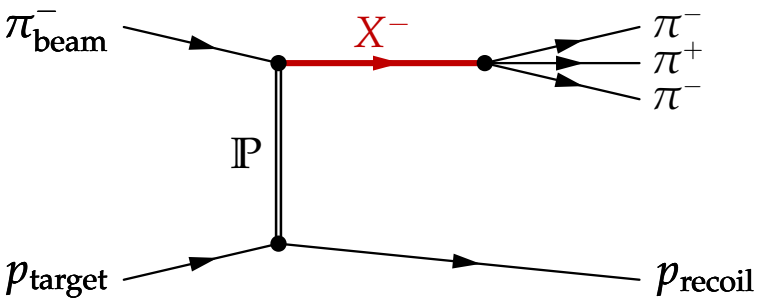

- exclusive measurement
- four-momentum transfer t' $< 0.5\,\text{GeV}$: Pomeron exchange $\mathbb{P}$
- rich structure in $\pi^-\pi^+\pi^-$ mass spectrum...
- ...and in the $\pi^+\pi^-$ subsystem

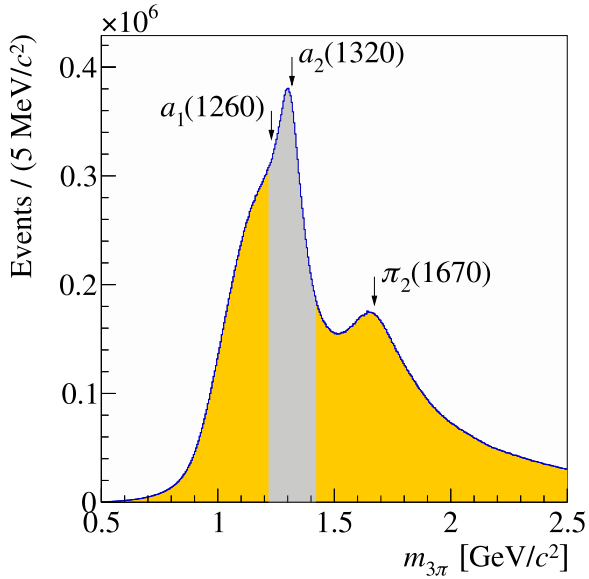

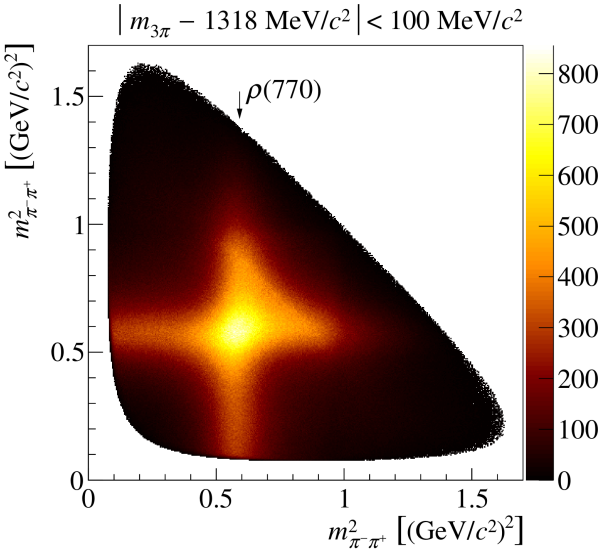

Diffractive 3π production

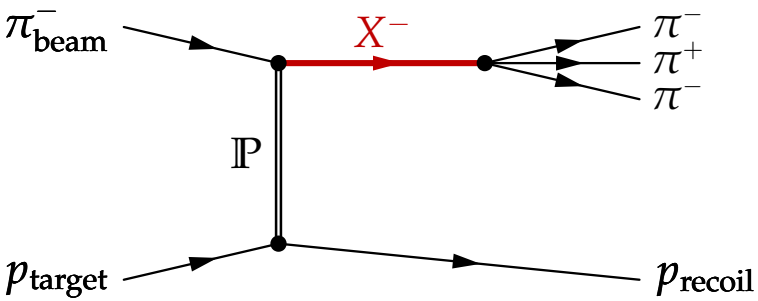

- exclusive measurement
- four-momentum transfer t' $< 0.5\,\text{GeV}$: Pomeron exchange $\mathbb{P}$
- rich structure in $\pi^-\pi^+\pi^-$ mass spectrum...
- ...and in the $\pi^+\pi^-$ subsystem
- Correlated with $m_{3\pi}$

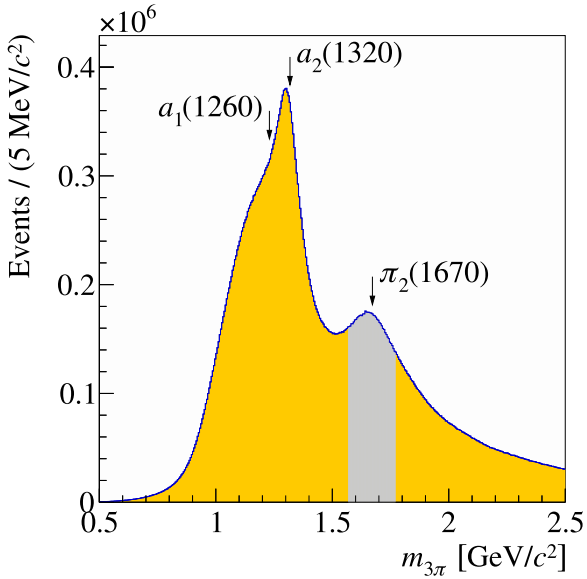

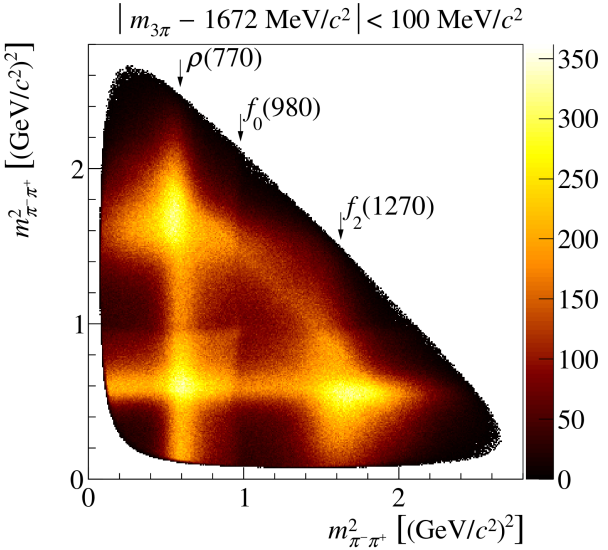

Diffractive 3π production

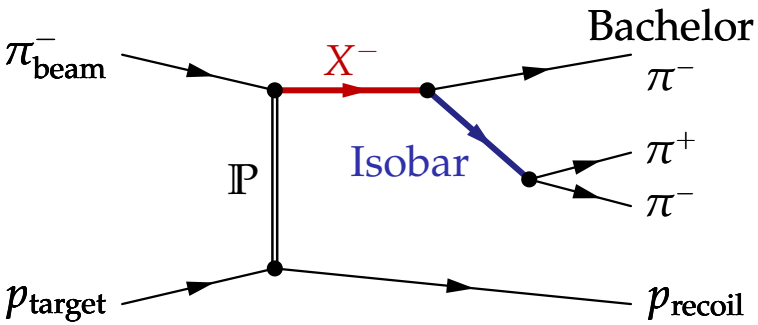

- exclusive measurement
- four-momentum transfer t' $< 0.5\,\text{GeV}$: Pomeron exchange $\mathbb{P}$
- rich structure in $\pi^-\pi^+\pi^-$ mass spectrum...
- ...and in the $\pi^+\pi^-$ subsystem
- Correlated with $m_{3\pi}$ $\rightarrow$ analysis with isobar model

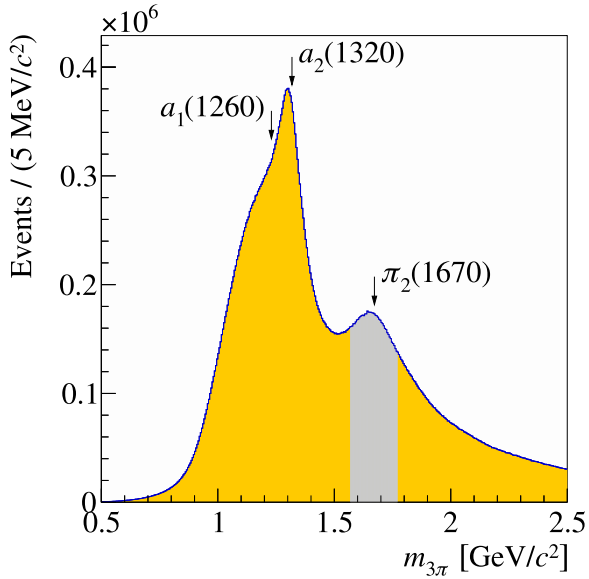

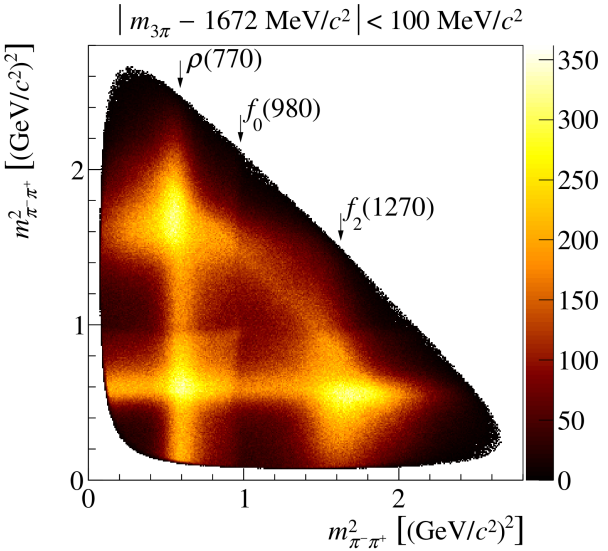

Analysis Procedure

(1) unbinned max-likelihood fit of partial waves to data in thin $m_{3\pi}$ slices and 11 t'bins

(2) fit dependence on $m_{3\pi}$ with Breit-Wigner reonance model (+BG)

Partial Waves

Intensity $\mathcal{I} = \left|\sum_{\text{waves}} T^{\text{wave}} \mathcal{A}^{\text{wave}}\right|^2$

$$J^{PC} M^{\varepsilon} \xi \pi L$$

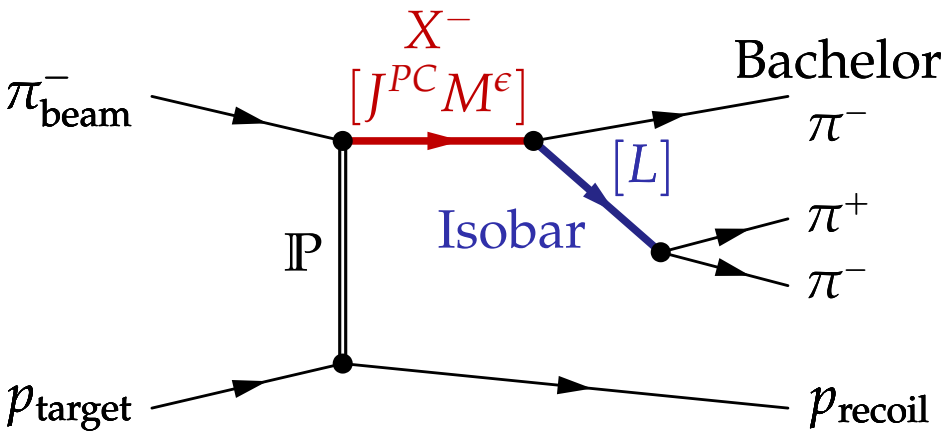

Partial Waves

Intensity $\mathcal{I} = \left|\sum_{\text{waves}} T^{\text{wave}} \mathcal{A}^{\text{wave}}\right|^2$

$$J^{PC} M^{\varepsilon} \xi \pi L$$

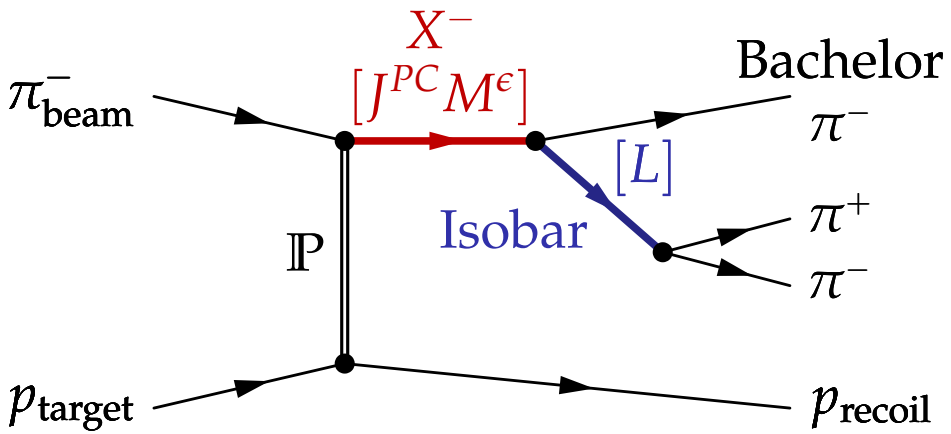

- J^{PC}: Spin, parity, charge-conjugation of X^-

Partial Waves

$$\text{Intensity } \mathcal{I} = \left|\sum_{\text{waves}} T^{\text{wave}} \mathcal{A}^{\text{wave}}\right|^2$$

$$J^{PC} M^{\varepsilon} \xi \pi L$$

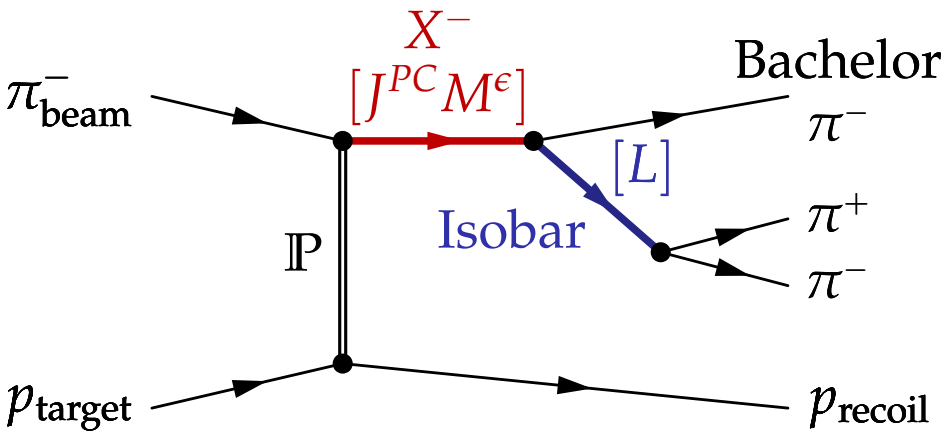

- J^{PC}: Spin, parity, charge-conjugation of X^-
- M^{ε}: Spin projection M of J on the incoming π^- direction (X^- rest system) and naturality ε of the exchange particle

Partial Waves

$$\text{Intensity } \mathcal{I} = \left|\sum_{\text{waves}} T^{\text{wave}} \mathcal{A}^{\text{wave}}\right|^2$$

$$J^{PC} M^{\varepsilon} \xi \pi L$$

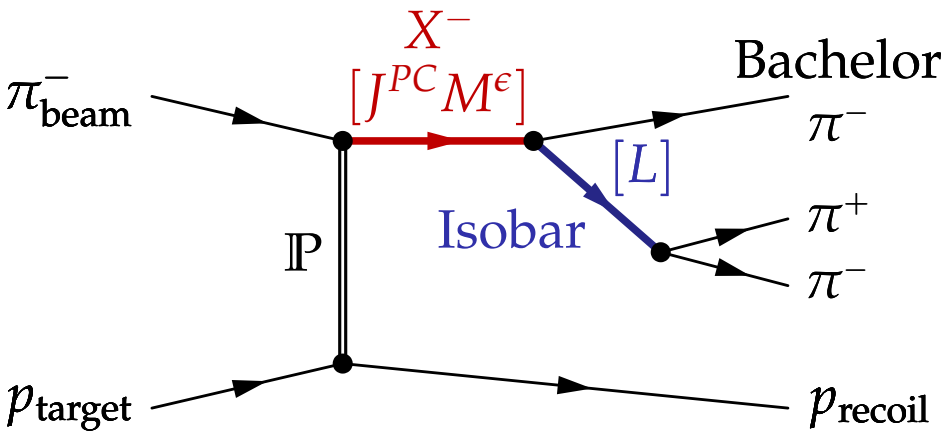

- J^{PC}: Spin, parity, charge-conjugation of X^-
- M^{ε}: Spin projection M of J on the incoming π^- direction (X^- rest system) and naturality ε of the exchange particle
- ξ: $\pi\pi$-isobar, e.g. $\rho(770)$, $f_2(1270)$

Partial Waves

Intensity $\mathcal{I} = \left|\sum_{\text{waves}} T^{\text{wave}} \mathcal{A}^{\text{wave}}\right|^2$

$$J^{PC} M^{\varepsilon} \xi \pi L$$

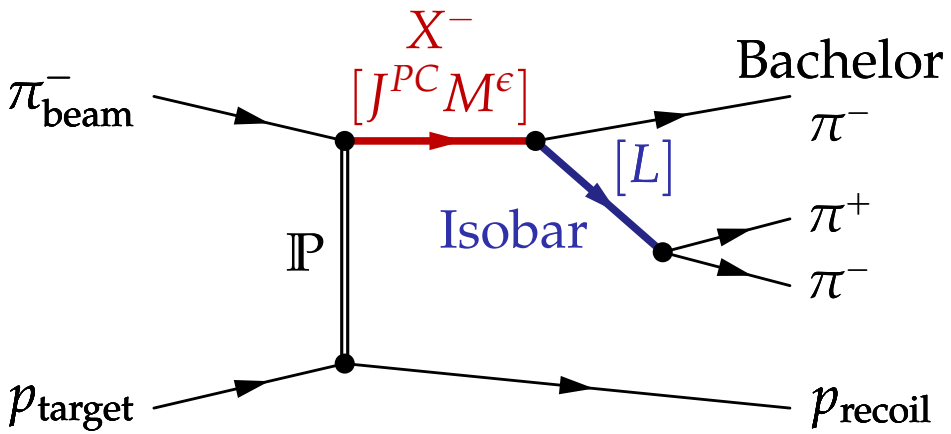

- J^{PC}: Spin, parity, charge-conjugation of X^-
- M^{ε}: Spin projection M of J on the incoming π^- direction (X^-rest system) and naturality ε of the exchange particle
- ξ: $\pi\pi$-isobar, e.g. $\rho(770)$, $f_2(1270)$
- π: bachelor π^-

Partial Waves

$$\text{Intensity } \mathcal{I} = \left|\sum_{\text{waves}} T^{\text{wave}} \mathcal{A}^{\text{wave}}\right|^2$$

$$J^{PC} M^{\varepsilon} \xi \pi L$$

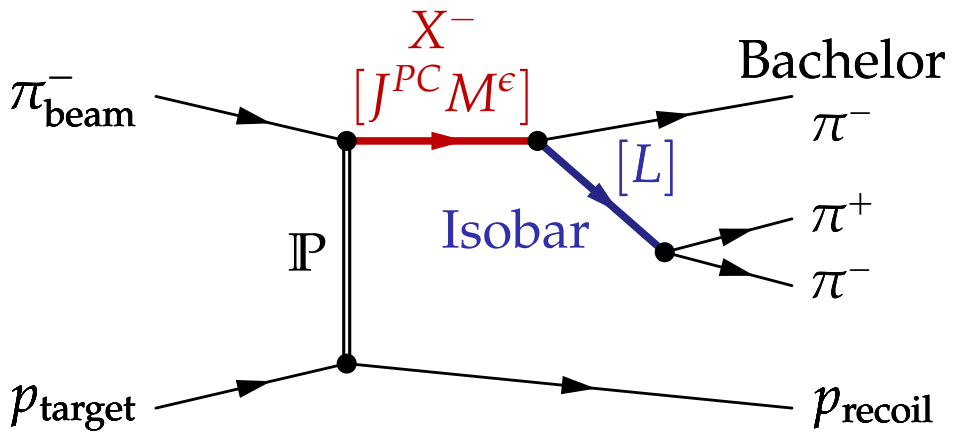

- J^{PC}: Spin, parity, charge-conjugation of X^-
- M^{ε}: Spin projection M of J on the incoming π^- direction (X^- rest system) and naturality ε of the exchange particle
- ξ: $\pi\pi$-isobar, e.g. $\rho(770)$, $f_2(1270)$
- π: bachelor π^-
- L: Orbital angular momentum between ξ and π

88 waves needed to describe the data (“hand-selected”)
interference terms $\rightarrow$ get (relative) phases

Step 1: Partial-Wave Analysis

Selected Waves (1 of 88) in two of the 11 independent t' bins

Low t'

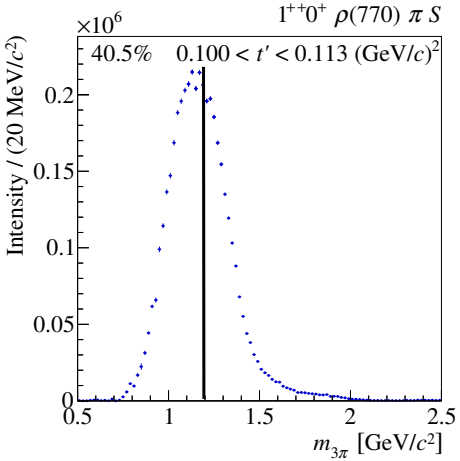

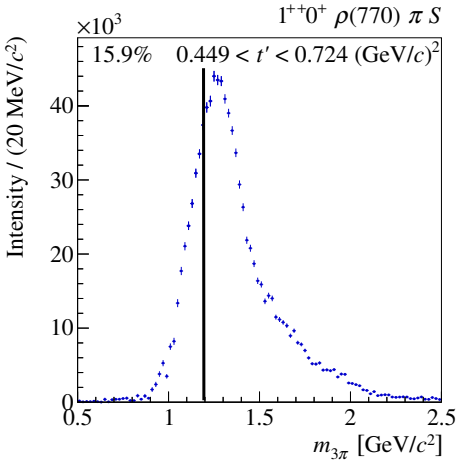

High t'

Step 1: Partial-Wave Analysis

Selected Waves (2 of 88) in two of the 11 independent t' bins

Low t'

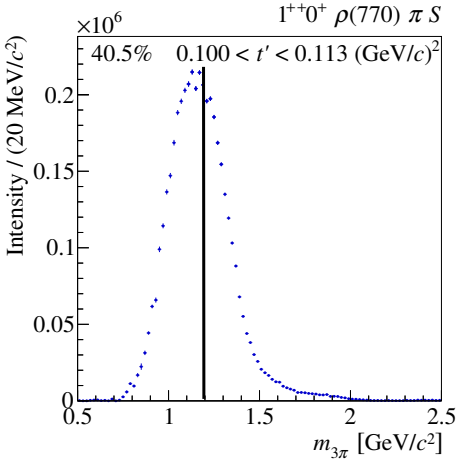

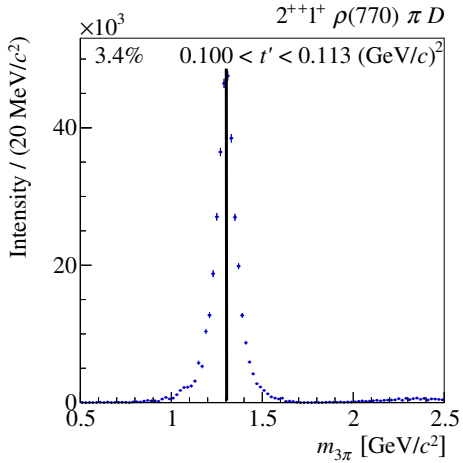

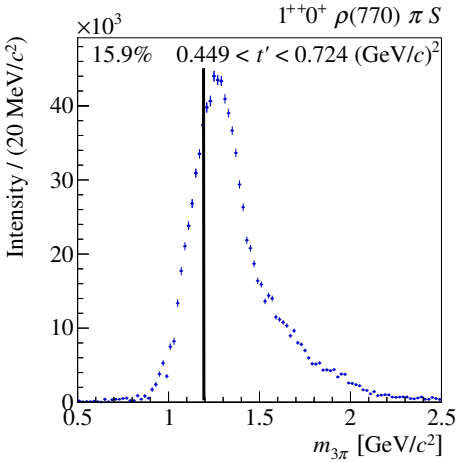

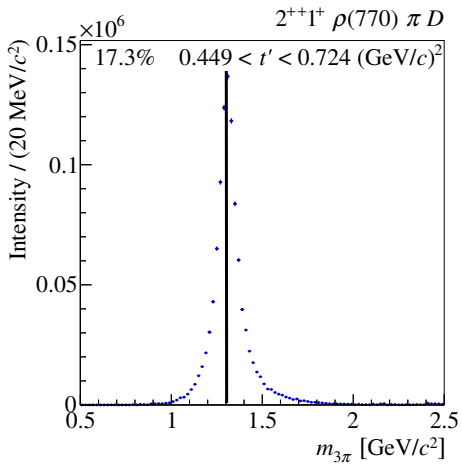

High t'

Step 1: Partial-Wave Analysis

Selected Waves (3 of 88) in two of the 11 independent t' bins

Low t'

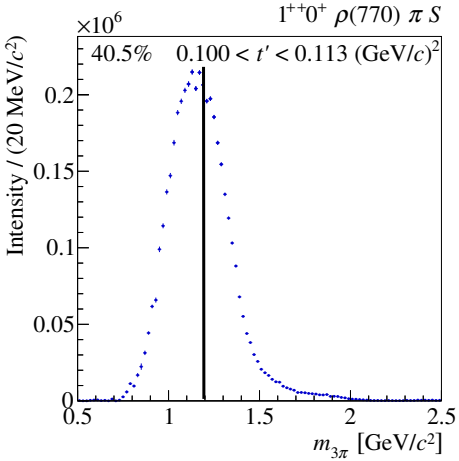

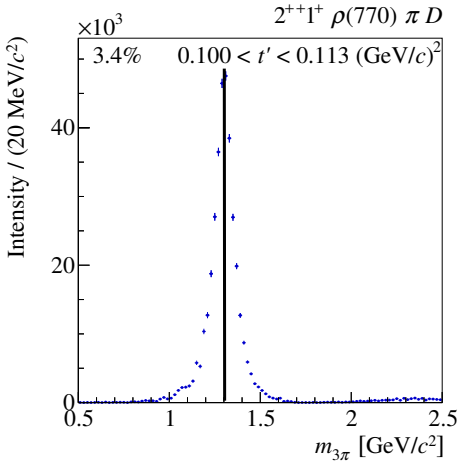

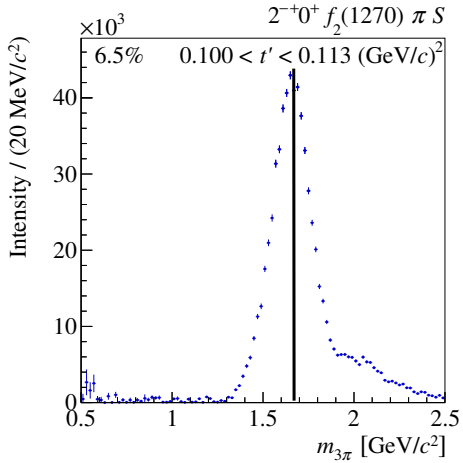

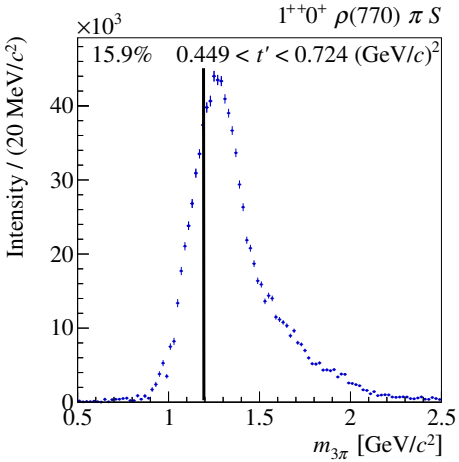

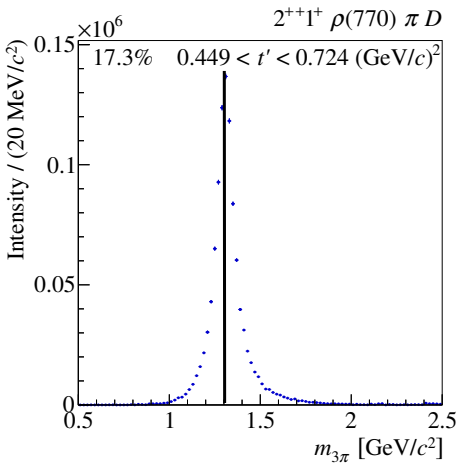

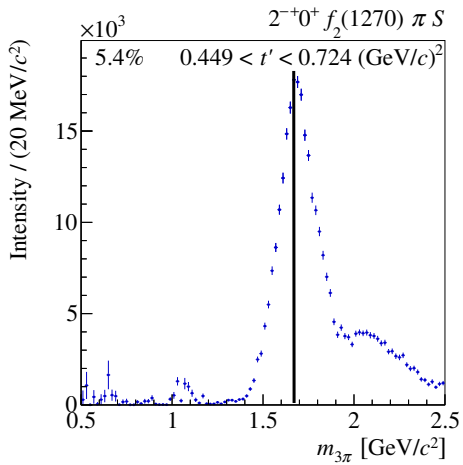

High t'

Step 1: Partial-Wave Analysis

Selected Waves (4 of 88) in two of the 11 independent t' bins

Low t'

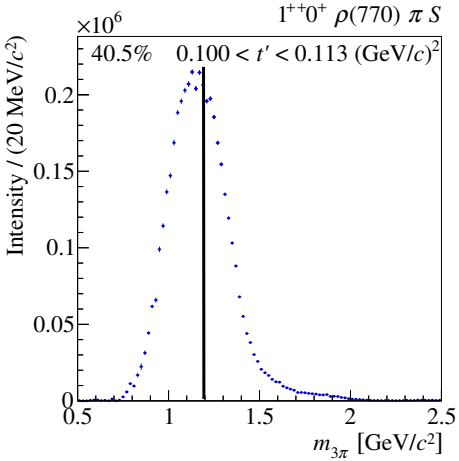

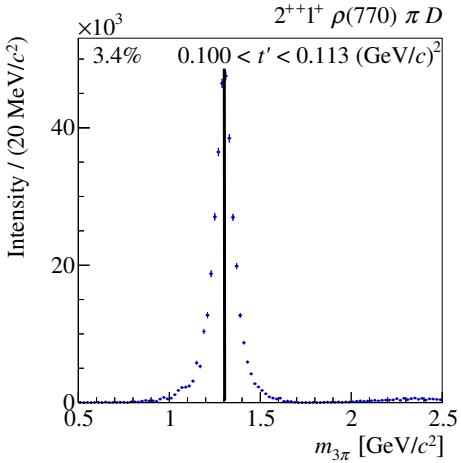

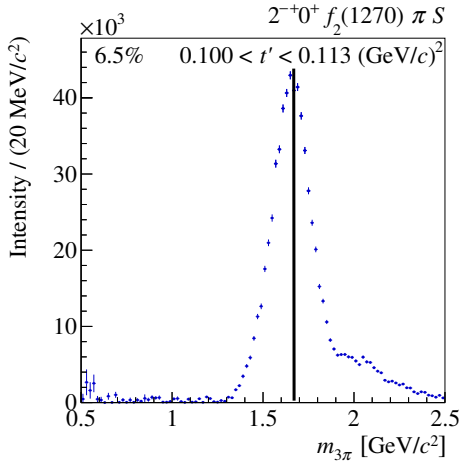

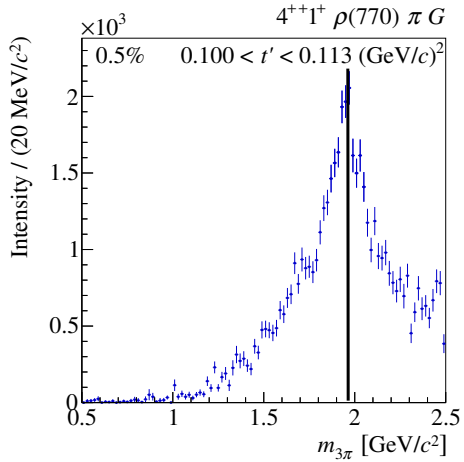

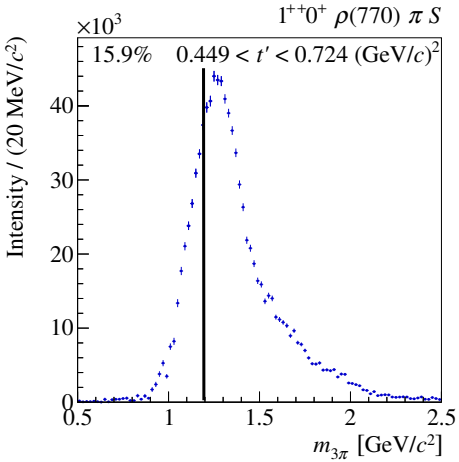

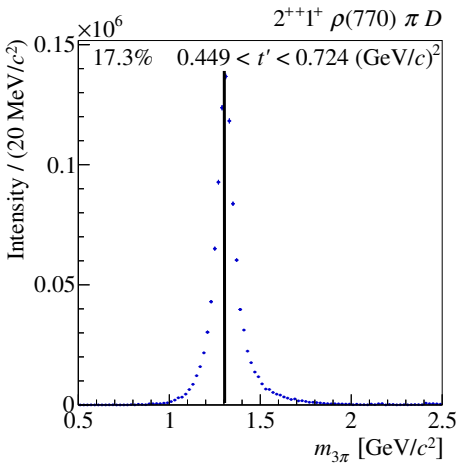

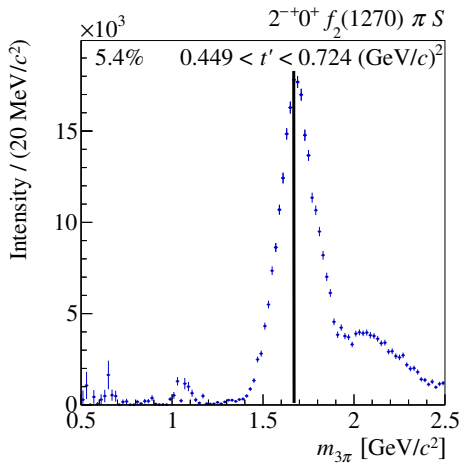

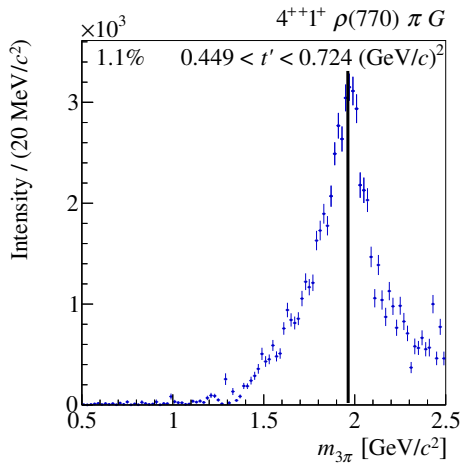

High t'

Step 2: Resonance model fit

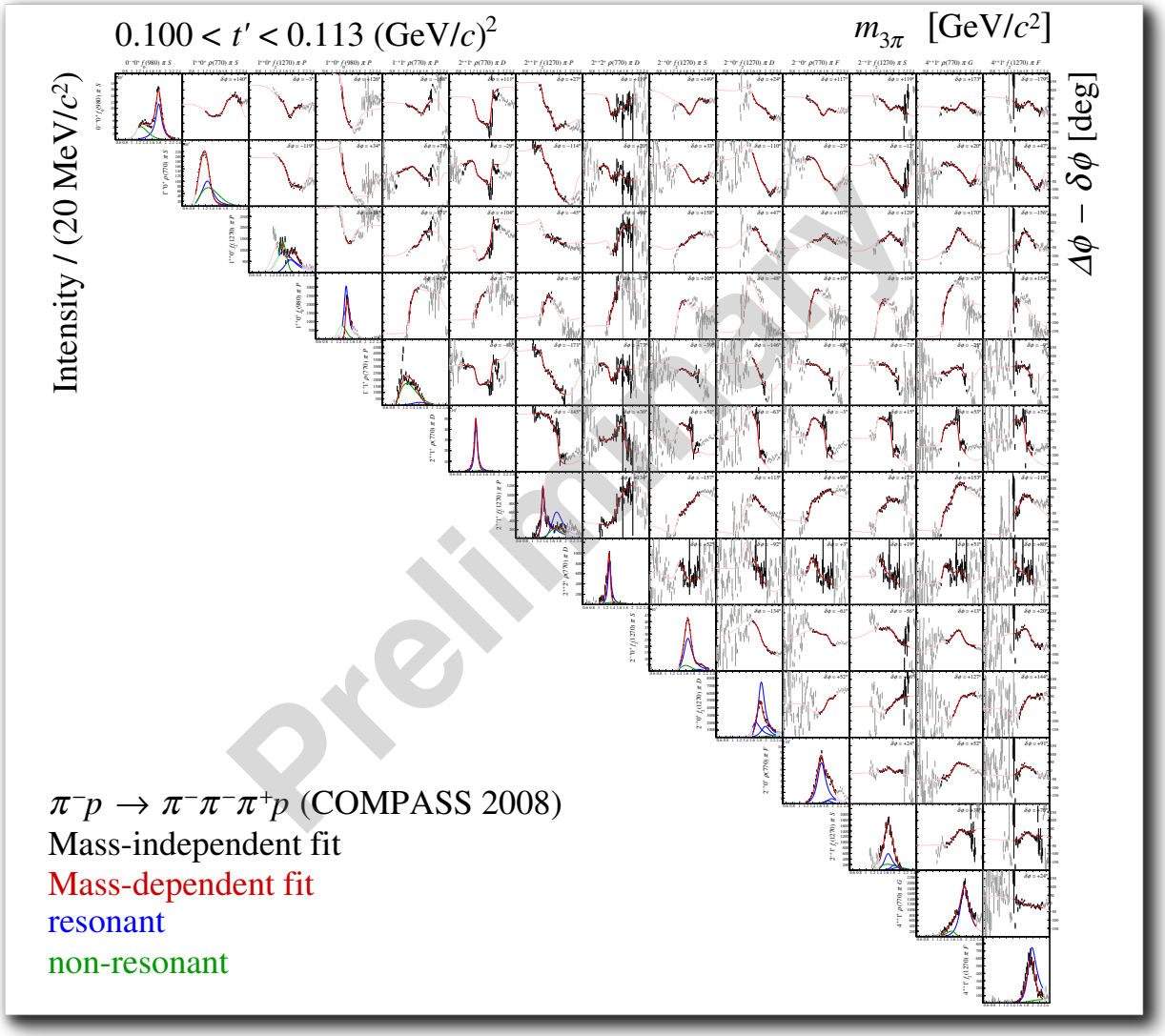

Step 2: Resonance model fit

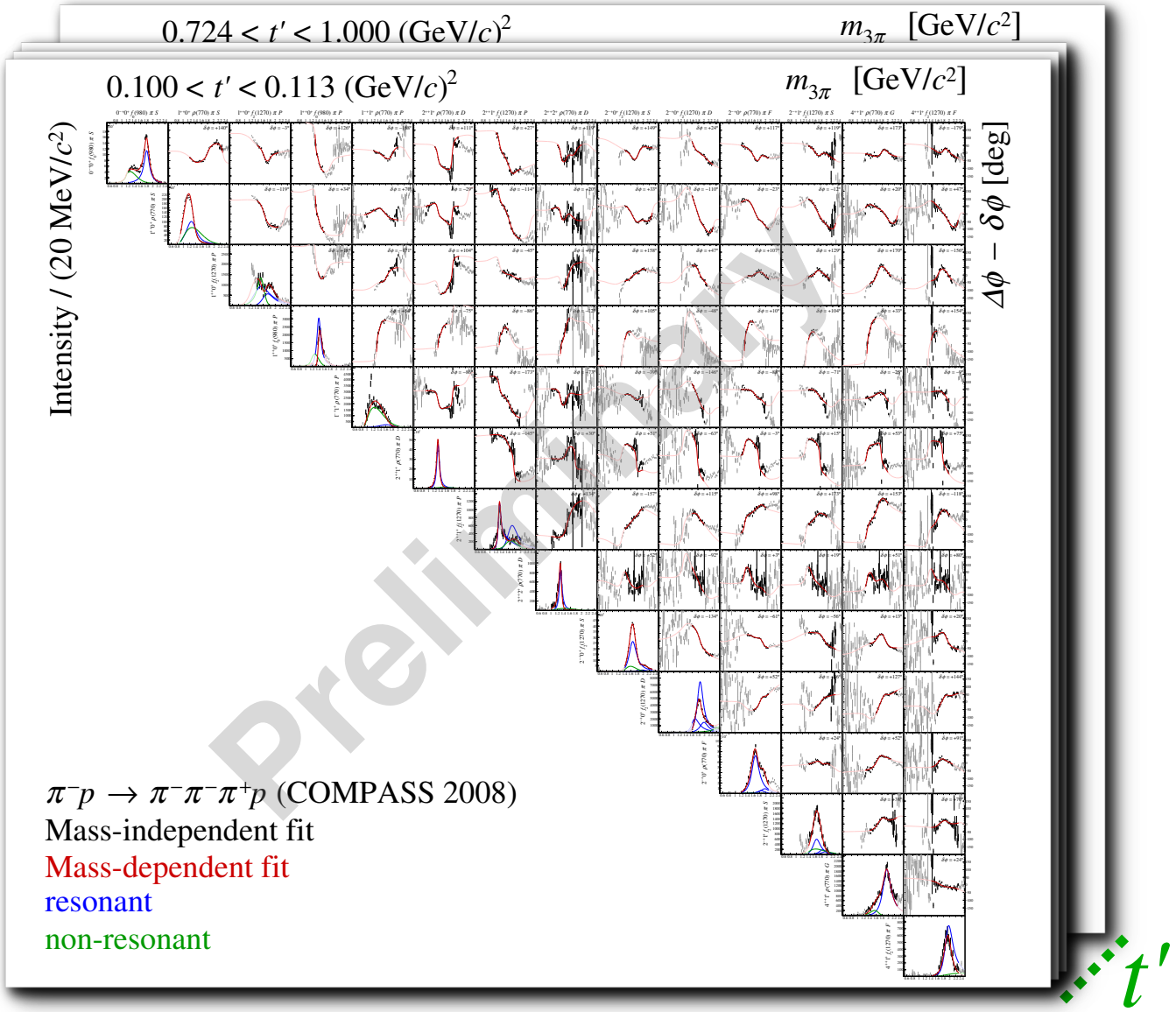

$\pi^- p \to \pi^-\pi^-\pi^+ p$ (COMPASS 2008)
Mass-independent fit
Mass-dependent fit
resonant
non-resonant

$\times 11$ bins in t'

$J^{PC} = 2^{++}$ sector

$J^{PC} = 2^{++}$ subsection

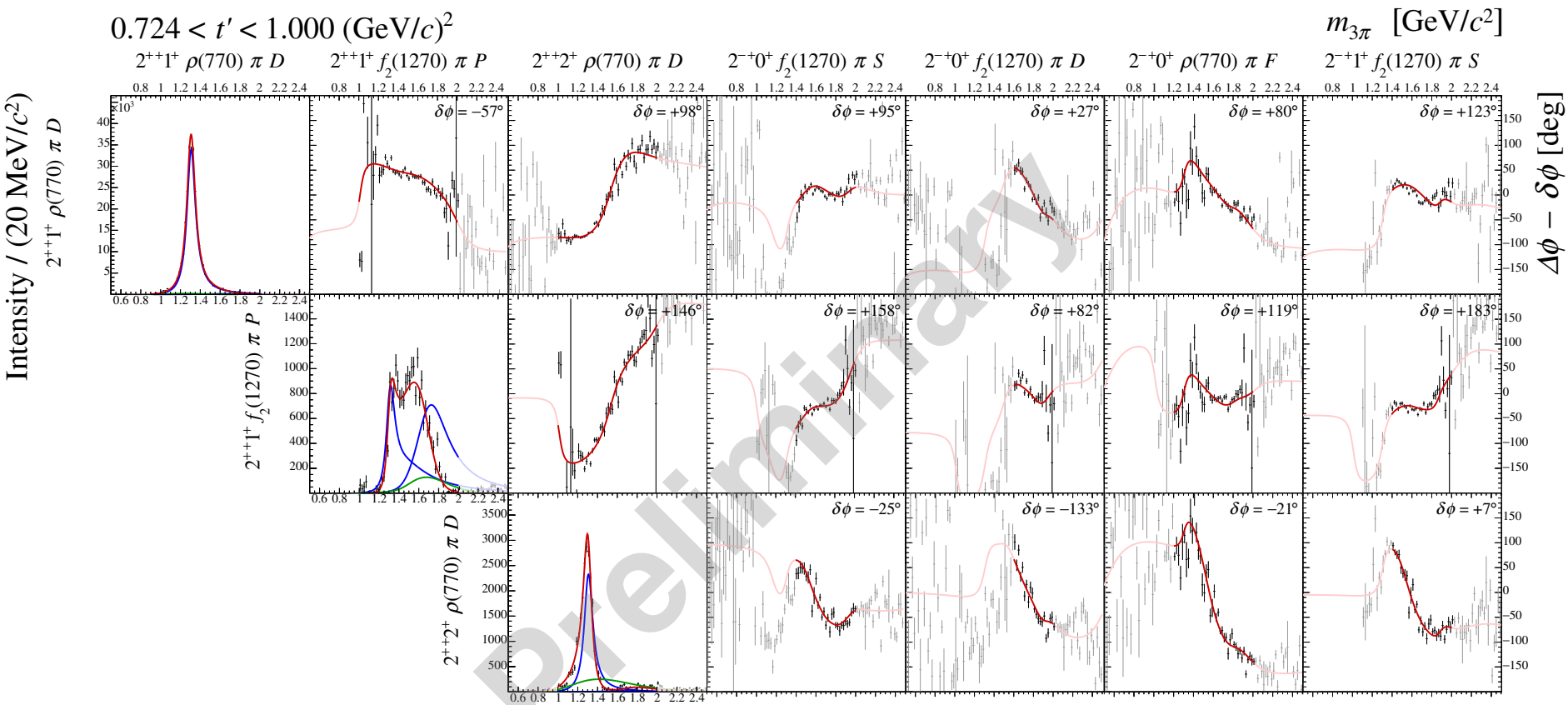

$\pi^- p \to \pi^-\pi^-\pi^+ p$ (COMPASS 2008)

Mass-independent fit

Mass-dependent fit

resonant

non-resonant

$J^{PC} = 2^{++}$ subsection

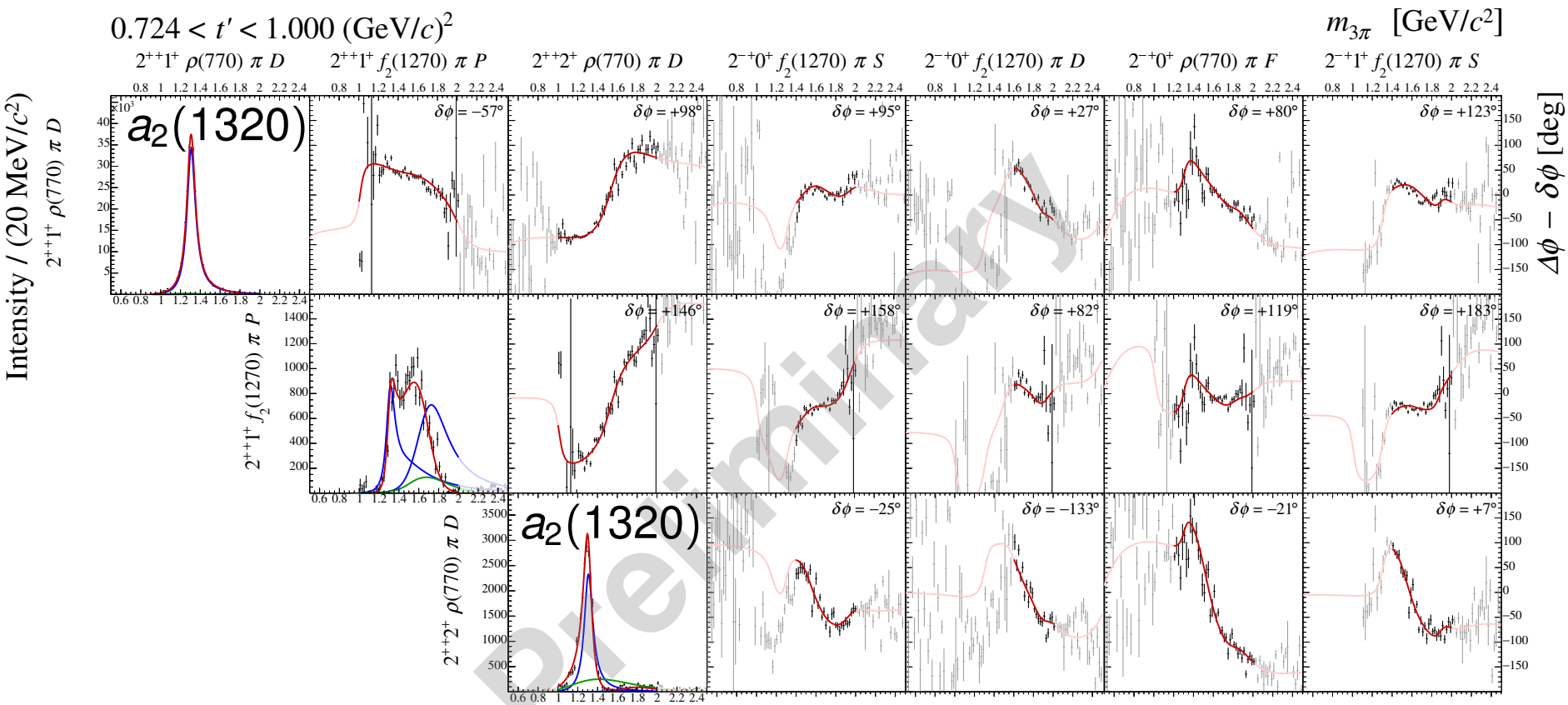

$\pi^- p \to \pi^-\pi^-\pi^+ p$ (COMPASS 2008)

Mass-independent fit

Mass-dependent fit

resonant

non-resonant

$J^{PC} = 2^{++}$ subsection

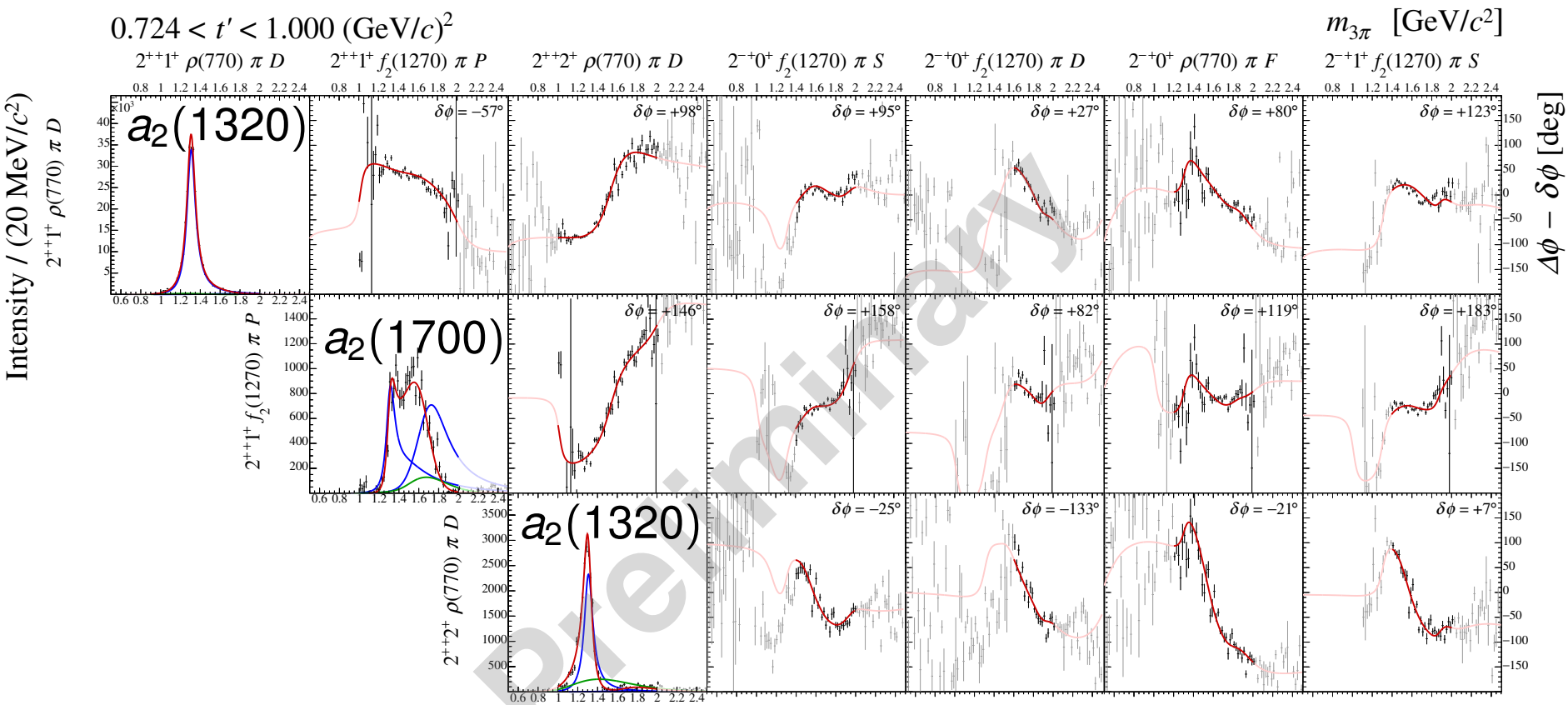

$\pi^- p \to \pi^-\pi^-\pi^+ p$ (COMPASS 2008)

Mass-independent fit

Mass-dependent fit

resonant

non-resonant

$J^{PC} = 4^{++}$ sector

$J^{PC} = 4^{++}$ subsection

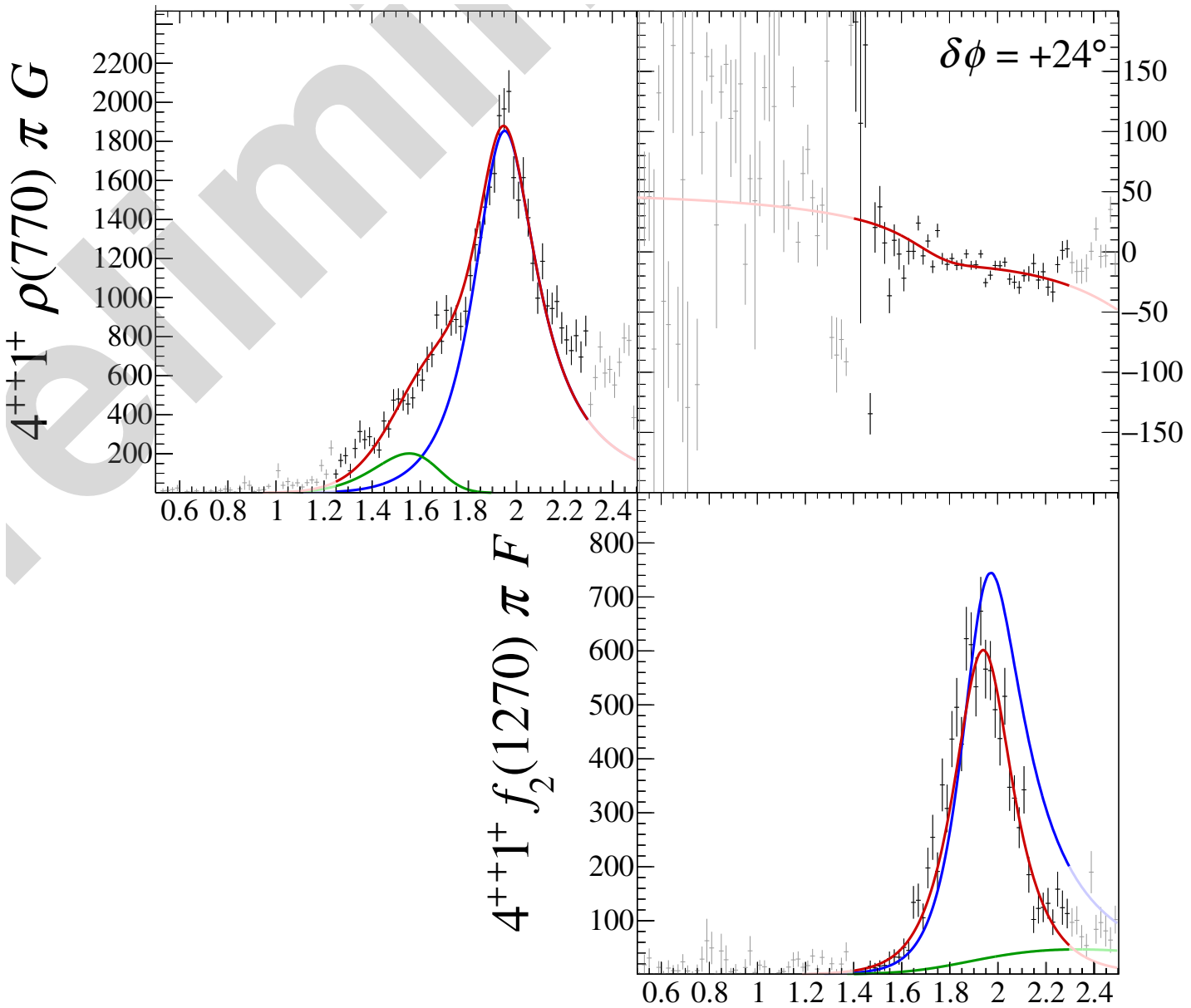

$J^{PC} = 4^{++}$ subsection

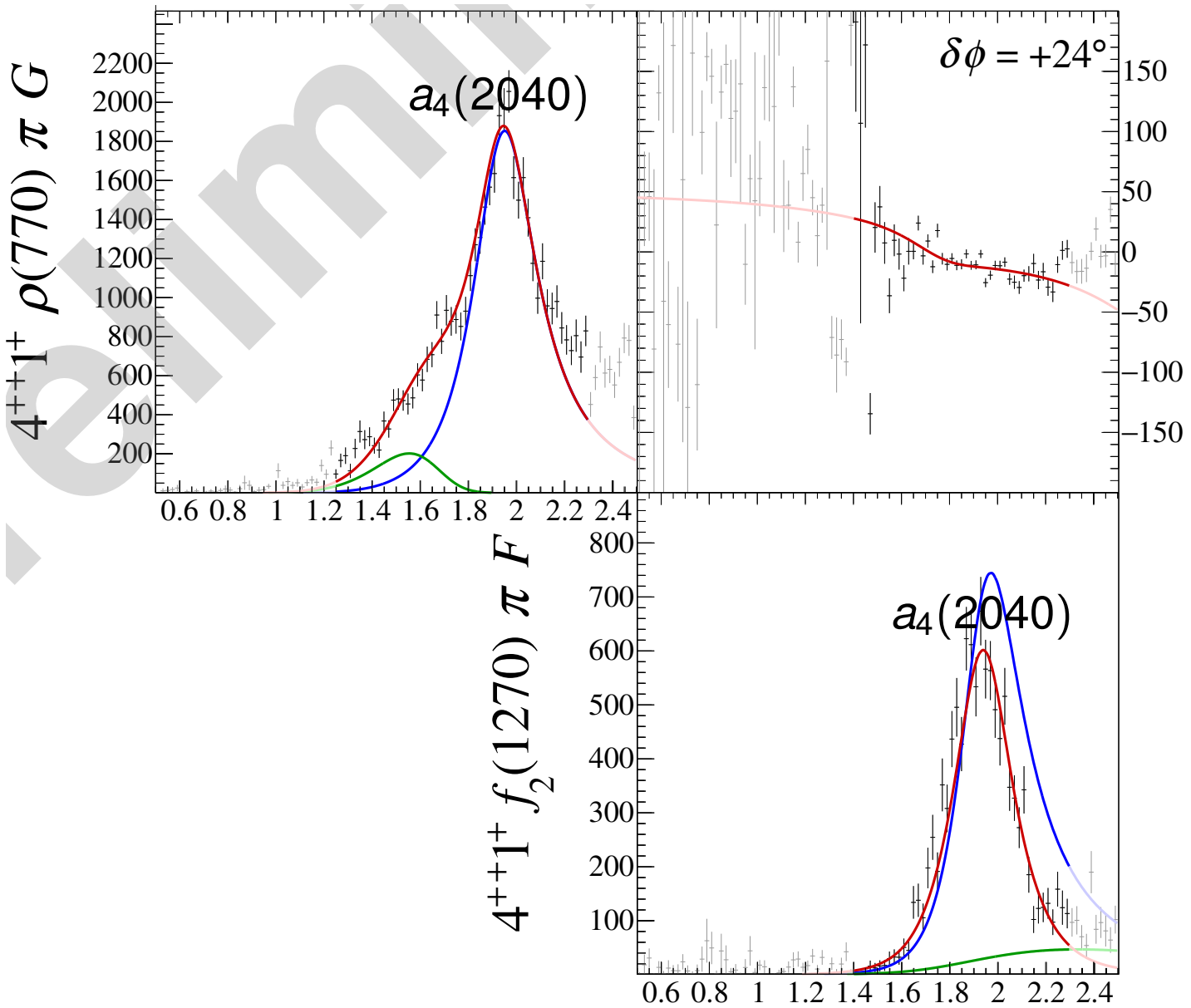

$J^{PC} = 1^{++}$ sector

$J^{PC} = 1^{++}$ subsection

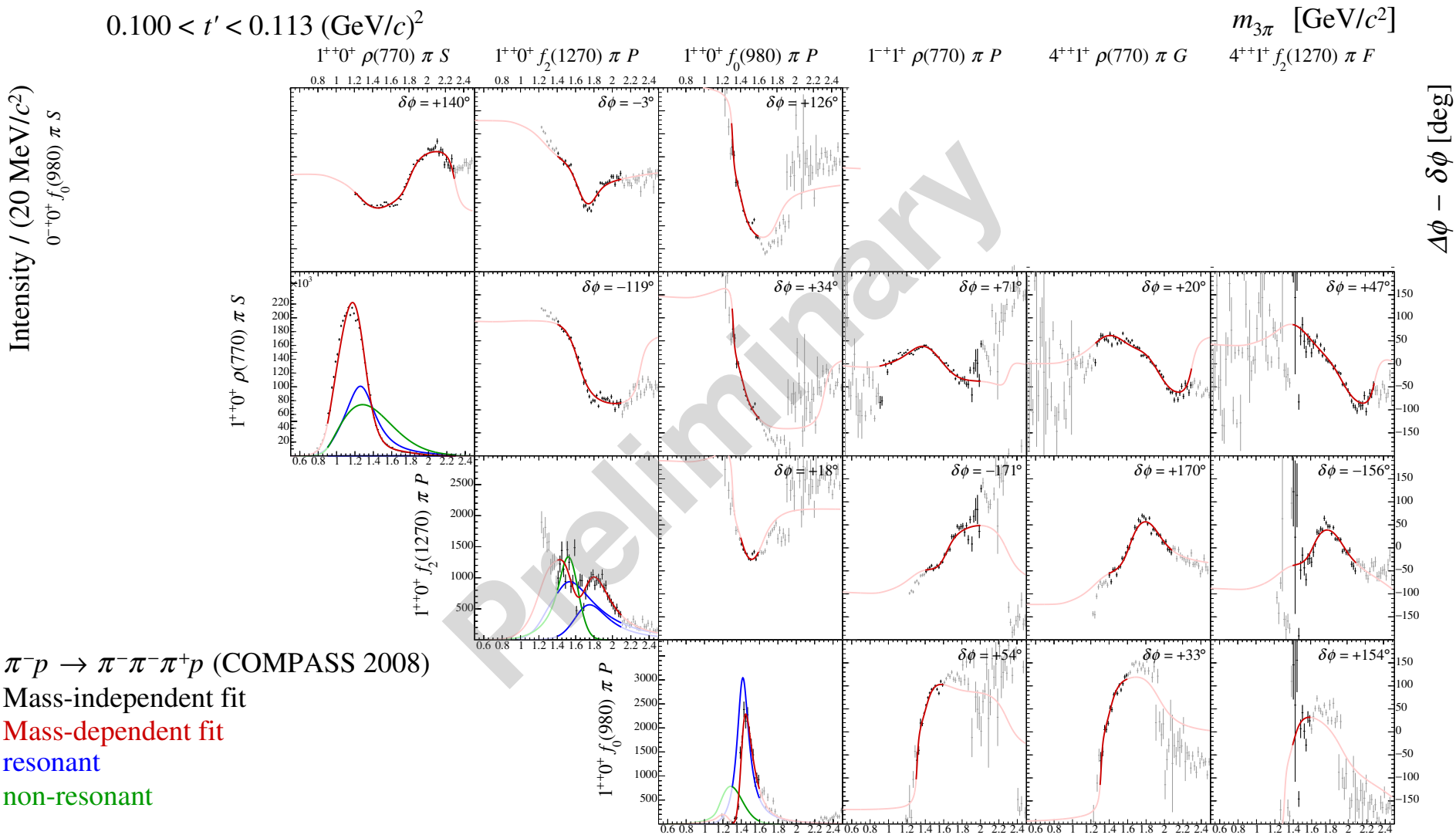

$\pi^- p \to \pi^-\pi^-\pi^+ p$ (COMPASS 2008)

Mass-independent fit

Mass-dependent fit

resonant

non-resonant

$J^{PC} = 1^{++}$ subsection

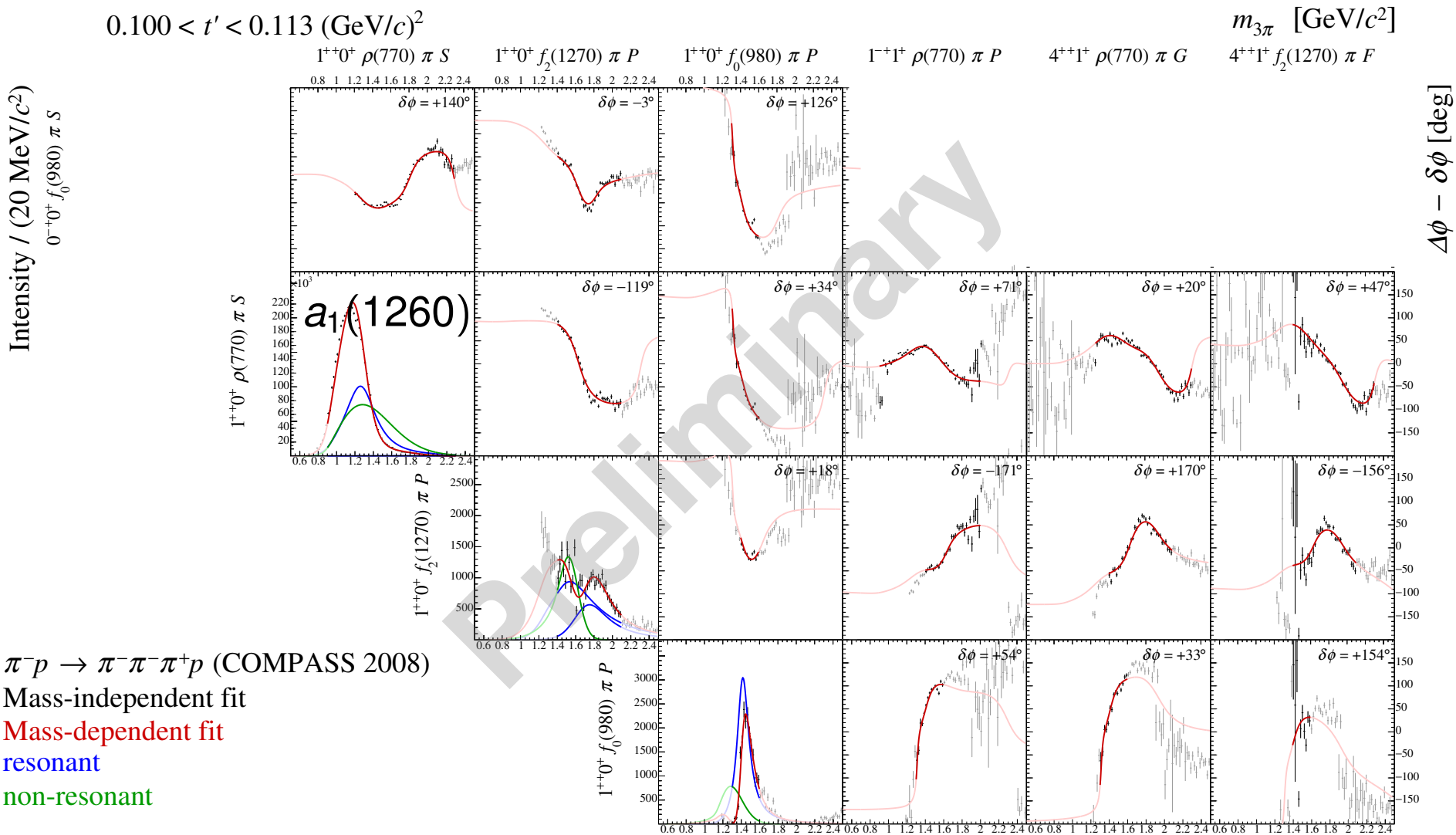

$\pi^- p \to \pi^-\pi^-\pi^+ p$ (COMPASS 2008)

Mass-independent fit

Mass-dependent fit

resonant

non-resonant

$J^{PC} = 1^{++}$ subsection

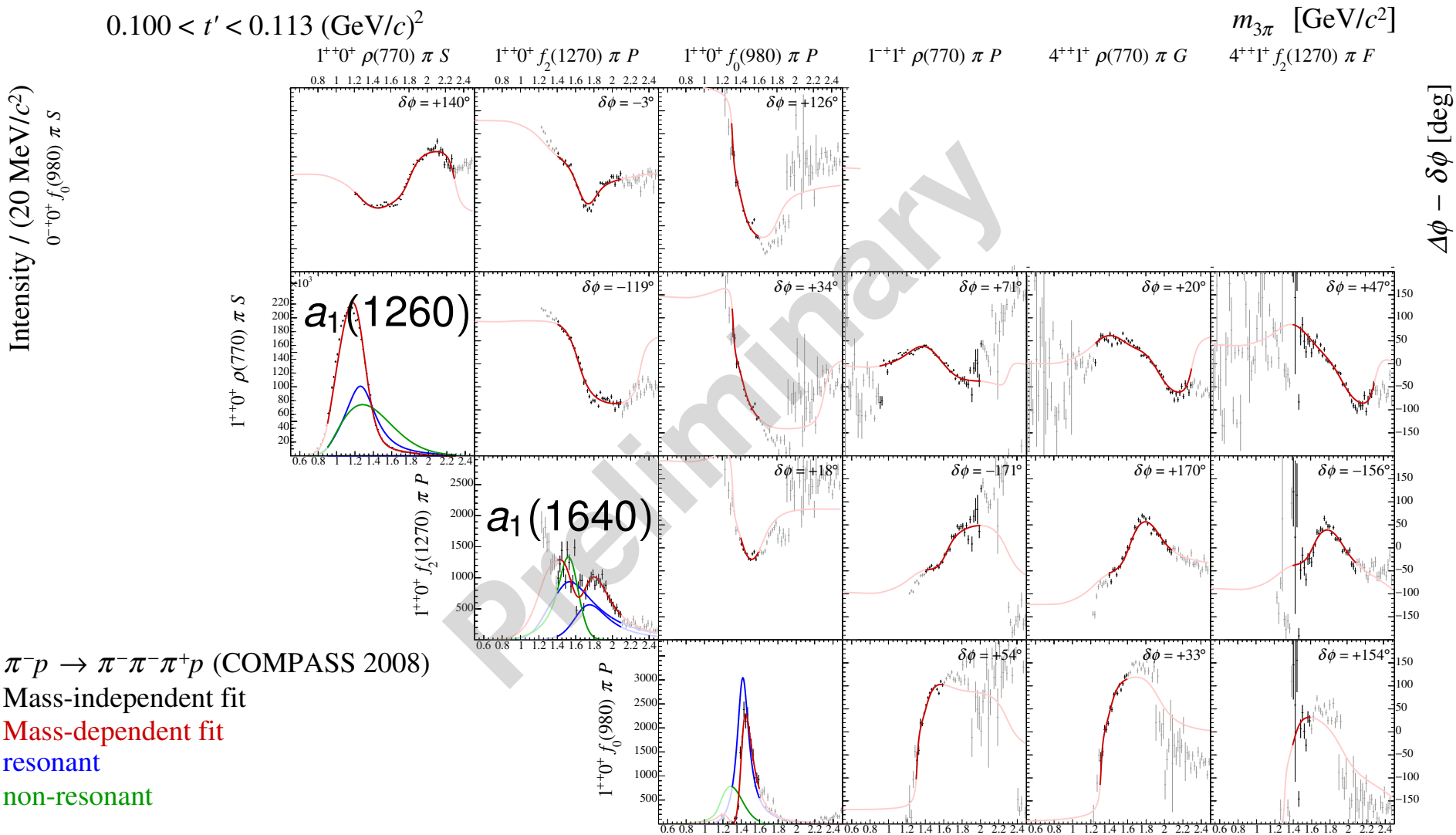

$\pi^- p \to \pi^-\pi^-\pi^+ p$ (COMPASS 2008)

Mass-independent fit

Mass-dependent fit

resonant

non-resonant

$J^{PC} = 1^{++}$ subsection

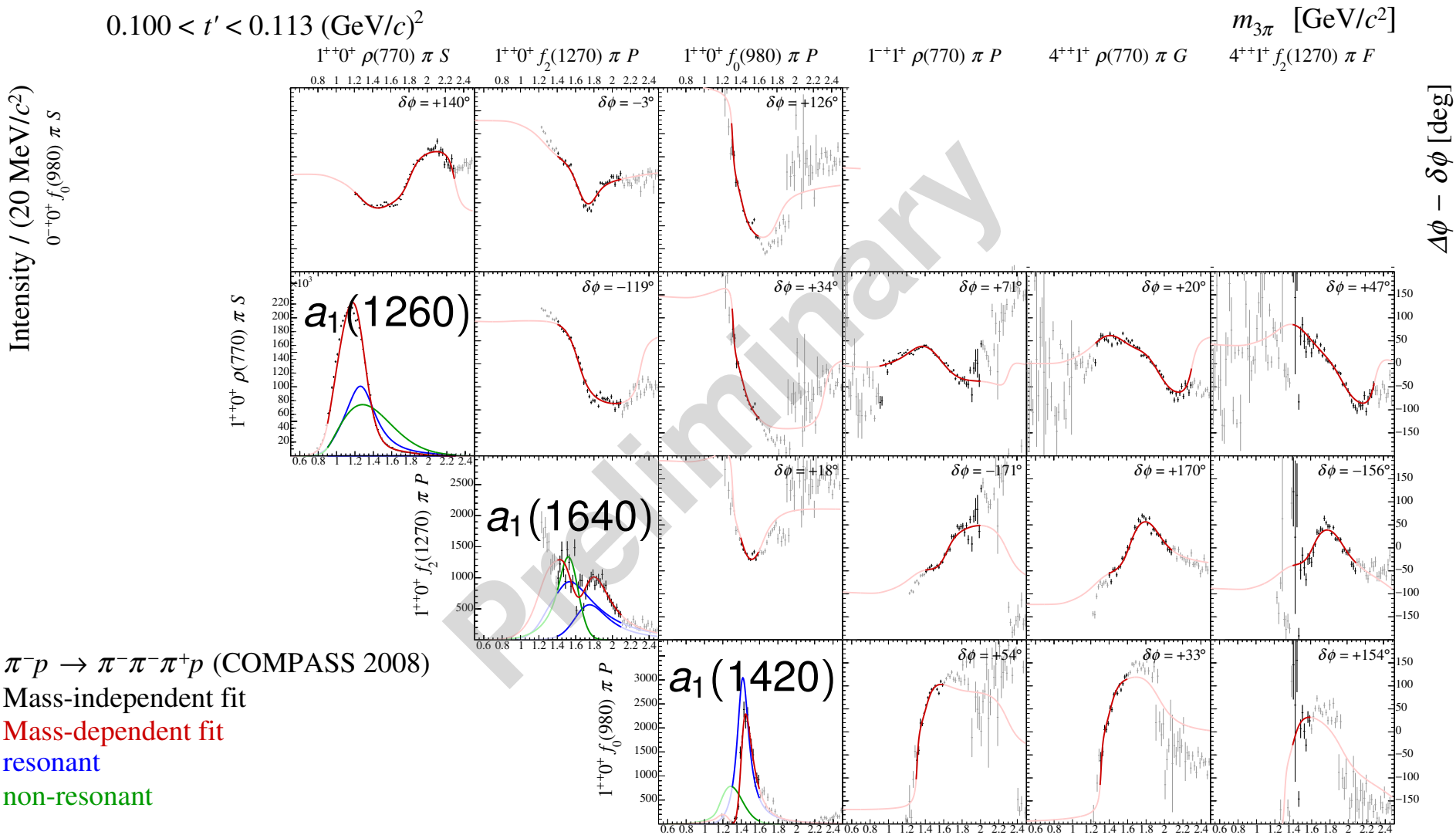

$\pi^- p \to \pi^-\pi^-\pi^+ p$ (COMPASS 2008)

Mass-independent fit

Mass-dependent fit

resonant

non-resonant

- resonance parameters do not depend on production mechanism

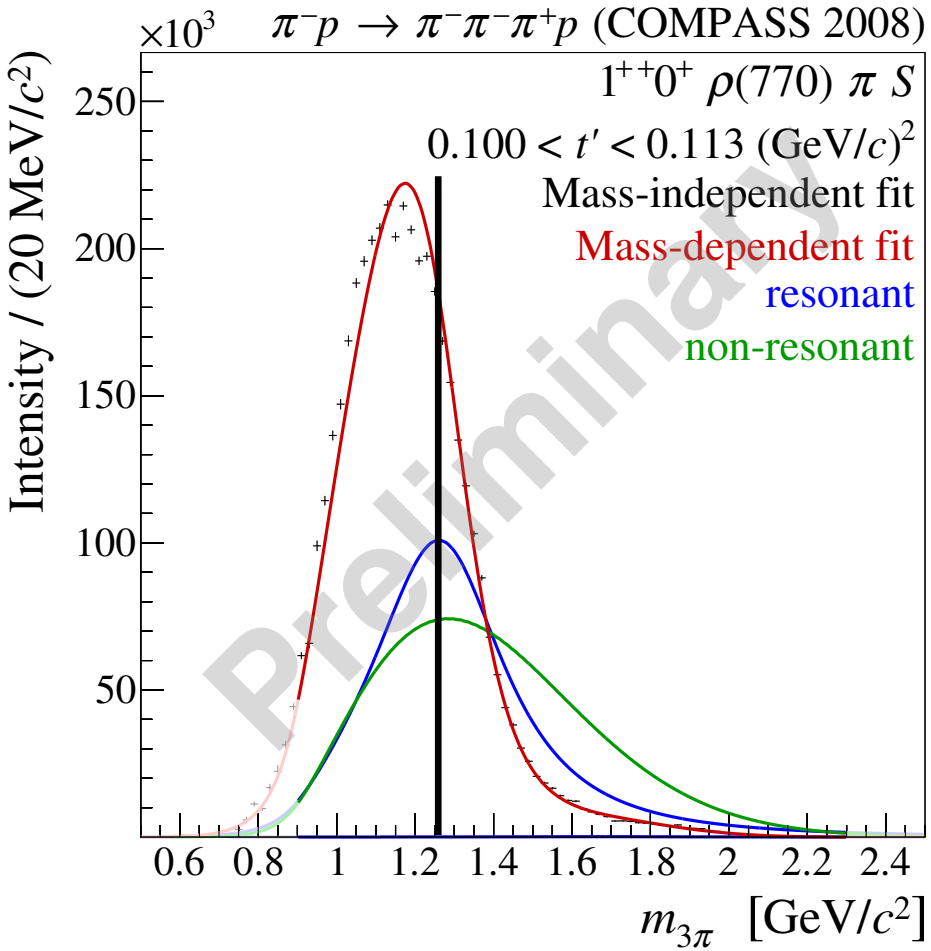

- resonance parameters do not depend on production mechanism
- couplings and non-resonant parts may vary with t'

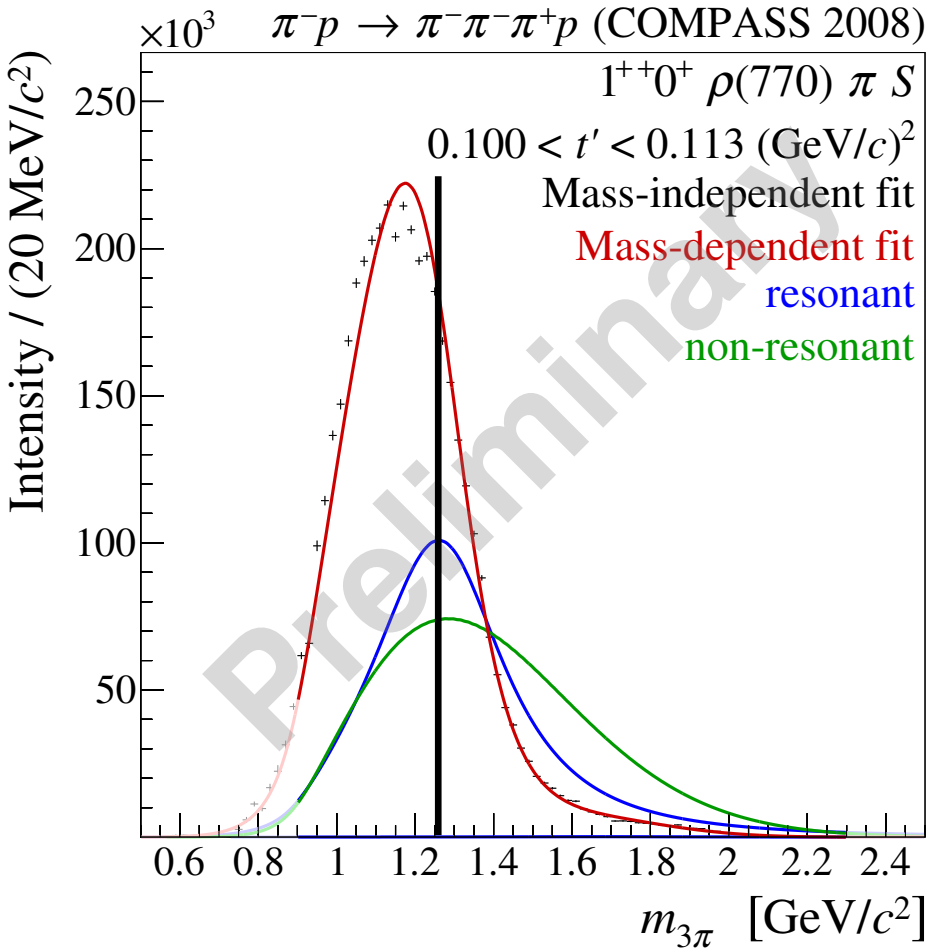

- resonance parameters do not depend on production mechanism
- couplings and non-resonant parts may vary with t'
- t'-resolved analysis: better disentanglement of resonant and non-resonant parts

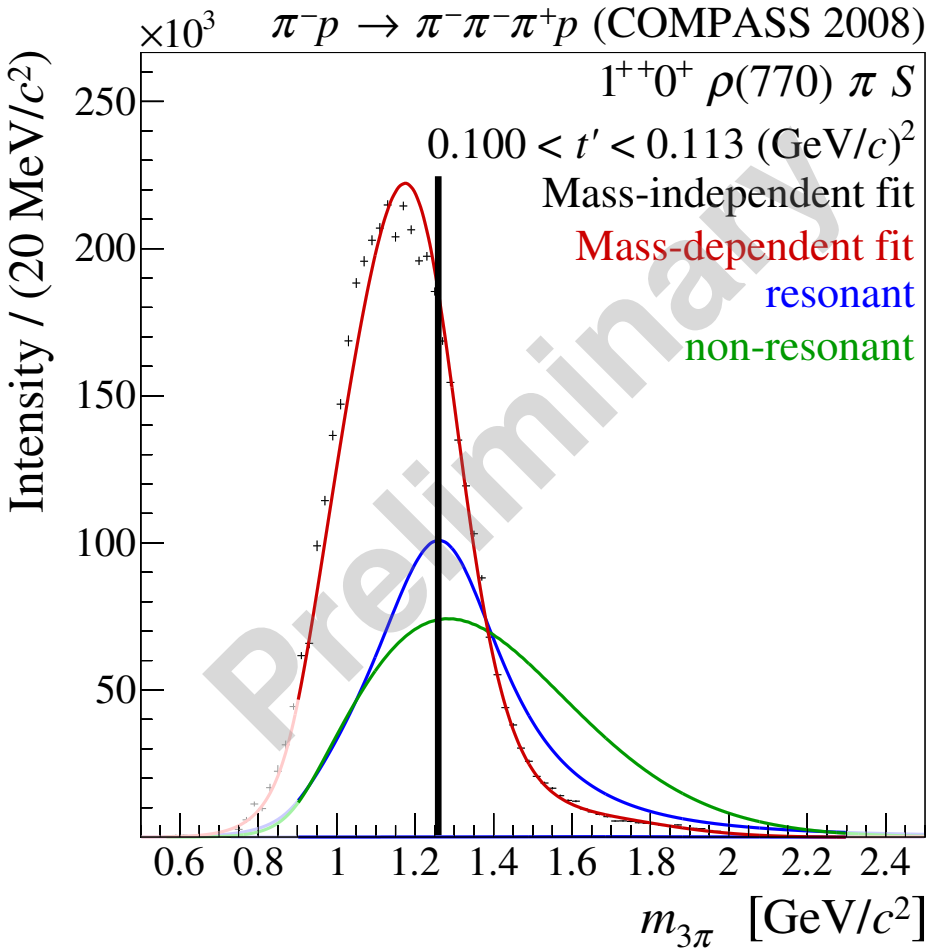

- resonance parameters do not depend on production mechanism
- couplings and non-resonant parts may vary with t'
- t'-resolved analysis: better disentanglement of resonant and non-resonant parts

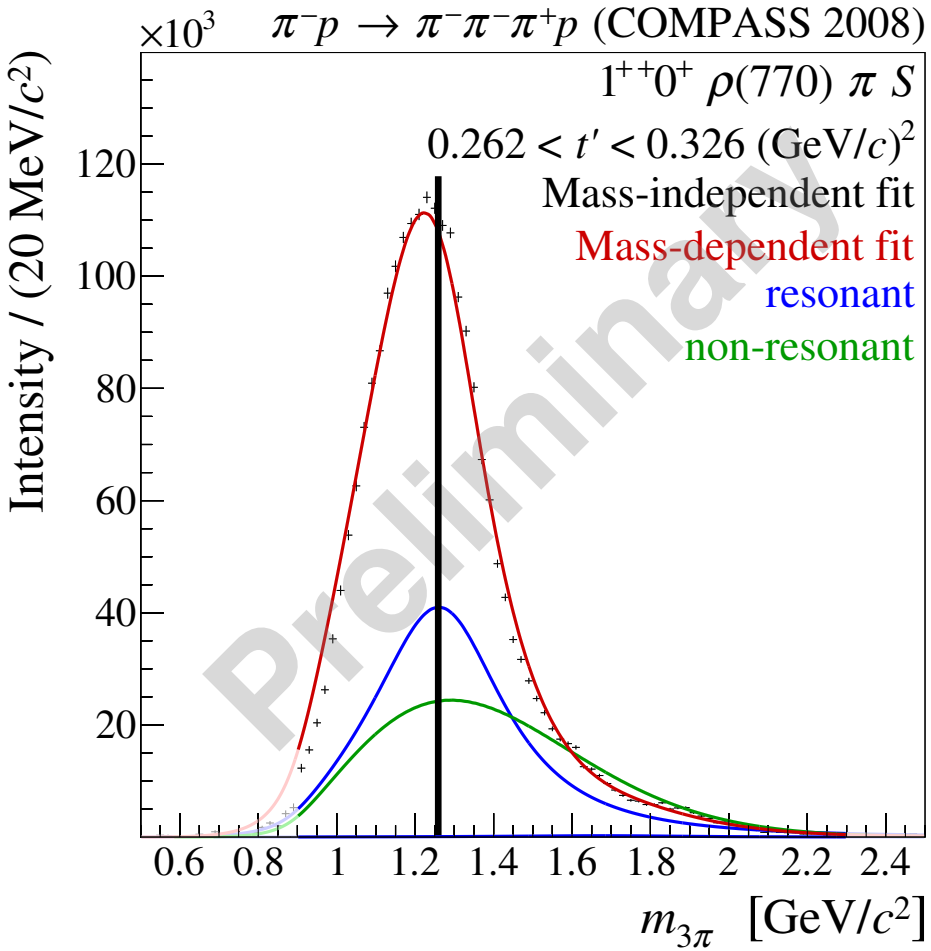

- resonance parameters do not depend on production mechanism
- couplings and non-resonant parts may vary with t'
- t'-resolved analysis: better disentanglement of resonant and non-resonant parts

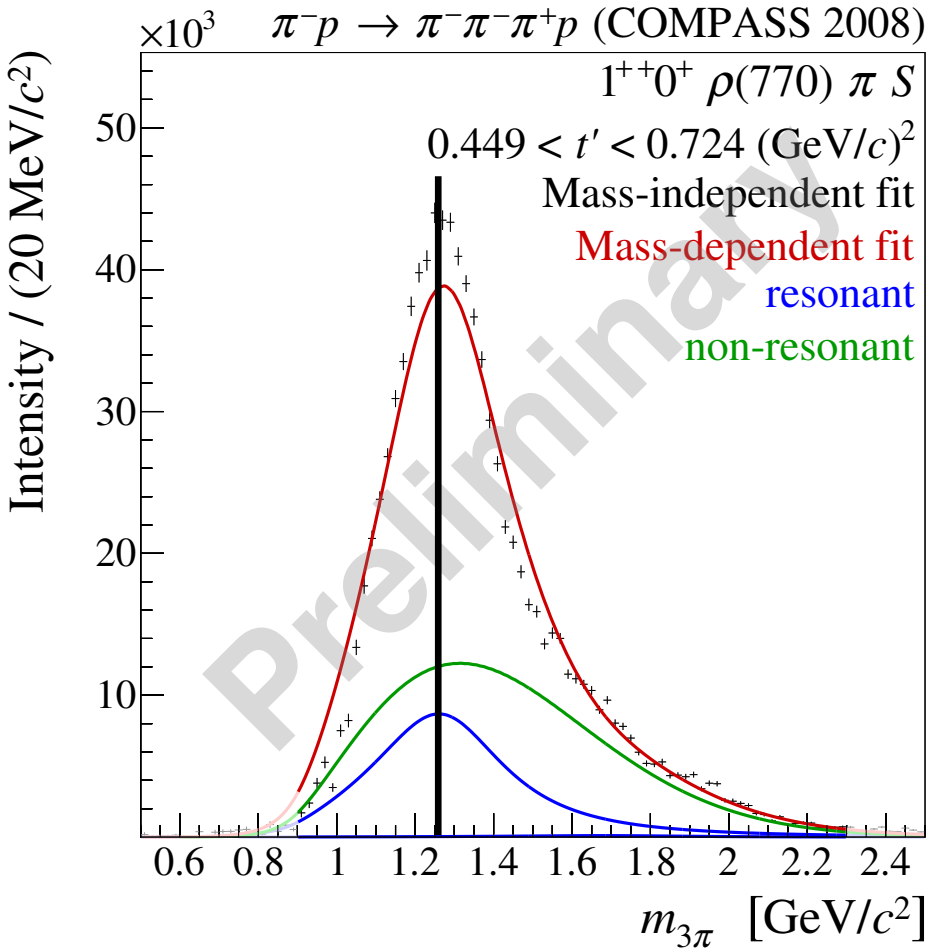

$a_1(1260)$

- resonance parameters do not depend on production mechanism
- couplings and non-resonant parts may vary with t'
- t'-resolved analysis: better disentanglement of resonant and non-resonant parts

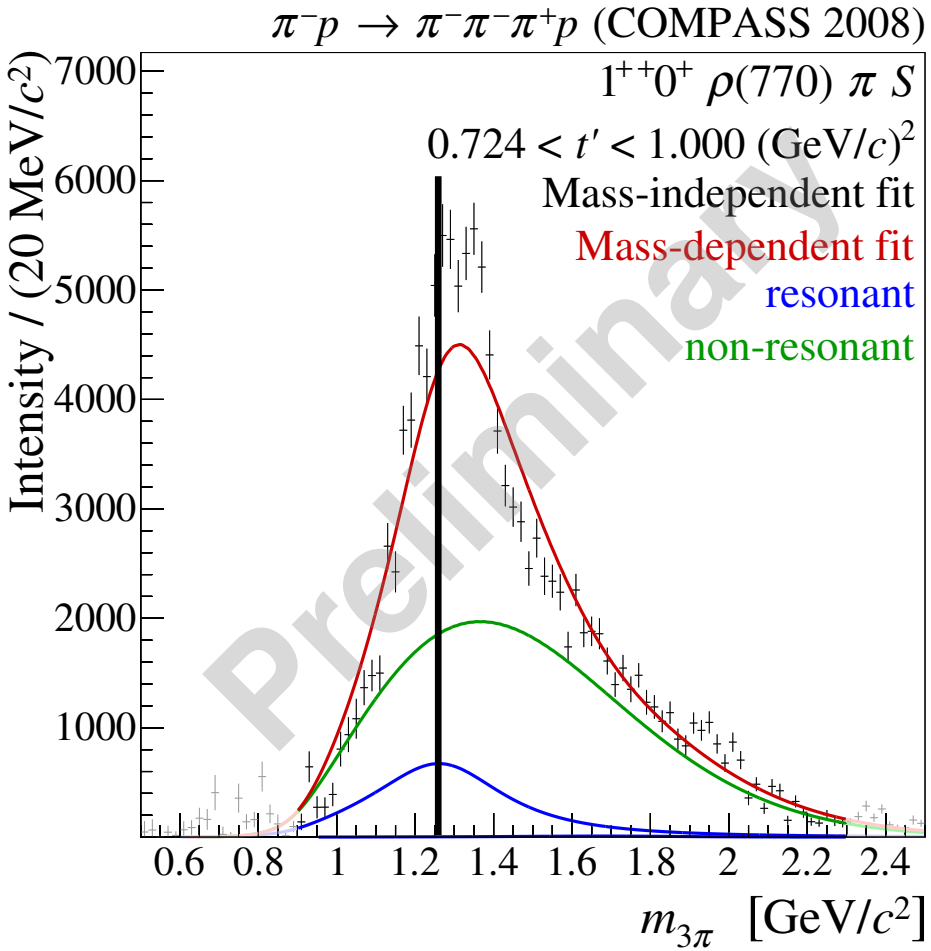

$a_1(1260)$

- resonance parameters do not depend on production mechanism
- couplings and non-resonant parts may vary with t'
- t'-resolved analysis: better disentanglement of resonant and non-resonant parts
- $a_1(1260)$ reproduced:

$$m^{fit} = 1298^{+13}_{-22}\ \text{MeV}/c^2$$
$$m^{PDG} = 1230 \pm 40\ \text{MeV}/c^2$$
$$\Gamma^{fit} = 403^{+0}_{-100}\ \text{MeV}/c^2$$
$$\Gamma^{PDG} = 250 - 600\ \text{MeV}/c^2$$

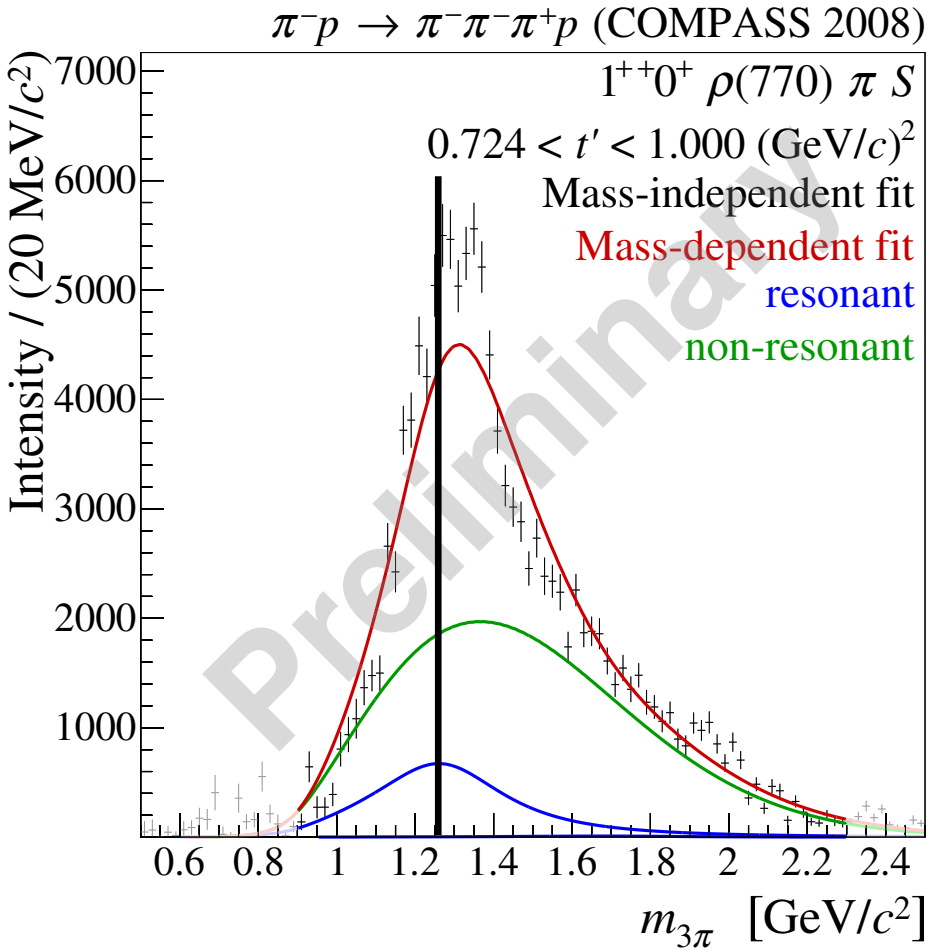

$a_1(1260)$

- resonance parameters do not depend on production mechanism
- couplings and non-resonant parts may vary with t'
- t'-resolved analysis: better disentanglement of resonant and non-resonant parts
- $a_1(1260)$ reproduced:
  $m^{fit} = 1298^{+13}_{-22}$ MeV/c^2
  $m^{PDG} = 1230 \pm 40$ MeV/c^2
  $\Gamma^{fit} = 403^{+0}_{-100}$ MeV/c^2
  $\Gamma^{PDG} = 250 - 600$ MeV/c^2
- weak signal for $a_1(1640)$

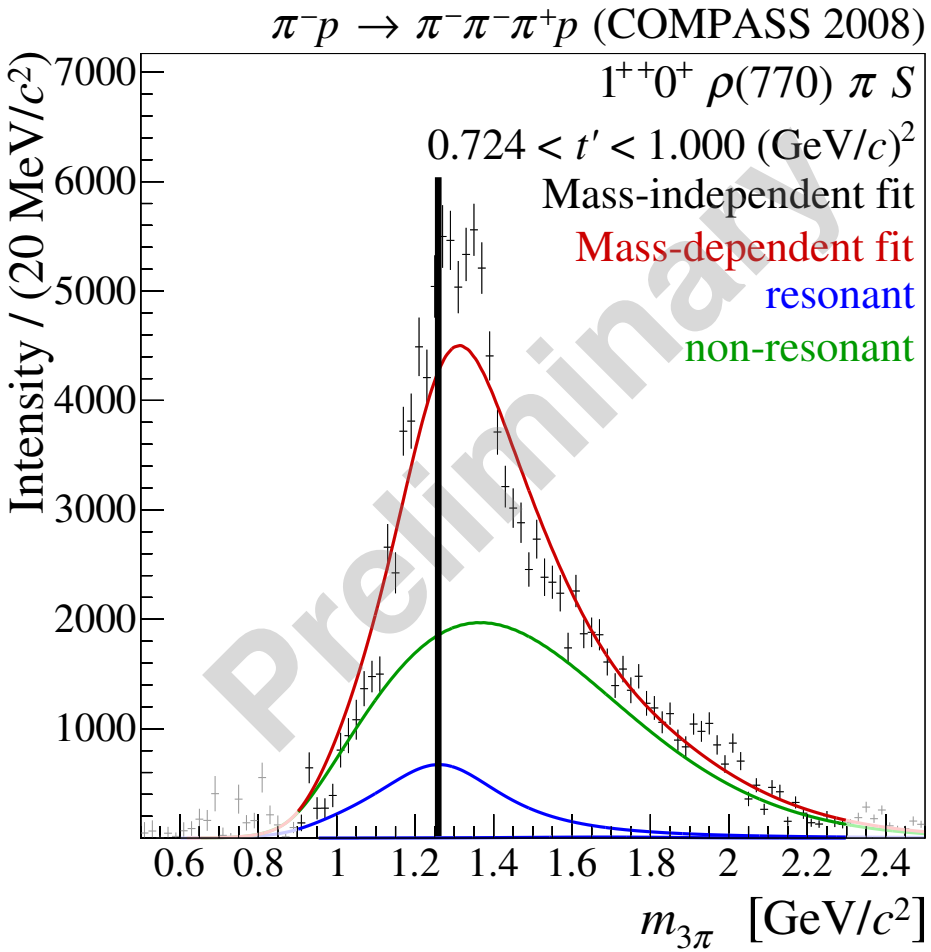

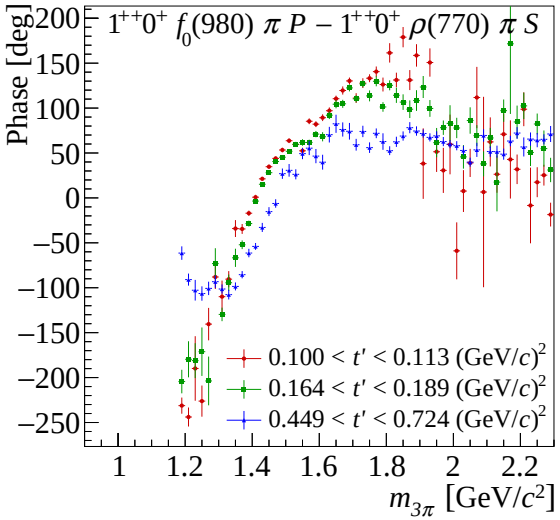
$1^{++}0^+$ $f_0(980)$ π P – $1^{++}0^+$ $\rho(770)$ π S
Phase [deg]
200
150
100
50
0
−50
−100
−150
−200
−250
1
1.2
1.4
1.6
1.8
2
2.2
$m_{3\pi}$ [GeV/c^2]
0.100 < t' < 0.113 (GeV/c)^2
0.164 < t' < 0.189 (GeV/c)^2
0.449 < t' < 0.724 (GeV/c)^2

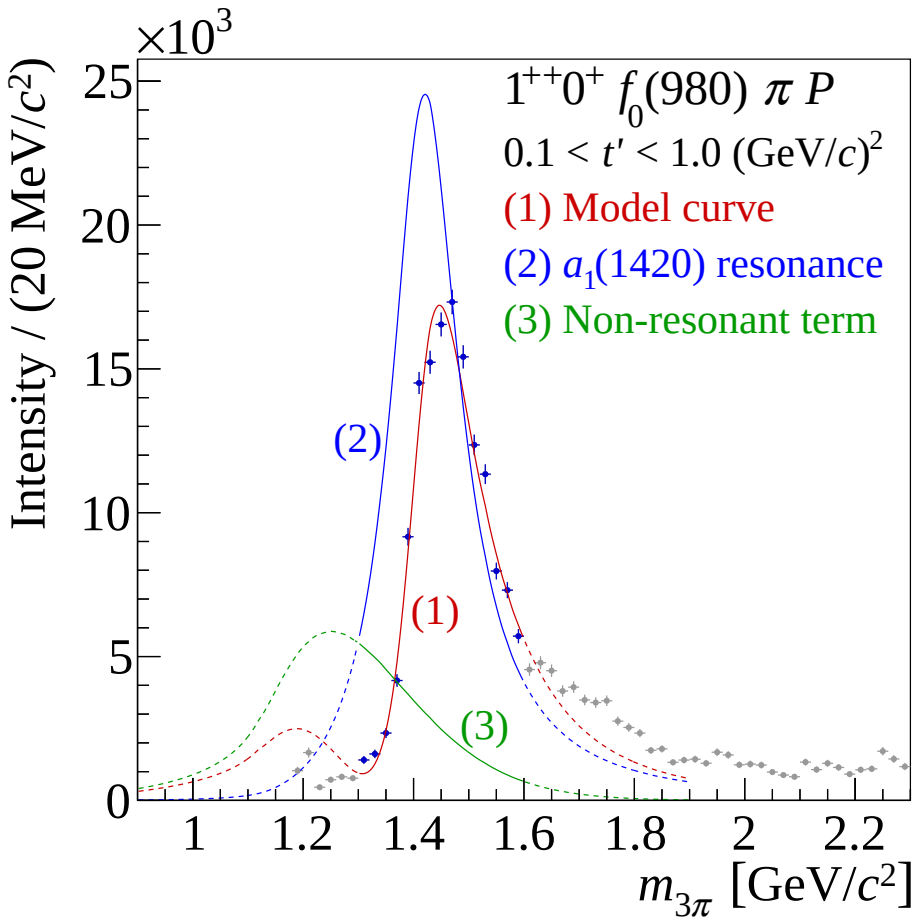
×10^3
Intensity / (20 MeV/c^2)
25
20
15
10
5
0
1
1.2
1.4
1.6
1.8
2
2.2
$m_{3\pi}$ [GeV/c^2]
$1^{++}0^+$ $f_0(980)$ π P
0.1 < t' < 1.0 (GeV/c)^2
(1) Model curve
(2) $a_1(1420)$ resonance
(3) Non-resonant term
(1)
(2)
(3)

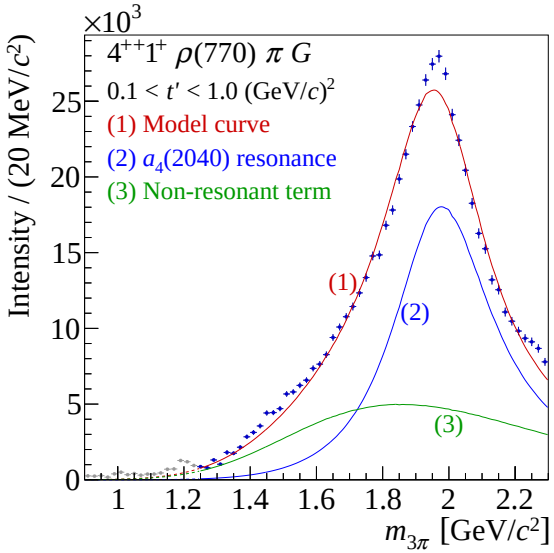
×10^3
4^++1^+ ρ(770) π G
0.1 < t' < 1.0 (GeV/c)^2
(1) Model curve
(2) a_4(2040) resonance
(3) Non-resonant term
Intensity / (20 MeV/c^2)
m_3π [GeV/c^2]

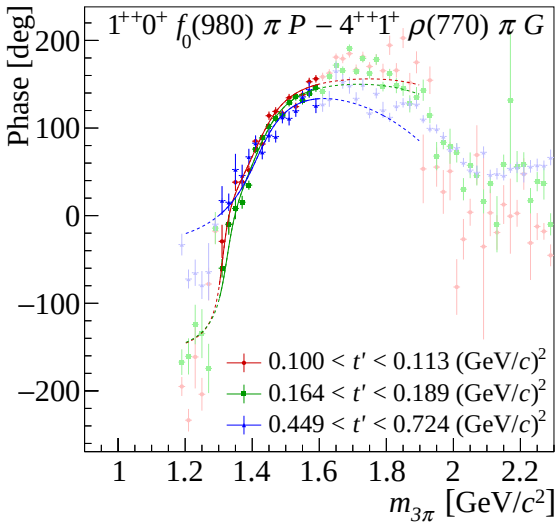
1^++0^+ f_0(980) π P − 4^++1^+ ρ(770) π G
0.100 < t' < 0.113 (GeV/c)^2
0.164 < t' < 0.189 (GeV/c)^2
0.449 < t' < 0.724 (GeV/c)^2
Phase [deg]
m_3π [GeV/c^2]

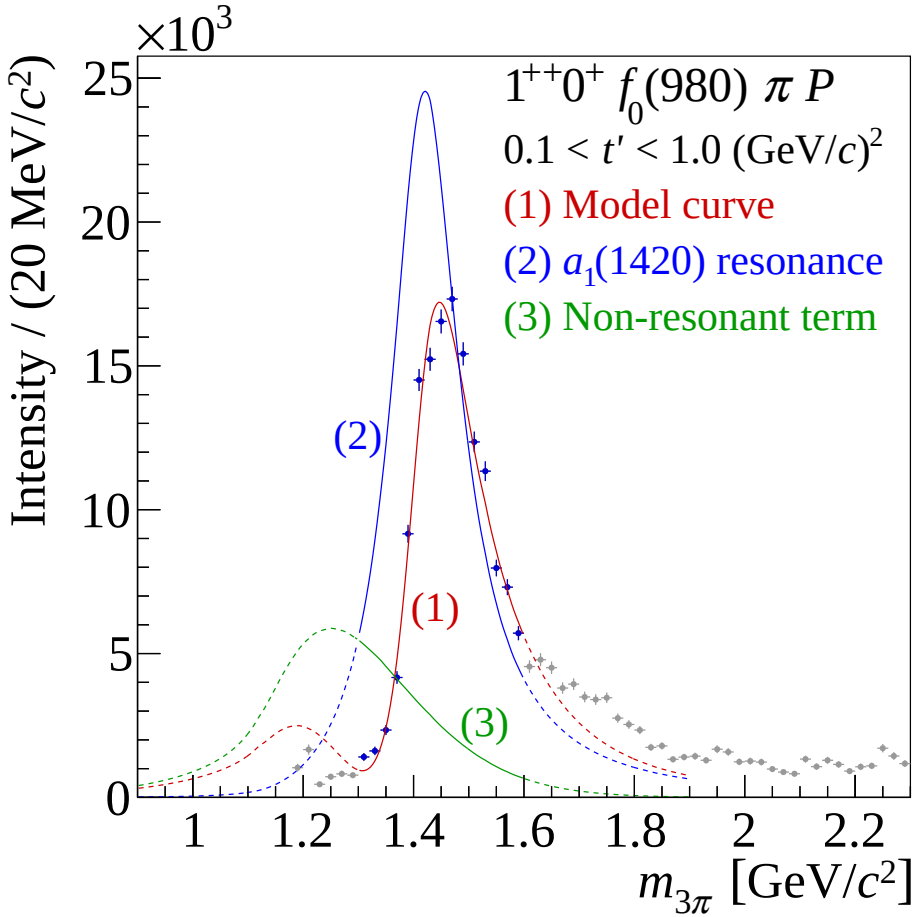
×10^3
1^++0^+ f_0(980) π P
0.1 < t' < 1.0 (GeV/c)^2
(1) Model curve
(2) a_1(1420) resonance
(3) Non-resonant term
Intensity / (20 MeV/c^2)
m_3π [GeV/c^2]

- new signal: $a_1(1420)$
- decay into $f_0(980)\pi$

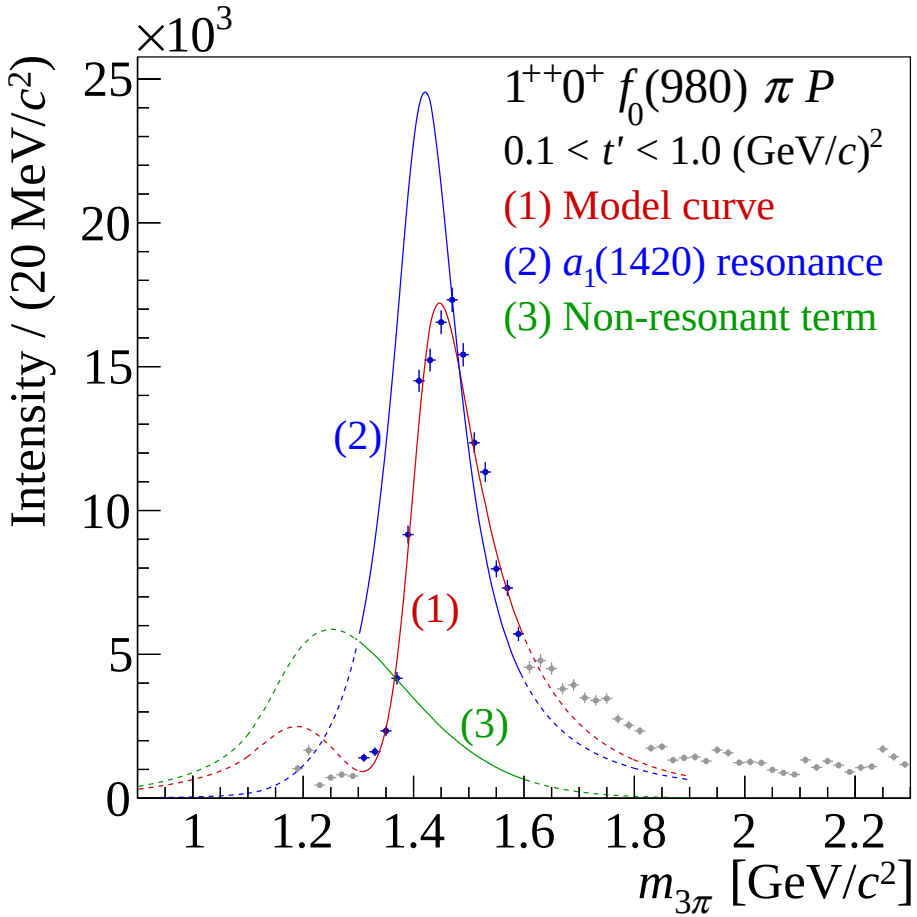

- new signal: $a_1(1420)$
- decay into $f_0(980)\pi$
- possible explanations:
  - triangle diagram
    Mikhasenko, Ketzer, Sarantsev
  - two-channel unitarized Deck amplitude
    Basdevant, Berger

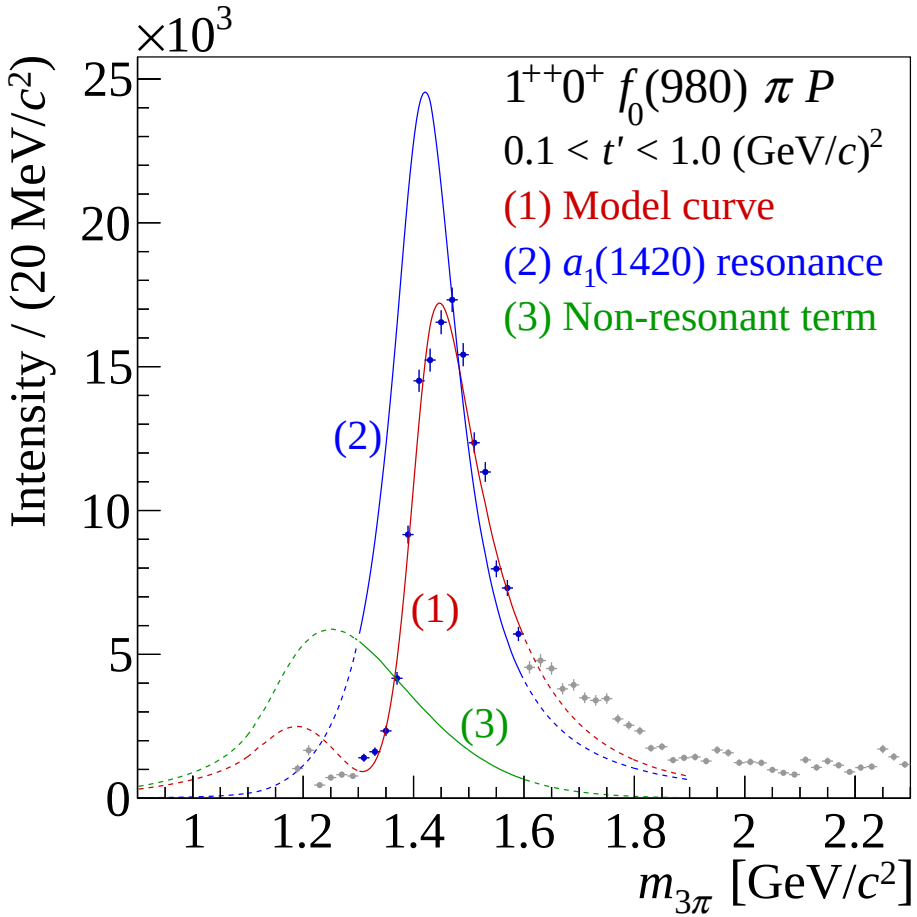

- new signal: $a_1(1420)$
- decay into $f_0(980)\pi$
- possible explanations:
  - triangle diagram
    Mikhasenko, Ketzer, Sarantsev
  - two-channel unitarized Deck amplitude
    Basdevant, Berger
- Mass:
  $m_{a_1(1420)} = 1411.8^{+1.0}_{-4.4}\,\mathrm{MeV}/c^2$
  Width:
  $\Gamma_{a_1(1420)} = 158^{+8}_{-8}\,\mathrm{MeV}/c^2$

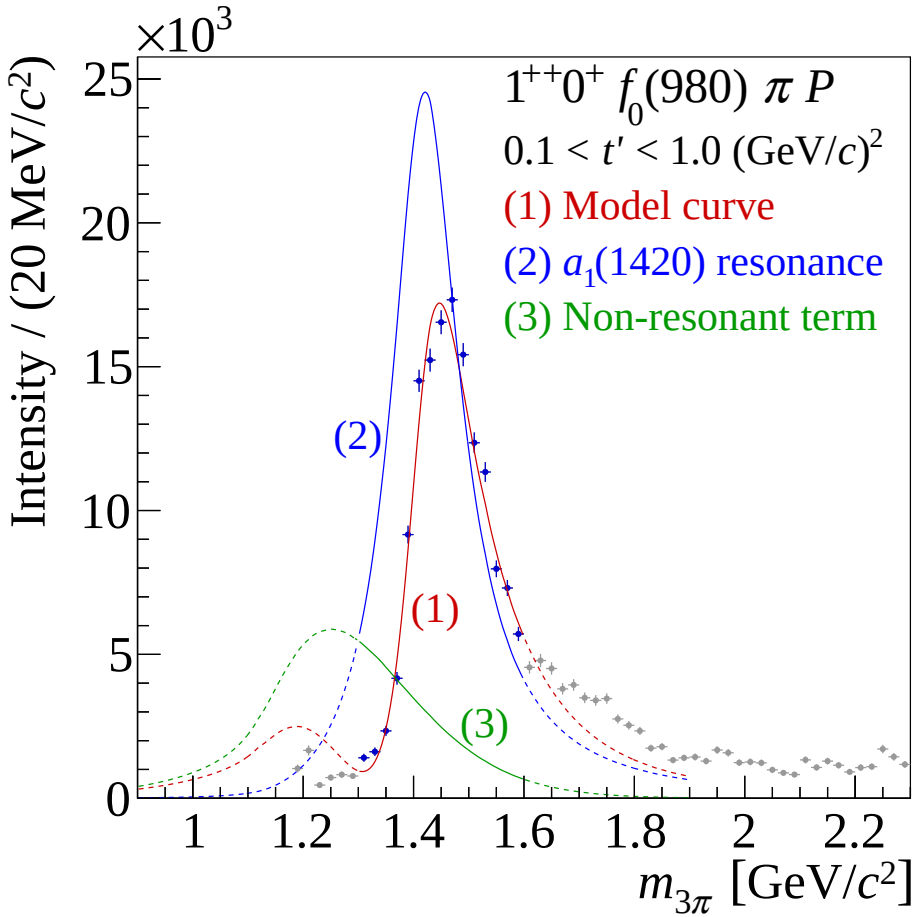

Summary of the a_J

$J^{PC} = 2^{++}$ sector:

- clearest resonance in the analysis: $a_2(1320)$
- excited $a_2(1700)$ also found

Summary of the a_J

$J^{PC} = 2^{++}$ sector:

- clearest resonance in the analysis: $a_2(1320)$
- excited $a_2(1700)$ also found

$J^{PC} = 4^{++}$ sector:

- $a_4(2040)$ resonance found

Summary of the a_J

$J^{PC} = 2^{++}$ sector:

- clearest resonance in the analysis: $a_2(1320)$
- excited $a_2(1700)$ also found

$J^{PC} = 4^{++}$ sector:

- $a_4(2040)$ resonance found

$J^{PC} = 1^{++}$ sector:

- $a_1(1260)$ and $a_1(1640)$ resonances in the main 1^{++} waves
- Distinguish from non-resonant part due to t' dependence
- New $a_1(1420)$ signal found in the $1^{++}0^+ f_0(980)\pi$ P wave

$$0^{-+}0^{+}f_0(980)\pi S$$

The $0^{-+}0^{+}f_0(980)\pi S$ wave

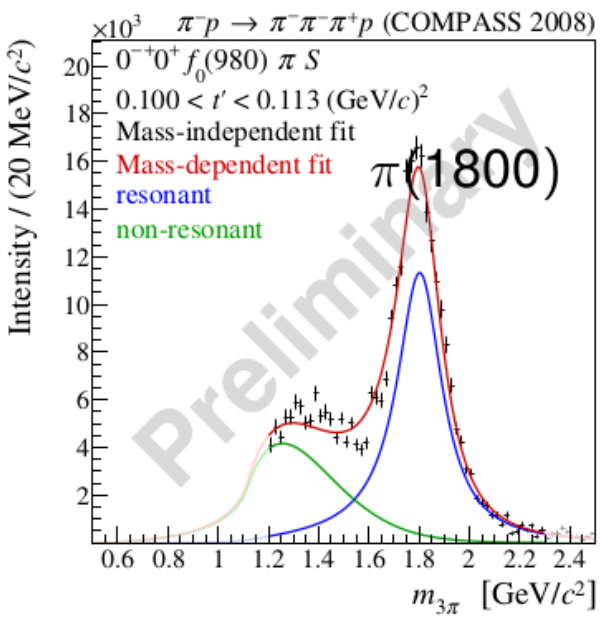

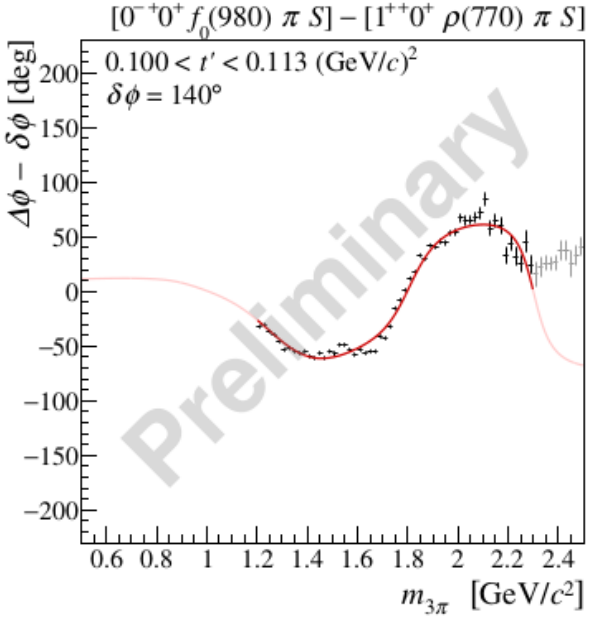

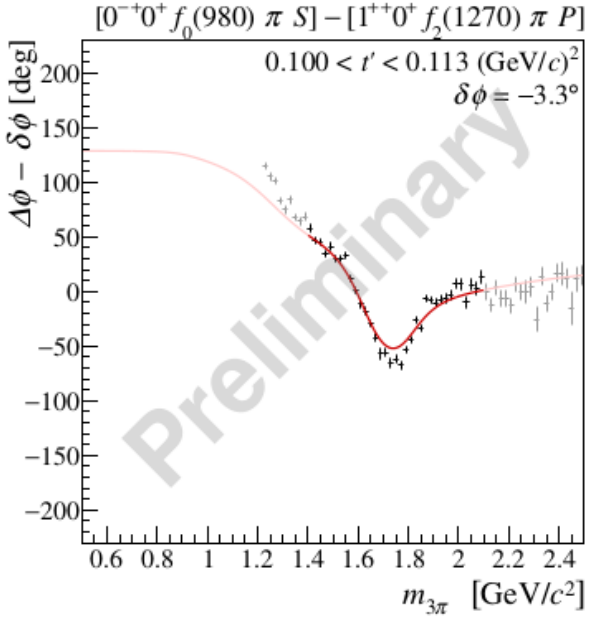

$$m_{\pi(1800)} = 1802.6^{+8}_{-3.5}\,\mathrm{MeV}/c^2\ ;\ \Gamma_{\pi(1800)} = 218^{+11}_{-6}\,\mathrm{MeV}/c^2$$

$$m^{\mathrm{PDG}}_{\pi(1800)} = 1812 \pm 12\,\mathrm{MeV}/c^2;\ \Gamma^{\mathrm{PDG}}_{\pi(1800)} = 208 \pm 12\,\mathrm{MeV}/c^2$$

$$1^{-+}1^{+}\rho(770)\pi P$$

The $1^{-+}1^{+}\rho(770)\pi P$ wave

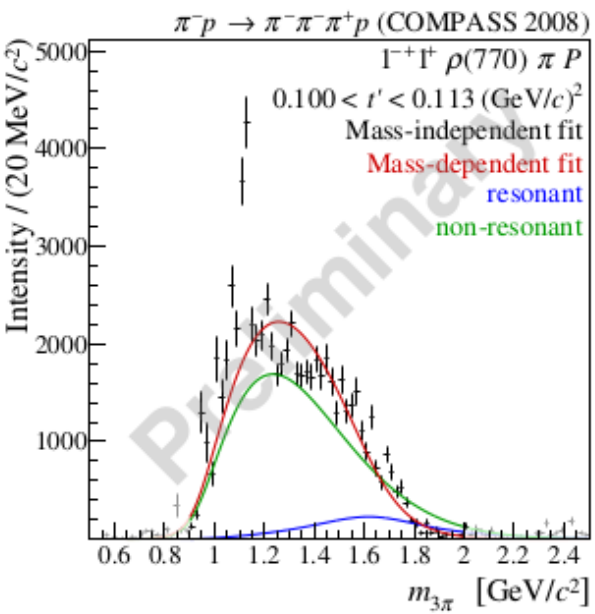

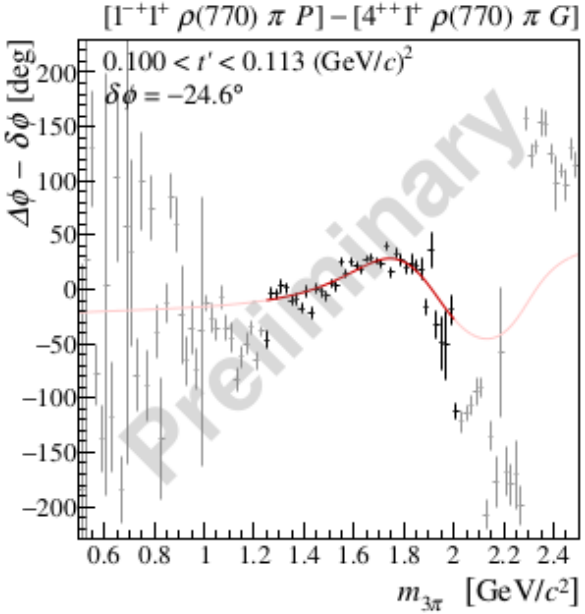

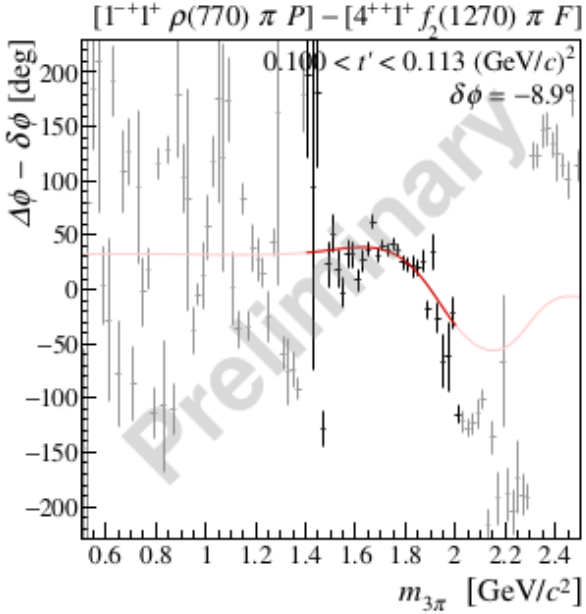

at low t' very weak resonant component

The $1^{-+}1^{+}\rho(770)\pi P$ wave

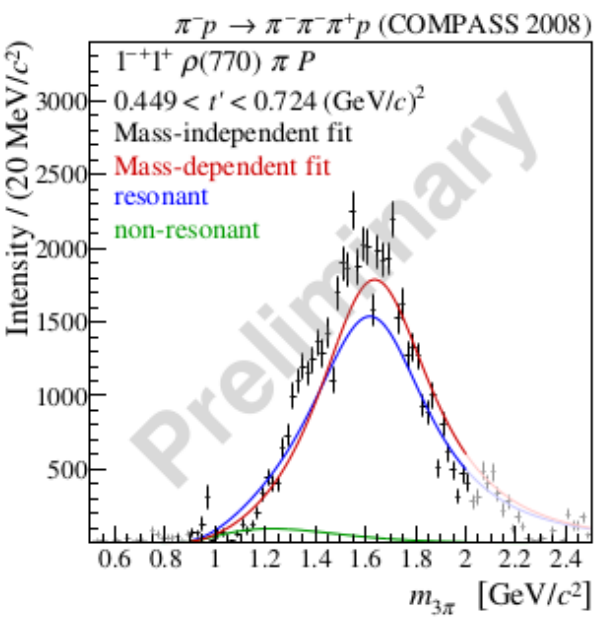

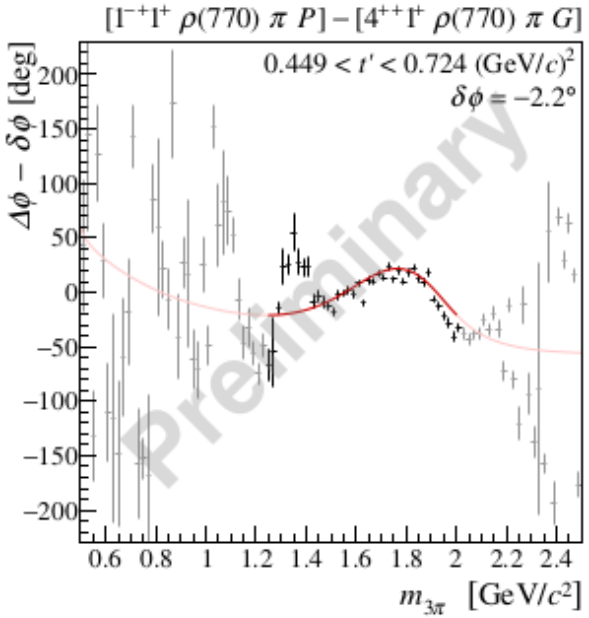

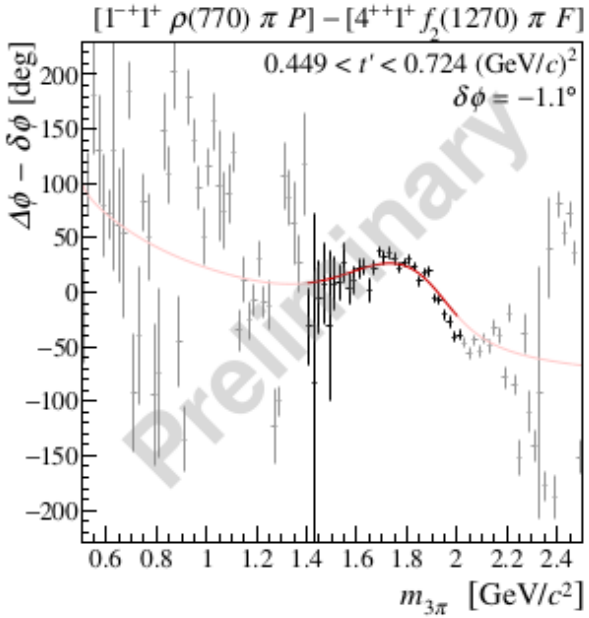

at higher t' resonant component dominant

The $1^{-+}1^{+}\rho(770)\pi P$ wave

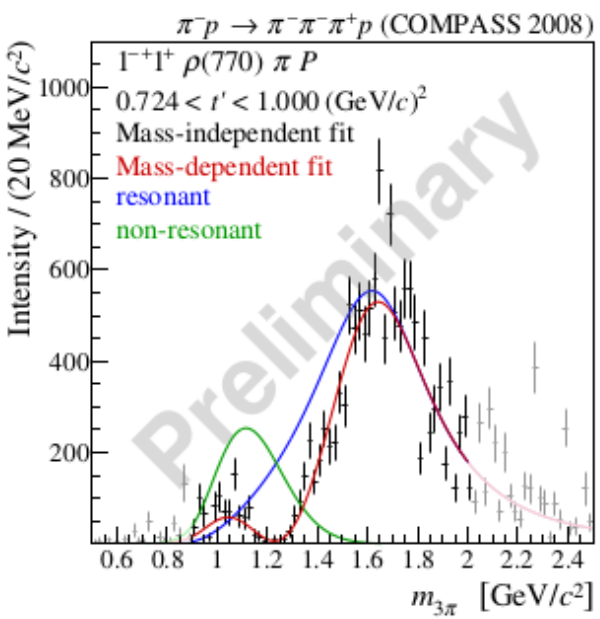

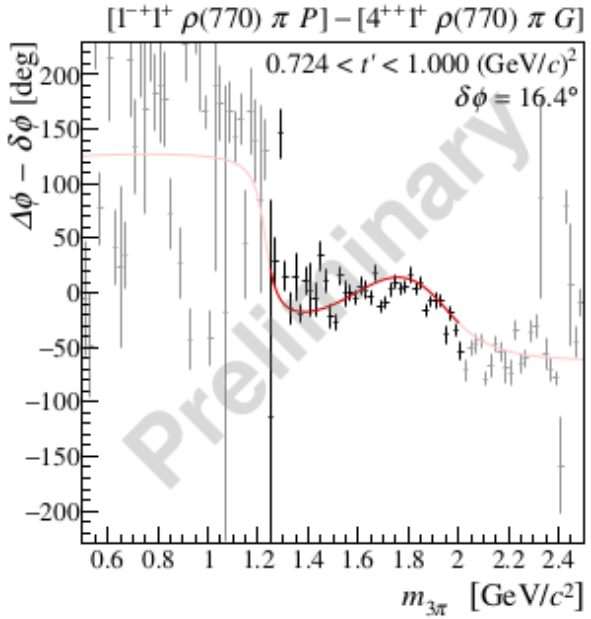

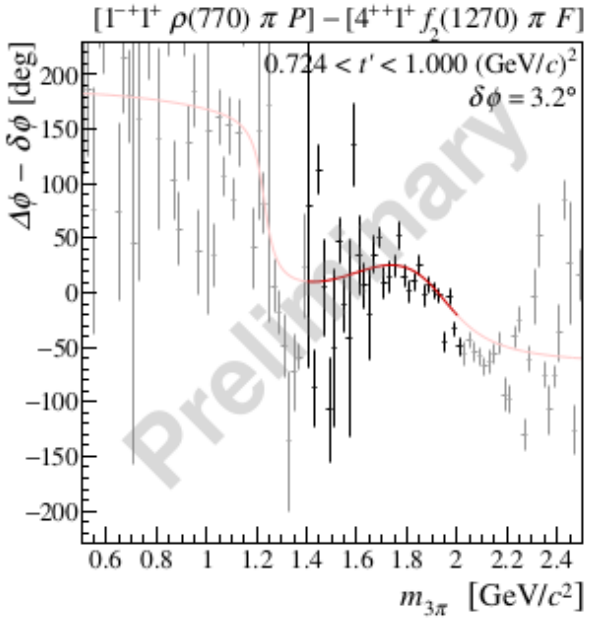

at higher t' resonant component dominant

The $1^{-+}1^{+}\rho(770)\pi P$ wave

Phase-motion

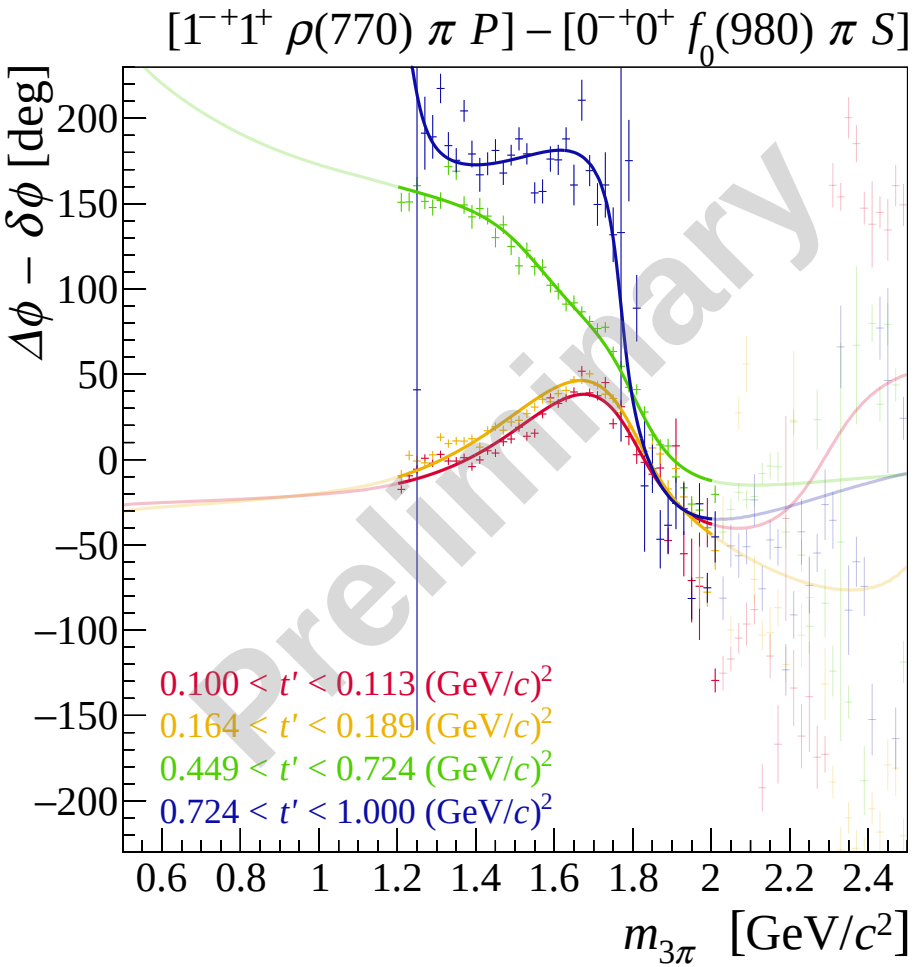

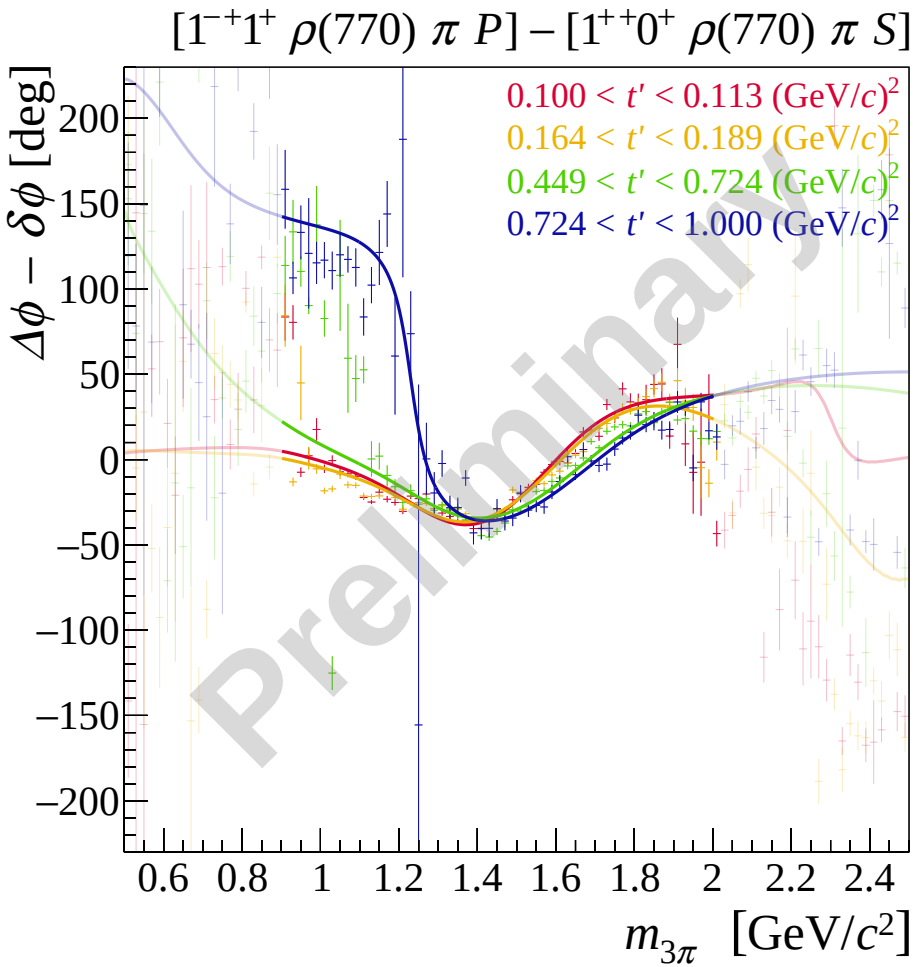

resonance very broad

$J^{PC} = 2^{-+}$ sector

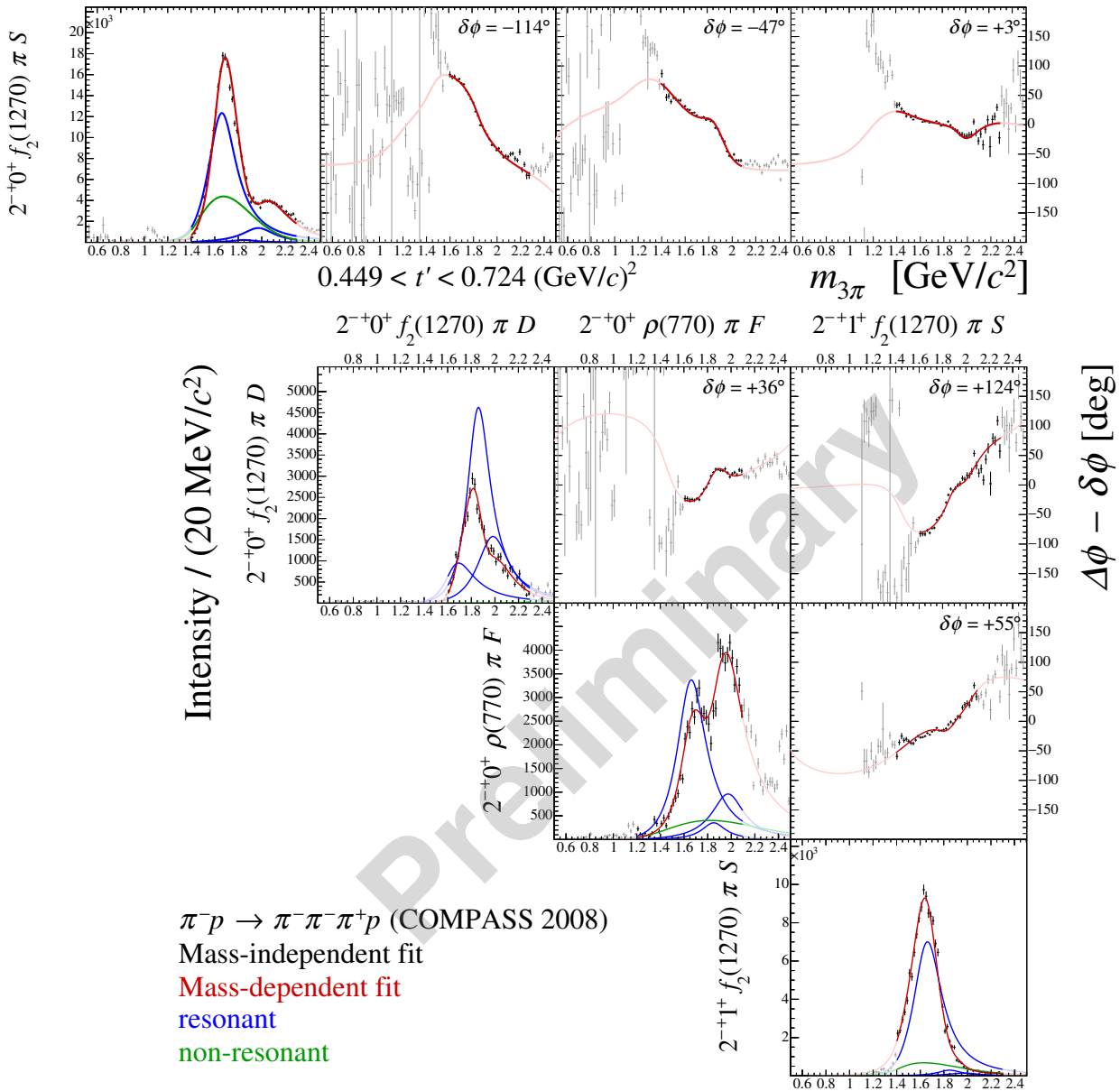
$2^{-+}0^{+}\, f_2(1270)\, \pi\, S$
$\delta\phi = -114°$
$\delta\phi = -47°$
$\delta\phi = +3°$
$0.449 < t' < 0.724\ (\mathrm{GeV}/c)^2$
$m_{3\pi}$ [GeV/c^2]
$2^{-+}0^{+}\, f_2(1270)\, \pi\, D$
$2^{-+}0^{+}\, \rho(770)\, \pi\, F$
$2^{-+}1^{+}\, f_2(1270)\, \pi\, S$
$\delta\phi = +36°$
$\delta\phi = +124°$
$\delta\phi = +55°$
Intensity / (20 MeV/c^2)
$\Delta\phi - \delta\phi$ [deg]
$\pi^- p \to \pi^-\pi^-\pi^+ p$ (COMPASS 2008)
Mass-independent fit
Mass-dependent fit
resonant
non-resonant
Preliminary

$J^{PC} = 2^{-+}$
Three $\pi_2(\ldots)$ resonances

$M = 0$

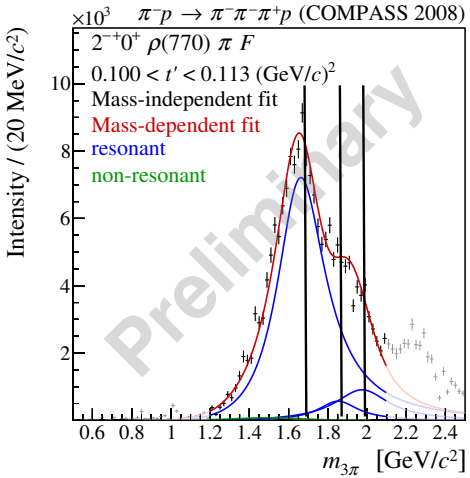

$M = 0$

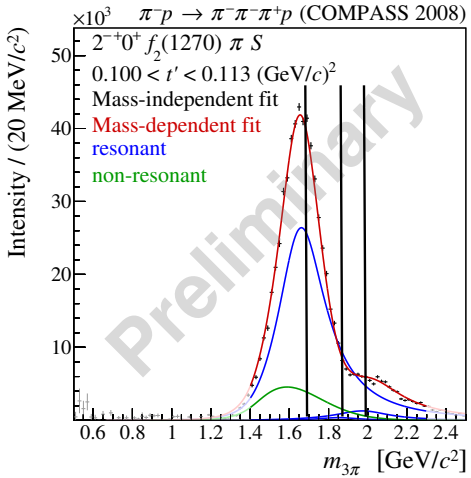

$M = 1$

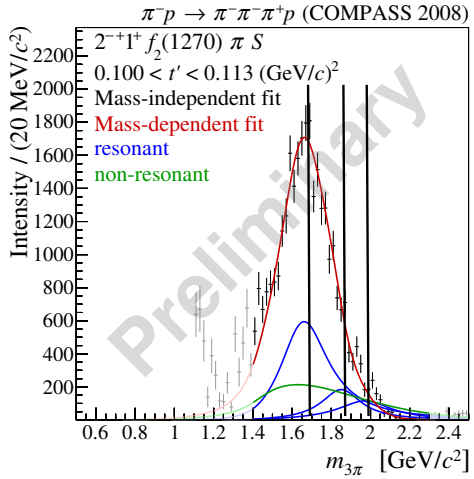

$M = 0$

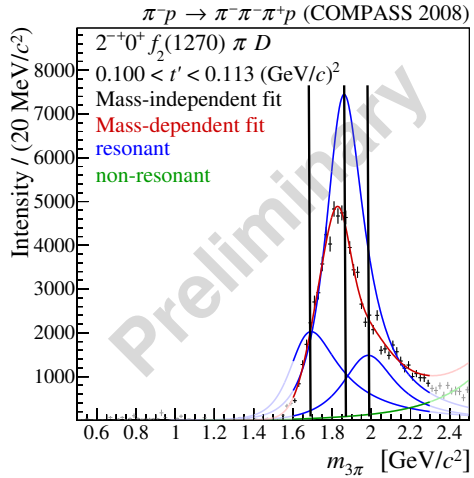

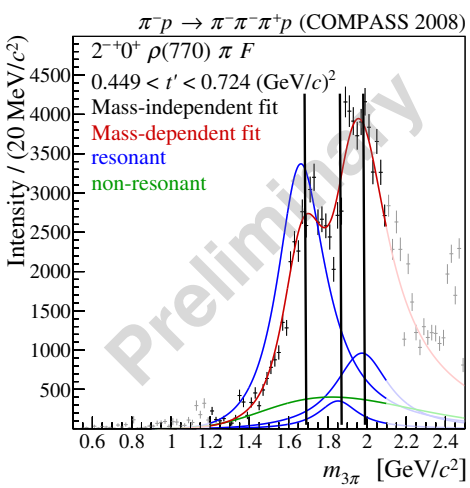

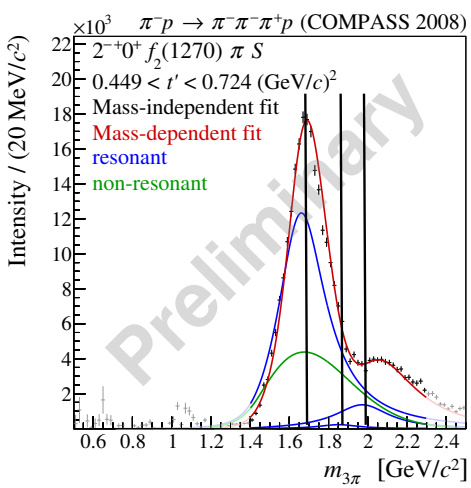

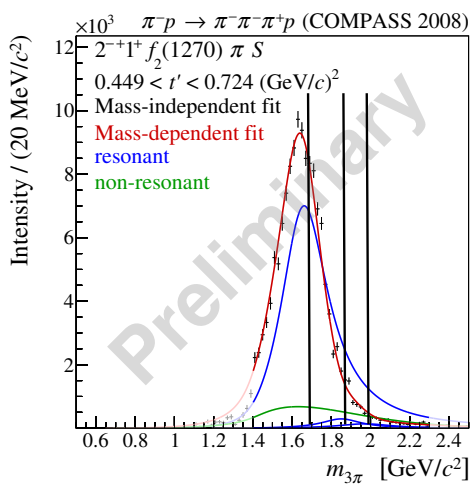

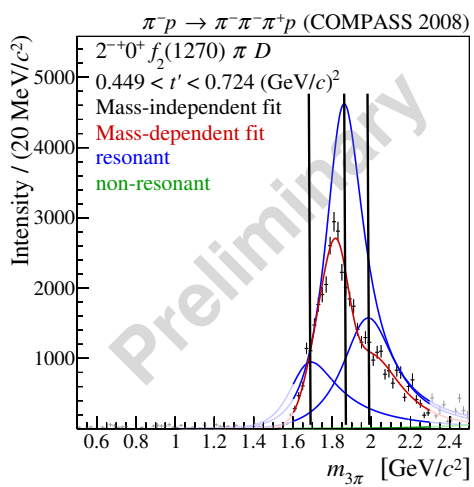

$J^{PC} = 2^{-+}$

Three $\pi_2(\ldots)$ resonances

$M = 0$ $M = 0$ $M = 1$ $M = 0$

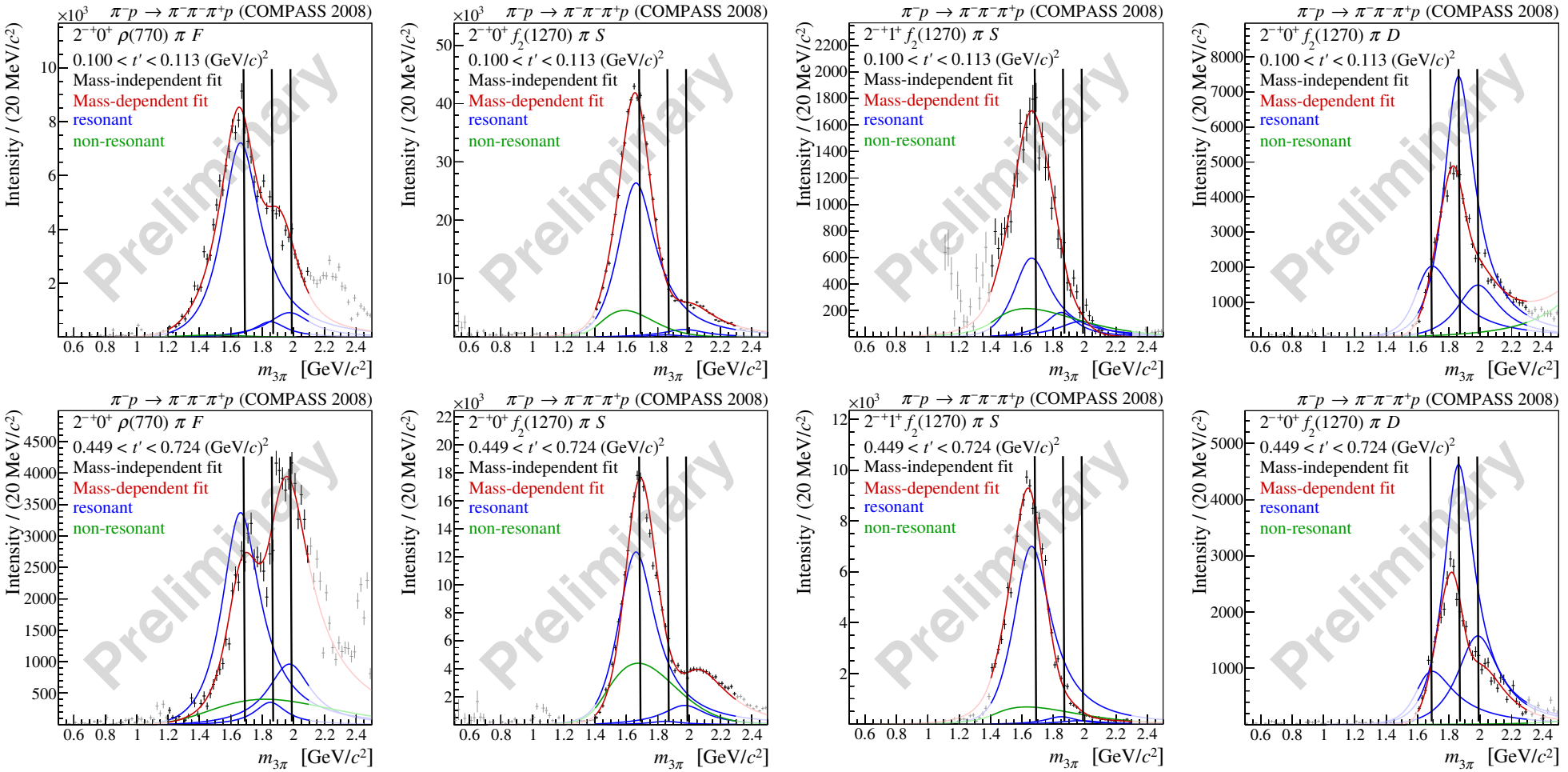

$\pi_2(1670)$, $\pi_2(1880)$ and $\pi_2(2005)$

Summary of π_J

$J^{PC} = 0^{-+}$ *sector*:

- One wave included: $0^{-+}0^{+}f_0(980)\pi S$
- $\pi(1800)$ resonance reproduced

Summary of π_J

$J^{PC} = 0^{-+}$ *sector*:

- One wave included: $0^{-+}0^{+}f_0(980)\pi S$
- $\pi(1800)$ resonance reproduced

$J^{PC} = 1^{-+}$ sector

- Spin-exotic $J^{PC} = 1^{-+}$ signal found
- One wave in the fit: $1^{-+}1^{+}\rho(770)\pi P$
- Resonance can't be explained within the simple quark model

Summary of π_J

$J^{PC} = 0^{-+}$ *sector*:

- One wave included: $0^{-+}0^{+}f_0(980)\pi S$
- $\pi(1800)$ resonance reproduced

$J^{PC} = 1^{-+}$ sector

- Spin-exotic $J^{PC} = 1^{-+}$ signal found
- One wave in the fit: $1^{-+}1^{+}\rho(770)\pi P$
- Resonance can't be explained within the simple quark model

$J^{PC} = 2^{-+}$ sector

- Three 2^{-+} resonances included
- $\pi_2(1670)$, $\pi_2(1880)$ and $\pi_2(2005)$
  - $\pi_2(1670)$ dominant in S-wave decays
  - $\pi_2(1880)$ dominant in D-wave decays
  - $\pi_2(2005)$ only seen once before

Summary of parameters for a_J resonances

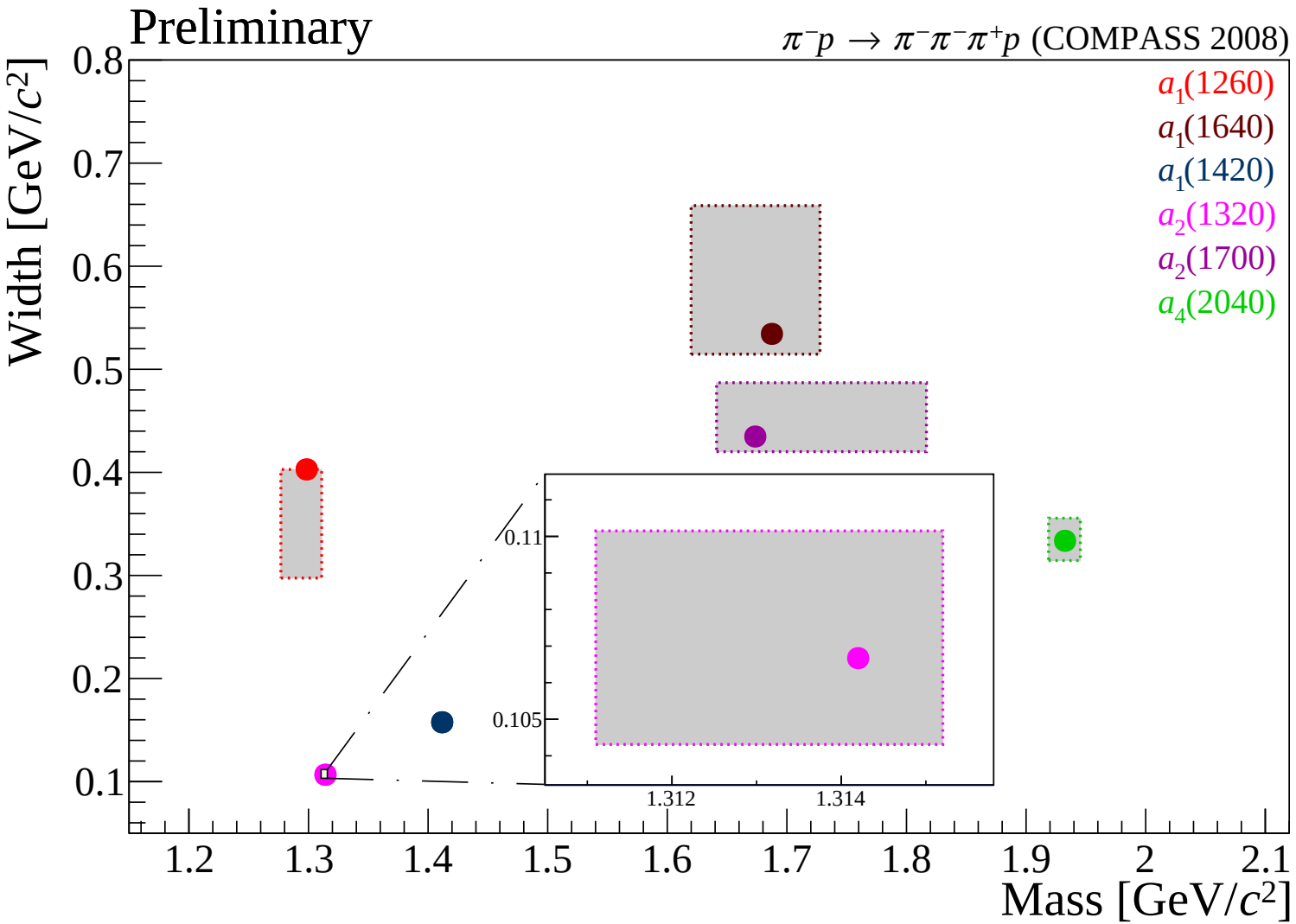

Summary of parameters for π_J resonances

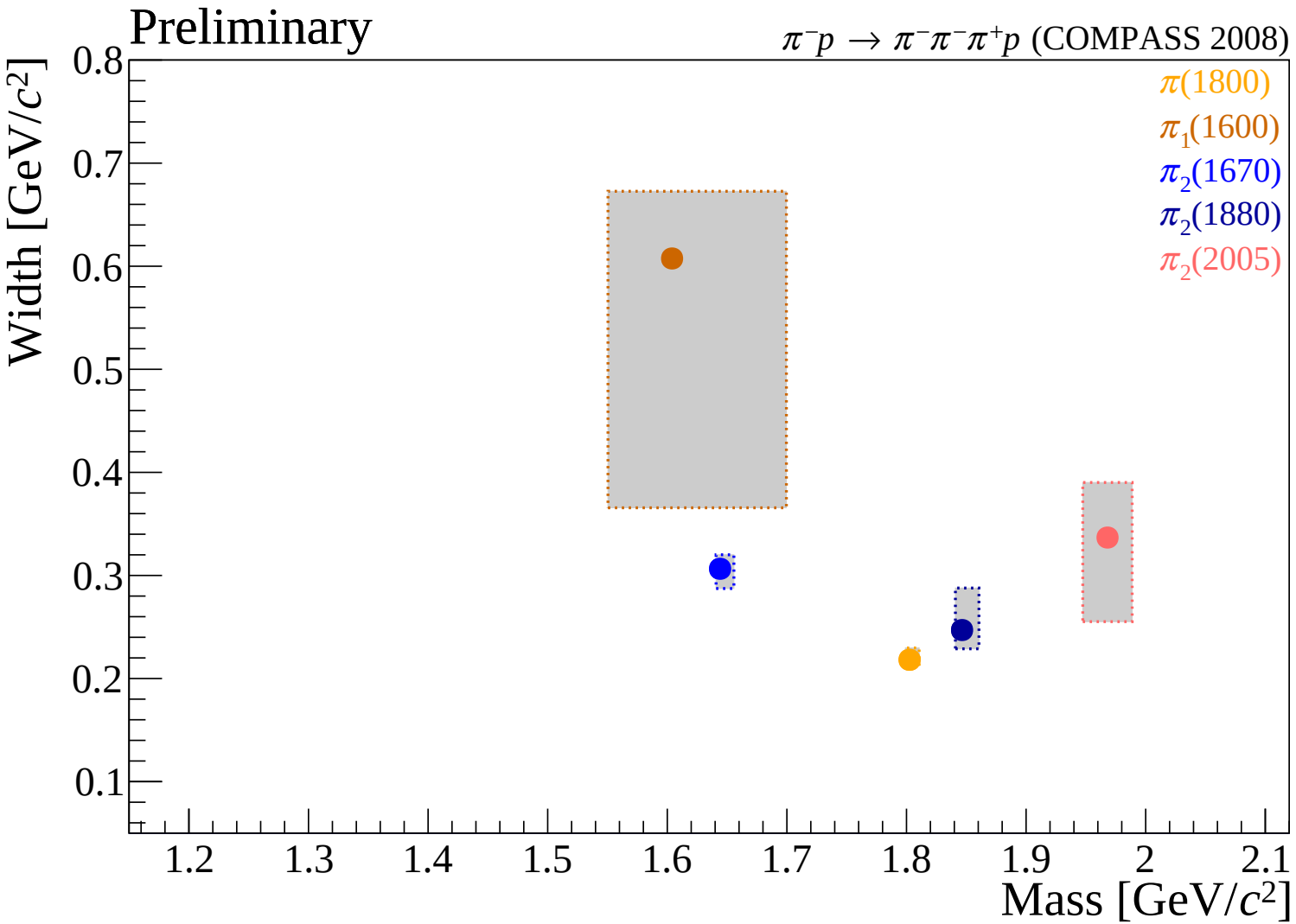

Results

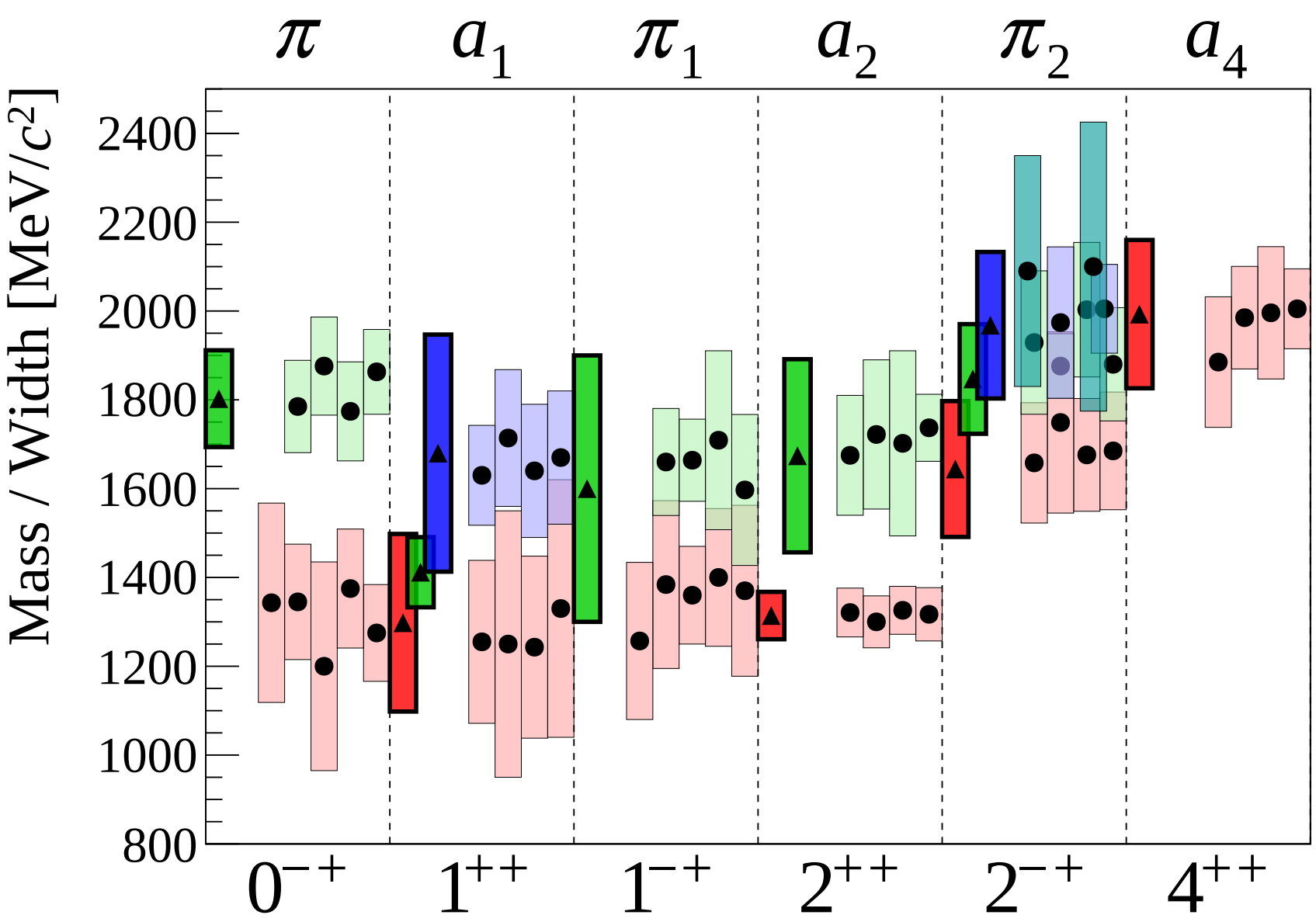
π
a_1
π_1
a_2
π_2
a_4
Mass / Width [MeV/c^2]
2400
2200
2000
1800
1600
1400
1200
1000
800
0^{-+}
1^{++}
1^{-+}
2^{++}
2^{-+}
4^{++}

Conclusions and Outlook

- 46 million events for $\pi^- p \to p\pi^-\pi^+\pi^-$ collected by COMPASS
- two-step analysis
  - partial-Wave Decomposition model of 88 waves
  - resonance-model fit
    - ⋆ subset of 14 waves
    - ⋆ main known resonances reproduced
    - ⋆ all resonance parameters determined in one single fit
    - ⋆ new signal: $a_1(1420)$
    - ⋆ exotic signal found
    - ⋆ extensive systematic studies performed

Conclusions and Outlook

- 46 million events for $\pi^- p \to p\pi^-\pi^+\pi^-$ collected by COMPASS
- two-step analysis
  - partial-Wave Decomposition model of 88 waves
  - resonance-model fit
    - ⋆ subset of 14 waves
    - ⋆ main known resonances reproduced
    - ⋆ all resonance parameters determined in one single fit
    - ⋆ new signal: $a_1(1420)$
    - ⋆ exotic signal found
    - ⋆ extensive systematic studies performed
- ongoing developments
  - refine non-resonant (Deck) background description
  - “de-isobaring” the model
  - relativistic spin coupling
- more channels to follow, including π^0, η

Conclusions and Outlook

- 46 million events for $\pi^- p \to p\pi^-\pi^+\pi^-$ collected by COMPASS
- two-step analysis
  - partial-Wave Decomposition model of 88 waves
  - resonance-model fit
    - ⋆ subset of 14 waves
    - ⋆ main known resonances reproduced
    - ⋆ all resonance parameters determined in one single fit
    - ⋆ new signal: $a_1(1420)$
    - ⋆ exotic signal found
    - ⋆ extensive systematic studies performed
- ongoing developments
  - refine non-resonant (Deck) background description
  - "de-isobaring" the model
  - relativistic spin coupling
- more channels to follow, including π^0, η
- lower statistics for incoming K^- beams
  $\to$ dedicated future programme with RF-separated beam?

Thank you for your attention!

Step 2: Resonance Model Fit

Spin-Density Matrix:

- Diagonal elements: Intensities: $\text{SDM}_{ii} = |T_i|^2$
- Off-diagonal elements: Phases: $\text{SDM}_{ij} = -\text{SDM}_{ji} = \arg\left(T_i T_j^*\right)$

Resonance model for Spin-Density Matrix

- 14×14 submatrix of 88×88 SDM
- Same model for every bin in t'
- Model resonances with Breit-Wigner amplitudes
- Add non-resonant background
  - Phenomenologial parametrization or Deck
- 722 free parameters
- 76505 data points

Extensive systematic studies

- 1000 Fit-attempts for the main fit $\rightarrow$ 30000 CpuH
  - Randomization of start-parameters
  - Release order of fit-parameters
- More than 200 systematic studies performed
- Studies include:
  - Variation of the set of fitted waves
  - Variation of the fit-model:
    - Resonance content
    - Resonance parametrizations
    - Non-resonant parametrizations
  - Variation of fit procedure:
    - Formulation of the χ^2 function
- 200 Fit attempts in every study $\rightarrow$ Over 40000 single fits in the systematic studies
- $\rightarrow$ Systematic uncertainties under control

Is Peak in $1^{++}\,0^{+}\,f_0(980)\pi P$ Wave a Model Artifact?

Novel analysis method (inspired by E791 analysis, PRD **73** (2006) 032204)

- Replace $J^{PC} = 0^{++}$ isobar parametrizations by piece-wise constant amplitudes in $m_{\pi^+\pi^-}$ bins
- Extract $m_{3\pi}$ dependence of 0^{++} isobar amplitude from data
  - Drastic reduction of model bias
  - *Caveat:* significant increase in number of fit parameters
- Result: the $a_1(1420)$ signal is indep. on the $f_0(980)$ description

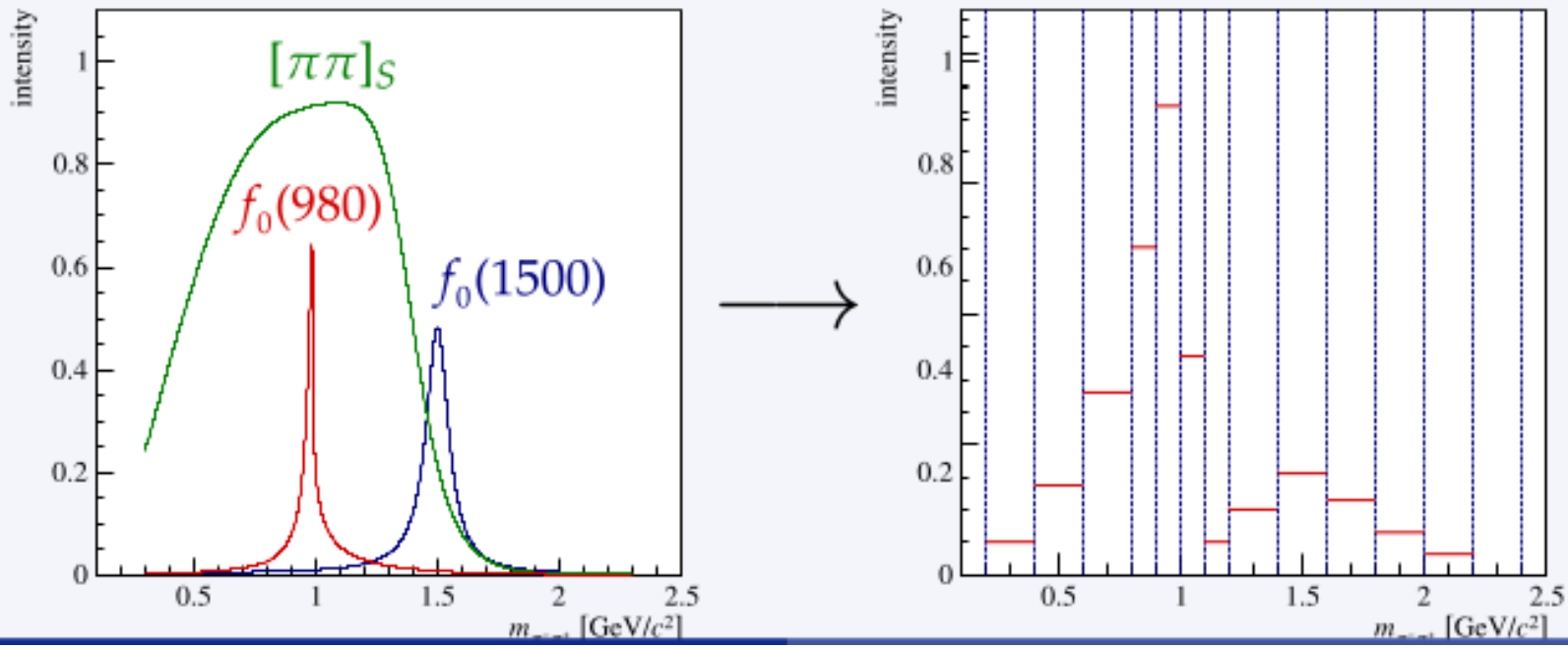

$\pi\pi$ S-Wave Amplitude in $J^{PC} = 1^{++}$ 3π Wave [arXiv:1509.00992]

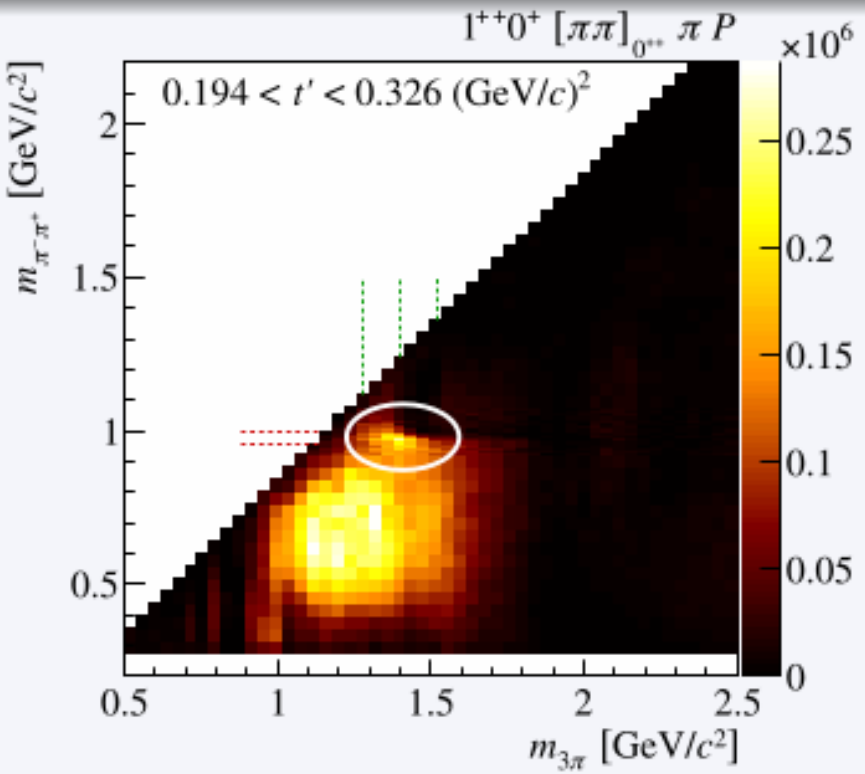

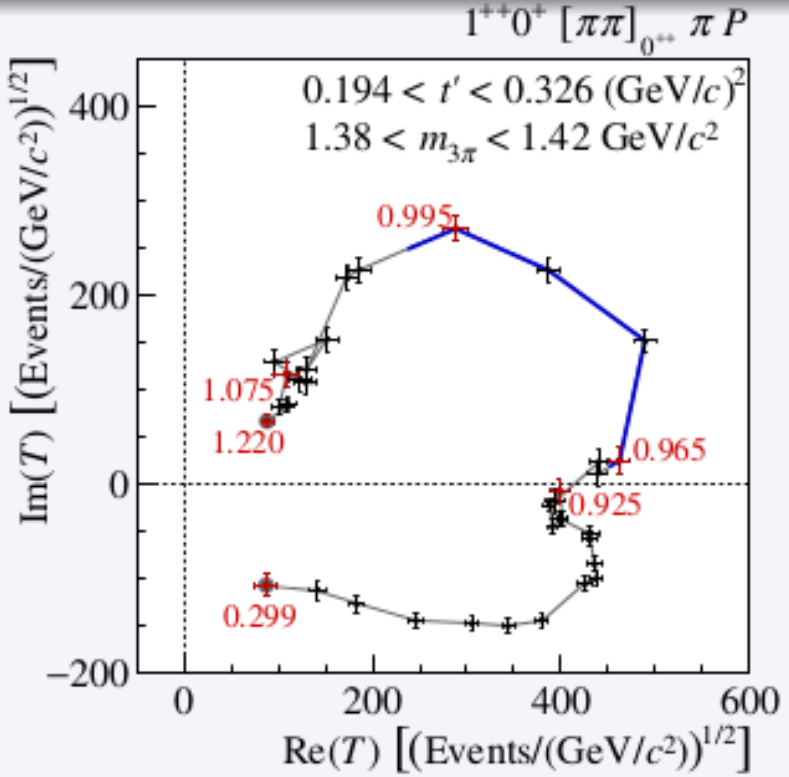

- Correlation of 3π intensity around $1.4\,\mathrm{GeV}/c^2$ with $f_0(980)$
- $f_0(980)$ semicircle in Argand diagram
- Confirms that $f_0(980)\,\pi$ signal is *not* an artifact of isobar parametrization

$\pi\pi$ S-Wave Amplitude in $J^{PC} = 1^{++}$ 3π Wave [arXiv:1509.00992]

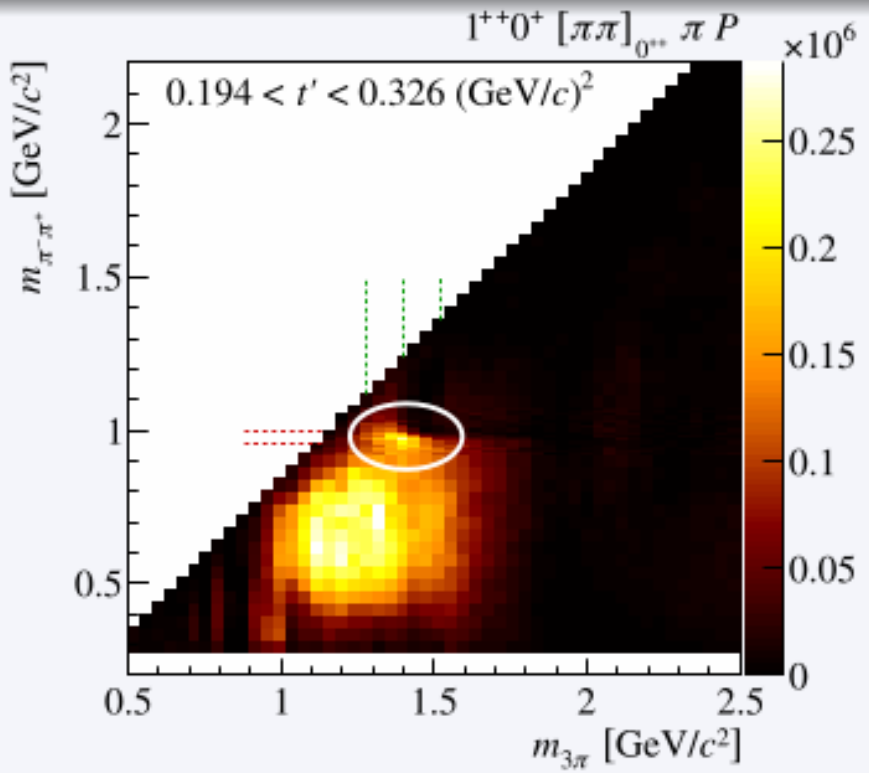

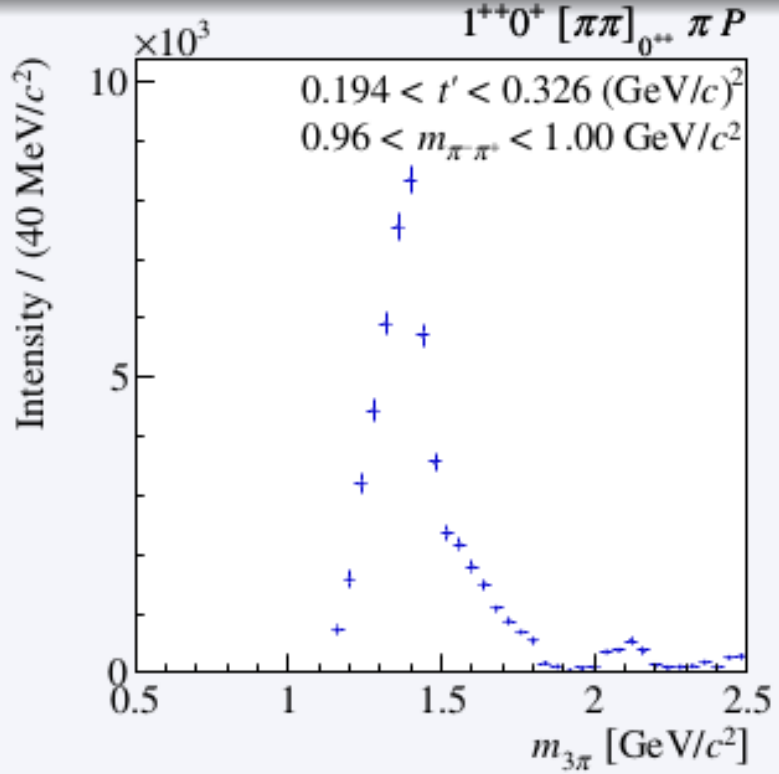

- Correlation of 3π intensity around $1.4\,\mathrm{GeV}/c^2$ with $f_0(980)$
- $f_0(980)$ semicircle in Argand diagram
- Confirms that $f_0(980)\,\pi$ signal is *not* an artifact of isobar parametrization

$\pi\pi$ S-Wave Amplitude in $J^{PC} = 0^{-+}$ 3π Wave [arXiv:1509.00992]

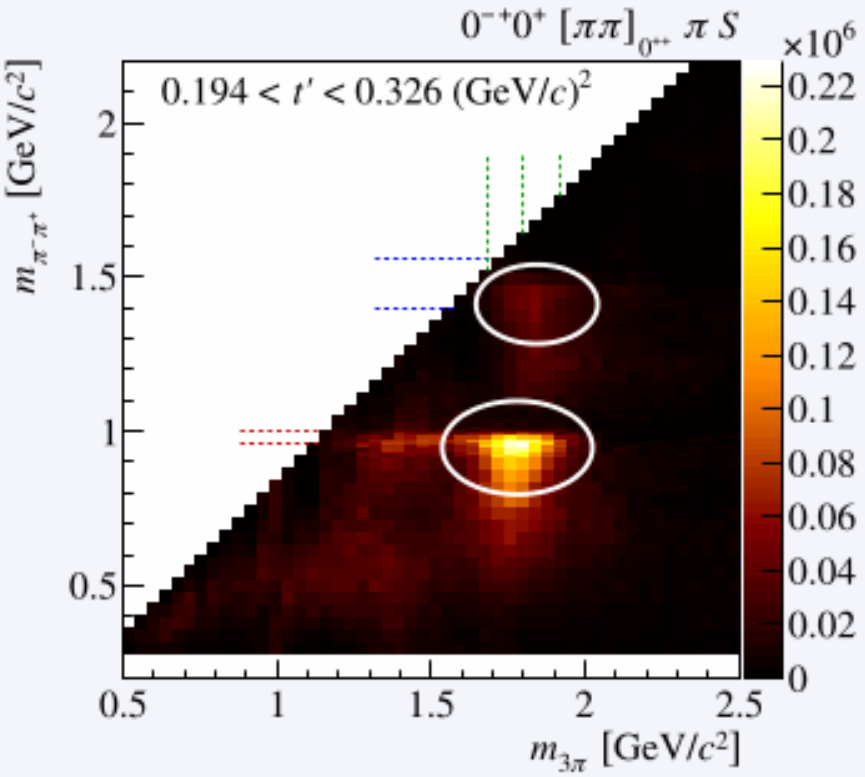

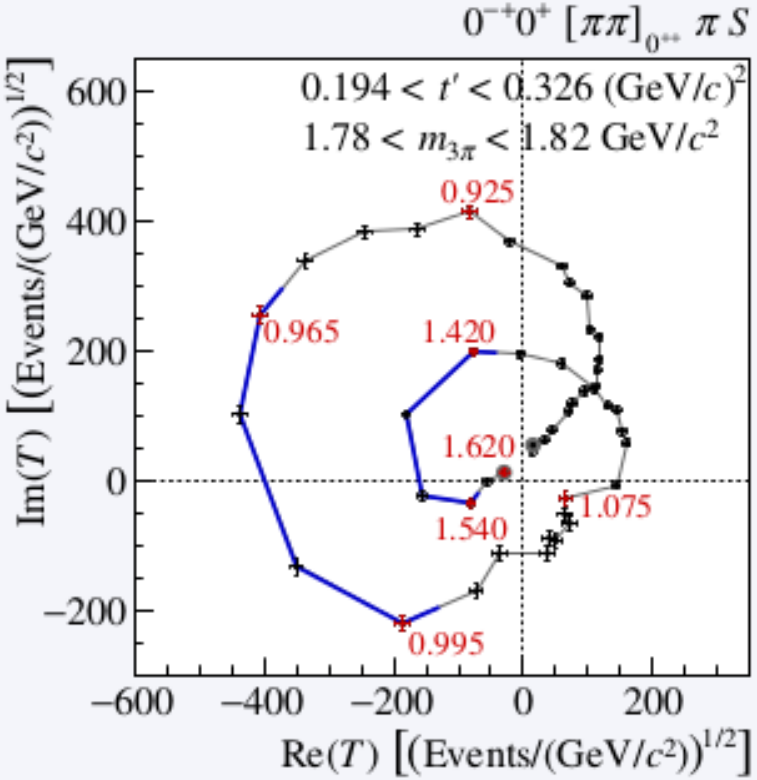

- Coupling of $\pi(1800)$ to $f_0(980)\pi$ and $f_0(1500)\pi$ decay modes

PWA of $\pi^- p \to \pi^- \eta^{(\prime)} p_{\text{recoil}}$

PLB **740** (2015) 303

- Odd-spin waves: spin-exotic quantum numbers
  - Disputed $J^{PC} = 1^{-+}$ resonance signals
    - $\pi_1(1400)$ in $\pi\eta$ and $\pi_1(1600)$ in $\pi\eta'$
- Comparison of $\pi\eta$ and $\pi\eta'$: information about flavor structure

Reconstruction from exclusive $\pi^-\pi^+\pi^-\gamma\gamma$ final state

- $\eta \to \pi^+\pi^-\pi^0$ with $\pi^0 \to \gamma\gamma$
- $\eta' \to \pi^+\pi^-\eta$ with $\eta \to \gamma\gamma$

$\pi^-\eta$ invariant mass

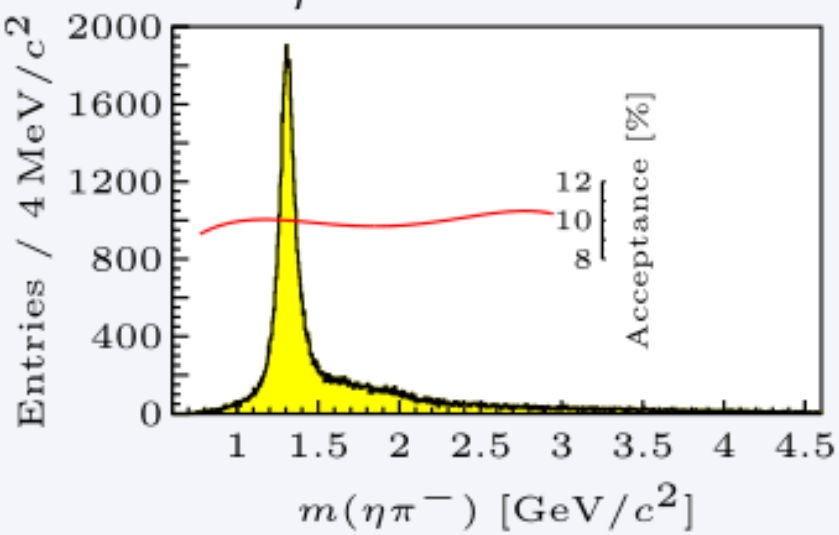

$\pi^-\eta'$ invariant mass

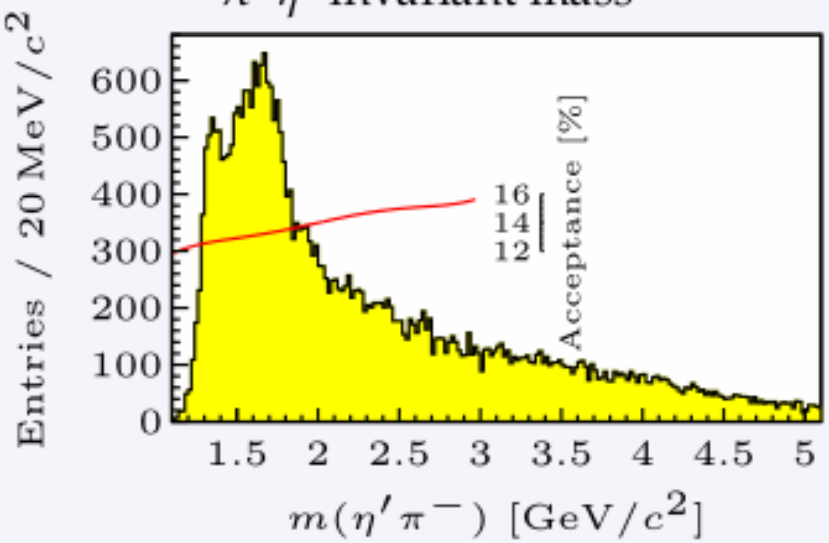

Comparison of $J^{PC} = 2^{++}$ Partial Waves

PLB **740** (2015) 303

Quark-line picture for $n = (u, d)$ and pointlike resonances

- $\pi^-\eta$ and $\pi^-\eta'$ partial-wave intensities for spin J related by
  - Different phase space and barrier factors
  - Branching fraction ratio b of η and η' into $\pi^-\pi^+\gamma\gamma$

$$N_J^{\pi\eta'}(m) \propto b \left[\frac{q^{\pi\eta'}(m)}{q^{\pi\eta}(m)}\right]^{2J+1} N_J^{\pi\eta}(m)$$

- q = breakup momentum

$\pi^-\eta$ final state

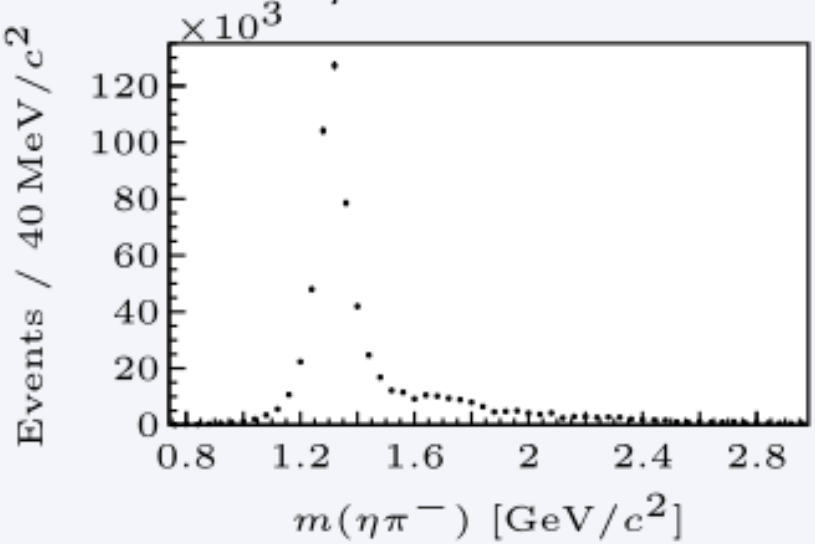

$\pi^-\eta'$ final state; $\pi^-\eta$ scaled

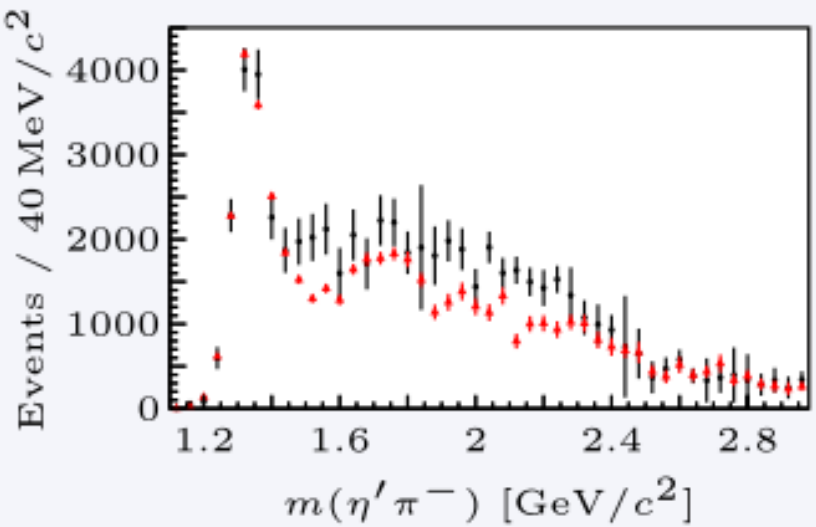

Even-Spin Waves

PLB **740** (2015) 303

$J^{PC} = 4^{++}$

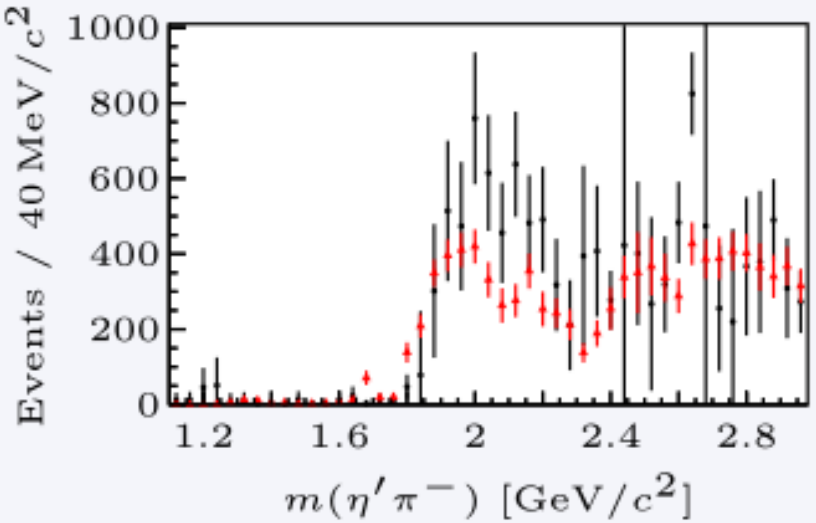

2^{++}

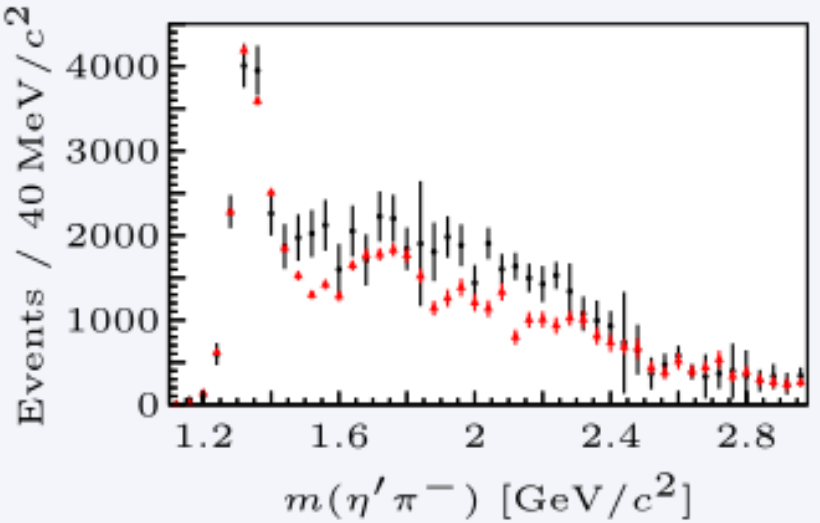

Phase: $4^{++} - 2^{++}$

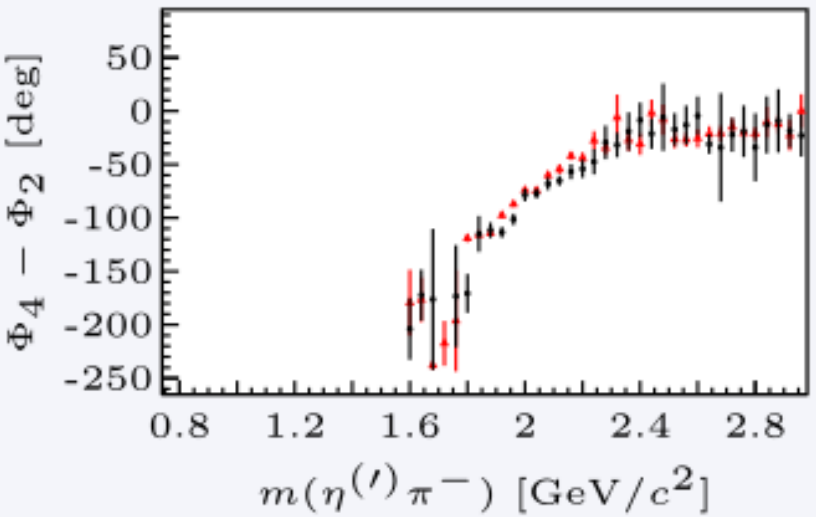

- Resonance-model fit (Breit-Wigner)
- $\dfrac{N(a_2 \to \pi\eta')}{N(a_2 \to \pi\eta)} = (5 \pm 2)\,\%$
- First-time measurement of $\dfrac{N(a_4 \to \pi\eta')}{N(a_4 \to \pi\eta)} = (23 \pm 7)\,\%$

$\pi^-\eta'$ final state; $\pi^-\eta$ scaled

$J^{PC} = 1^{-+}$ Spin-Exotic Wave

PLB **740** (2015) 303

Spin-exotic $J^{PC} = 1^{-+}$

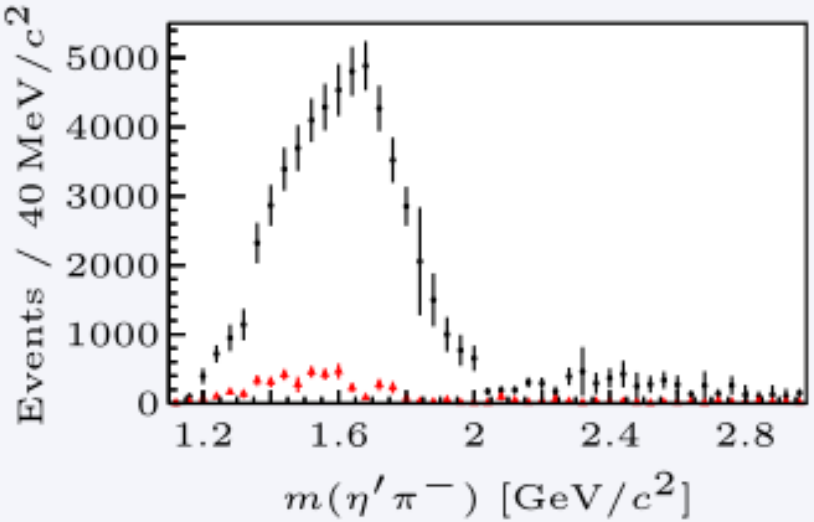

2^{++}

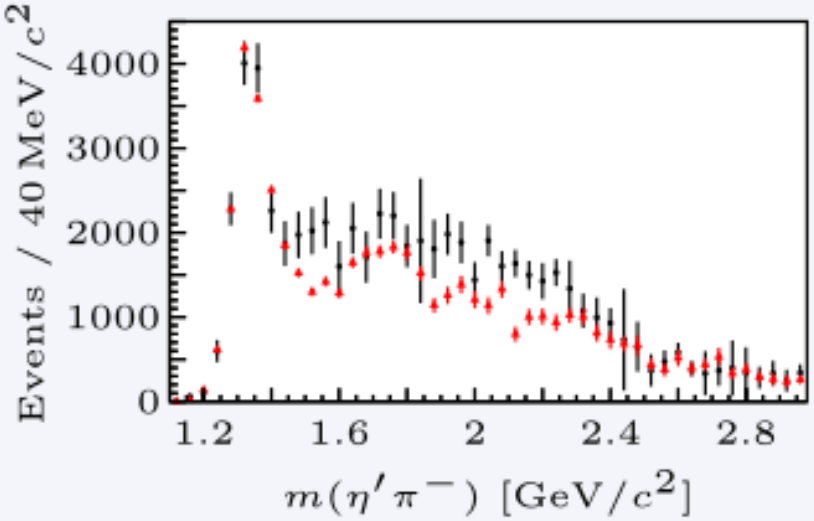

Phase: $1^{-+} - 2^{++}$

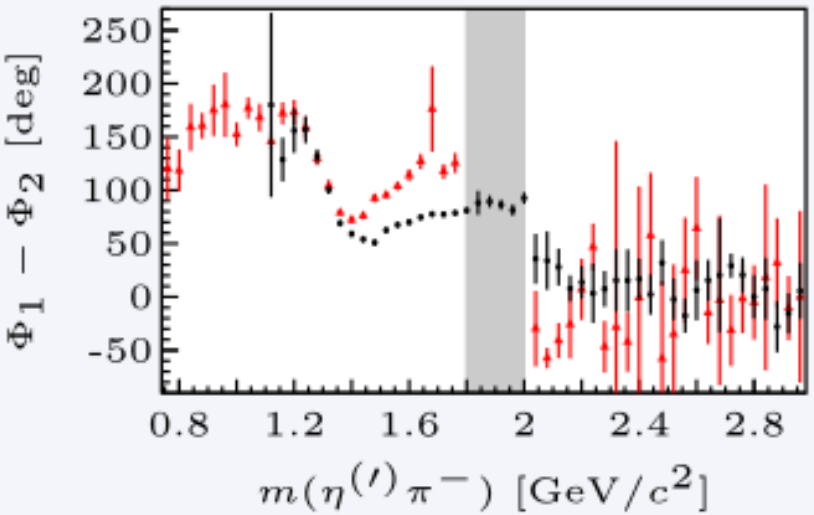

- 1^{-+} intensities very different
- Suppression in $\pi\eta$ channel predicted for intermediate $|q\bar{q}g\rangle$ state
- Different phase motion in 1.6 GeV/c^2 region

$\pi^-\eta'$ final state; $\pi^-\eta$ scaled

2004 Primakoff results

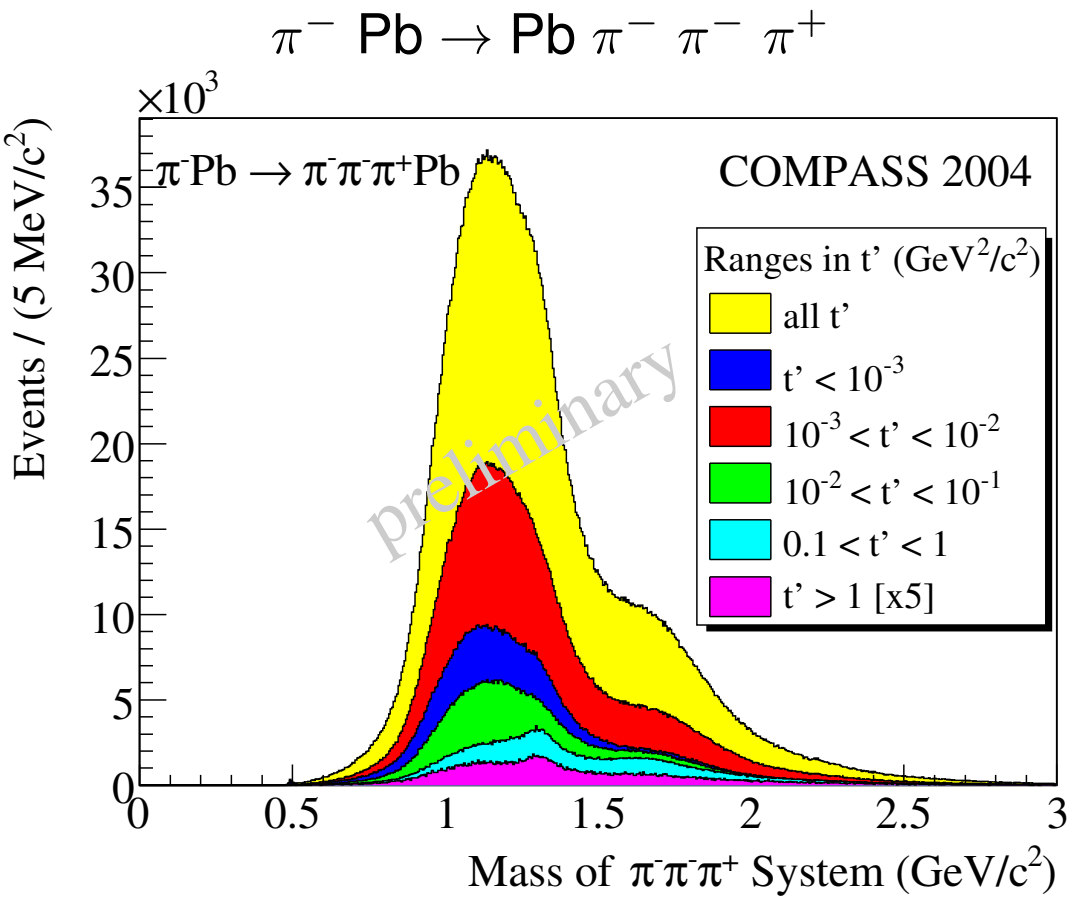

- "Low t'": $10^{-3} < t' < 10^{-2}$ $\sim$ 2 000 000 events
- "Primakoff region": $t' < 10^{-3}$ $\sim$ 1 000 000 events

Chiral dynamics in $\pi\gamma \to 3\pi$

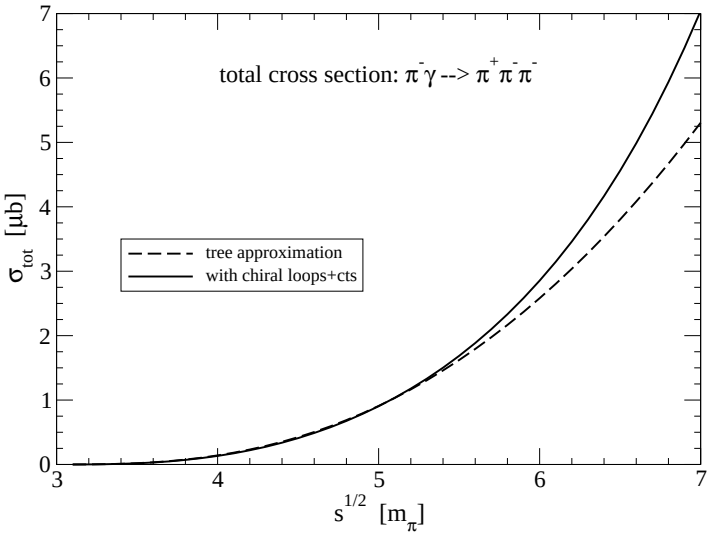

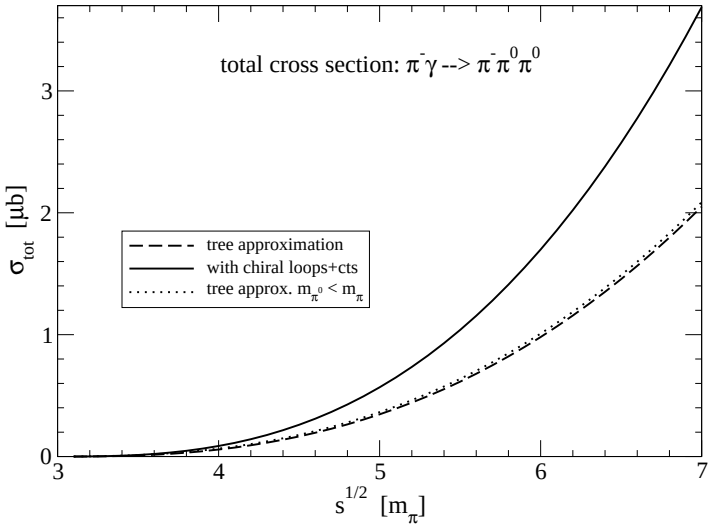

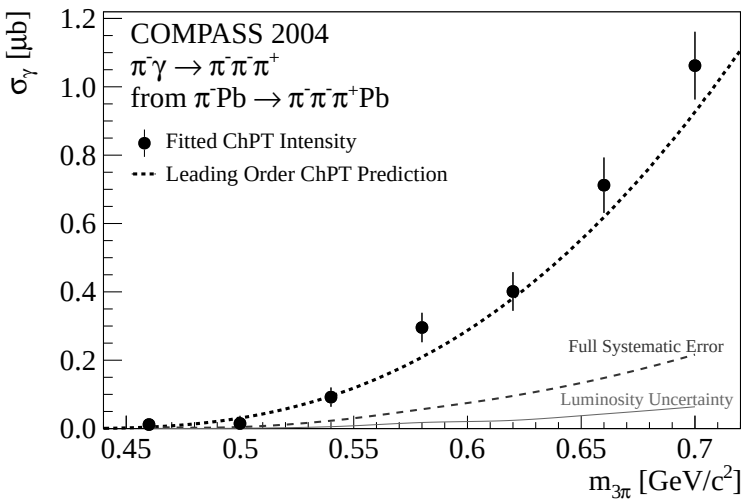

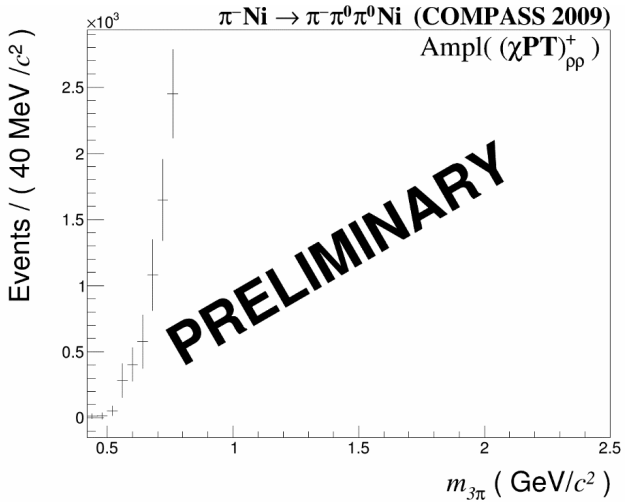

published in PRL 108 (2012) 192001

normalization: analysis ongoing

Radiative Coupling of $a_2(1320)$ and $\pi_2(1670)$

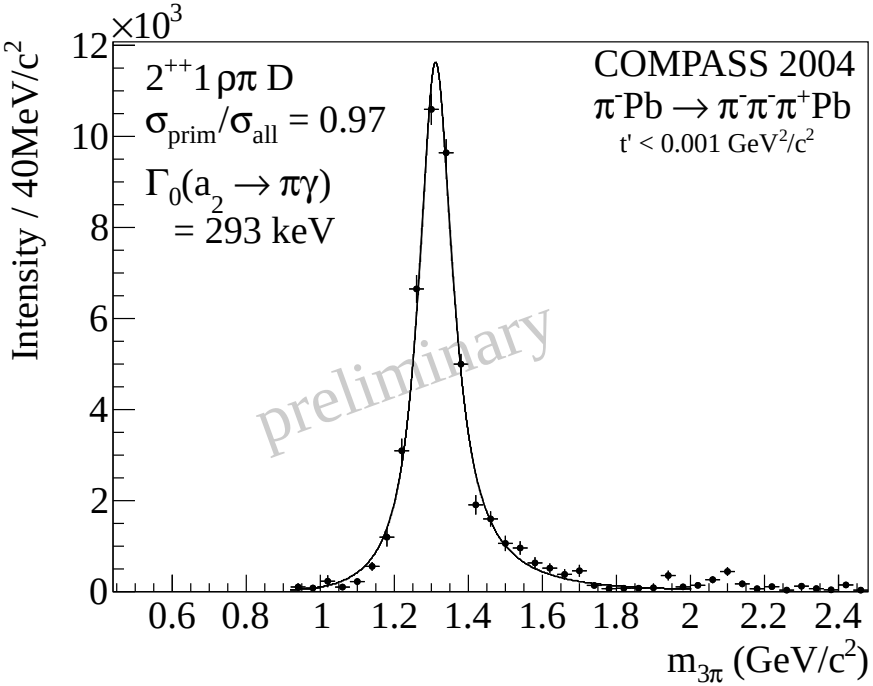

$\Gamma_0(a_2(1320) \to \pi\gamma)$ *M2*

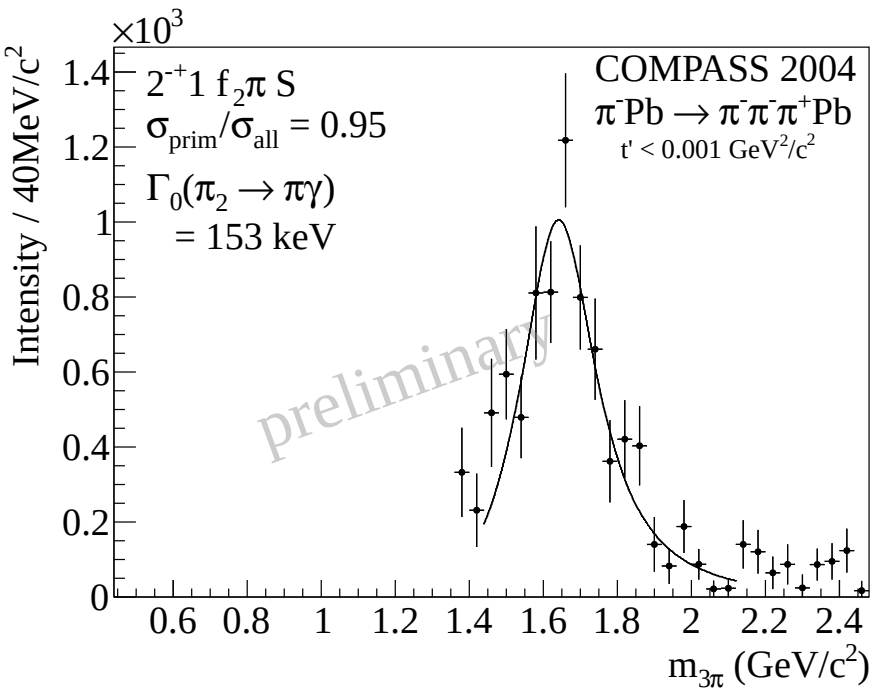

$\Gamma_0(\pi_2(1670) \to \pi\gamma)$ *E2*

$\Leftrightarrow$ meson w.f.'s: $\Gamma_{i\to f} \propto |\langle \Psi_f | e^{-i\vec{q}\cdot\vec{r}}\, \hat{\epsilon}\cdot\vec{p}\, | \Psi_i \rangle|^2$, VMD

- normalization via beam kaon decays
- large Coulomb correction

published in EPJ A50 (2014) 79